NON-BOILING HEAT TRANSFER IN HORIZONTAL AND NEAR HORIZONTAL DOWNWARD INCLINED GAS-LIQUID TWO PHASE FLOW

By

TABASSUM AZIZ HOSSAINY

Bachelor of Science in Mechanical Engineering

Islamic University of Technology

Gazipur, Dhaka

2009

Submitted to the Faculty of the
Graduate College of the
Oklahoma State University
in partial fulfillment of
the requirements for
the Degree of
MASTER OF SCIENCE
July, 2014

NON-BOILING HEAT TRANSFER IN HORIZONTAL AND NEAR HORIZONTAL DOWNWARD INCLINED GAS-LIQUID TWO PHASE FLOW

Thesis Approved:

Dr. Afshin Ghajar

Thesis Adviser

Dr. Khaled A. Sallam

Dr. AJ Johannes

ACKNOWLEDGEMENTS

I would like to extend my thanks and deepest gratitude to my Advisor Dr. Afshin J. Ghajar for all his support, valuable advice and guidance throughout my graduate study at OSU, which helped me to become a better student and researcher. I would also like to thank my committee members Dr. Khaled A. Sallam and Dr. AJ Johannes for giving their valuable time to act as committee members in their busy schedule. I would like to thank all my labmates, Swanand Bhagwat, Kalapatapu Srinaga Bharat Chandra, Edgar Lares Barboza, Adekunle Oyewole and Mehmet Mollamahmutoglu for all their support and friendship. Special thanks to my friends Kalapatapu Srinaga Bharath Chandra, Edgar Lares Barboza and Adekunle Oyewole for making my time as a graduate student a memorable one.

My ultimate thanks and love for my mother for teaching me the value of sincerity, hard work and integrity; her endless support, inspiration and sacrifice has made it possible for me to come this far in life and pursue my higher studies. I would also like to thank my brother and sister who have always been a source of inspiration.

Name: HOSSAINY, TABASSUM AZIZ

Date of Degree: JULY, 2014

Title of Study: NON-BOILING HEAT TRANSFER IN HORIZONTAL AND NEAR HORIZONTAL DOWNWARD INCLINED GAS-LIQUID FLOW

Major Field: MECHANICAL ENGINEERING

Abstract: Heat transfer in non-boiling gas-liquid two phase flow has significant practical applications in chemical and petroleum industry. To date, majority of the research in this field have been conducted for two phase flow in horizontal and vertical pipe systems. To explore and enhance the general understanding of heat transfer in non-boiling two phase flow, the main focus of this work is to experimentally measure local and average convective heat transfer coefficients for different flow patterns in horizontal and near horizontal downward inclined two phase flow. In total, 380 experiments are carried out in a 12.5 mm I.D. schedule 10S stainless steel pipe at 0, -5, -10 and -20 degrees pipe orientations using air-water as fluid combination. For each pipe orientation, the superficial gas and liquid Reynolds number is varied from 200 to 19,000 and 2000 to 18,000, respectively. The measured values of the average two phase heat transfer coefficient are found to be in a range of 500 W/m^2K to 7700 W/m^2K. Comparisons are drawn between the two phase heat transfer coefficients in the above mentioned pipe orientations. It is found that the increase in inclination of the pipe in downward direction causes the two phase heat transfer coefficient to decrease. This trend of two phase heat transfer data is explained based on the flow visualization and establishing its connection with the flow pattern structure and the two phase flow physics. Performance of the existing two-phase heat transfer correlations available in the literature is investigated by using the experimental data. Among general and Reynolds analogy based correlations, Shah (1981) and Bhagwat *et al.* (2012) are the best performing correlations. A new correlation is also proposed to improve the performance of the Reynolds analogy based correlation which has successfully predicted 96% of the data points within ±30%.

TABLE OF CONTENTS

Chapter Pages

CHAPTER I **1**

INTRODUCTION **1**

1.1 Basic Definitions and Terminology 5

1.2 Basic Flow Patterns 9

1.3 Research Objectives 11

1.4 Brief Outline 12

CHAPTER II **14**

LITERATURE REVIEW **14**

2.1 General Heat Transfer Correlations 16

2.2 Pressure Drop and Heat Transfer Relationship Based Correlations 25

CHAPTER III **32**

EXPERIMENTAL SETUP **32**

3.1 Details of Experimental Setup 32

3.2 Data Acquisition System 38

3.3 Experimental Procedure 40

3.4 Validation of the Experimental Setup 42

3.4.1 Single Phase Heat Transfer Uncertainty 42

3.4.2 Two Phase Heat Transfer Uncertainty 43

3.4.3 Comparison of Single Phase Heat Transfer Measurements with Correlations 44

CHAPTER IV **46**

RESULTS AND DISCUSSION **46**

4.1 Flow Patterns and Flow Pattern Maps 47

4.2 Heat Transfer 53
4.2.1 Effect of Flow Patterns and Pipe Orientation on Two Phase Heat Transfer Coefficient 53
4.2.2 Heat Transfer Correlation Performance 72
4.2.3 Correlation Development 85
CHAPTER V 91
SUMMARY, CONCLUSIONS & RECOMMENDATIONS 91
5.1 Summary of Findings 91
5.2 Future Recommendations 94
REFERENCES 96
APPENDIX A 103
UNCERTAINTY ANALYSIS 103

LIST OF TABLES

Table Page

Table 2.1 List of selected correlations for the heat transfer data analysis 29

Table 3.1 Two phase heat transfer uncertainties at different flow patterns 43

Table 3.2 Single phase heat transfer correlations 44

Table 4.1 Number of data points in different flow patterns at different pipe inclinations 53

Table 4.2 Heat transfer coefficient performance for 0 degree 75

Table 4.3 Heat transfer coefficient performance for -5 degree 76

Table 4.4 Heat transfer coefficient performance for -10 degree 77

Table 4.5 Heat transfer coefficient performance for -20 degree 78

Table 4.6 Heat transfer coefficient performance for all inclinations 79

Table 4.7 Specific value of the exponents of the proposed correlation $h_{TP}/h_L = (\varphi_L)^p (F_p)^q$ in different inclinations 88

Table 4. 8 Comparison of performance Bhagwat et al. (2012) and proposed correlation 88

Table A.1 Single phase heat transfer uncertainty (Best Case RUN 0001) 108

Table A. 2 Single phase heat transfer uncertainty (Worst case RUN 0018) 108

Table A. 3 Two phase heat transfer uncertainty (Best case RUN 151) 109

Table A. 4 Two phase heat transfer uncertainty (Worst case RUN 1150) 109

LIST OF FIGURES

Figure Page

Figure 3.1 Experimental setup circuit diagram 33

Figure 3.2 Experimental setup 33

Figure 3.3 Coriolis flow meters 37

Figure 3.4 Experimental setup validation with single phase heat transfer correlation 45

Figure 4.1 Flow regime map for horizontal and downward inclined two phase flow (Adapted from Hossainy *et al.* (2014)) 49

Figure 4.2 Representative photographs of stratified flow for horizontal, -5^o, -10^o and-20^o at Re_{SL}=2600, Re_{SG}=700 50

Figure 4.3 Representative photographs of slug flow for horizontal, -5^o, -10^o and-20^o at Re_{SL}=7400, Re_{SG}=700 51

Figure 4.4 Representative photographs of intermittent flow for horizontal, -5^o, -10^o and-20^o at Re_{SL}=12000, Re_{SG}=14000 52

Figure 4.5 Variation of two phase heat transfer coefficient at fixed Re_{SL} and increasing Re_{SG} (a) 0 degree, (b) -5 degree, (c) -10 degree, (d) -20 degree 55

Figure 4.6 Average percentage decrease in h_{TP} for different inclinations with reference to horizontal orientation. 58

Figure 4.7 Comparison of $h_{TP,\theta}/h_{TP,0}$ at different inclinations at (a) Re_{SG} = 279, (b) Re_{SG} = 2800, (c) Re_{SG} = 4500, (d) Re_{SG} = 9000, (e) Re_{SG} = 13000 61

Figure 4.8 Comparison of two phase heat transfer coefficient h_{TP} at different liquid Re_{SL}, (a) Re_{SL} = 2600, (b) Re_{SL} = 5100, (c) Re_{SL} = 7400, (d) Re_{SL} = 9800. 64

Figure 4.9 Comparison of top and bottom surface h_{TP} for (a) 0 degree, (b) -5 degree, (c) -10 degree, (d) -20 degree at Re_{SL} = 12,500 68

Figure 4.10 (a) Top surface, (b) Bottom surface h_{TP} comparison in slug flow regime Re_{SL} = 7400 70

Figure 4.11(a) Top surface h_{TP} comparison, (b) Bottom surface h_{TP} comparison at Re_{SL} = 12,000 in the intermittent flow region 71

Figure 4.12 Performance of correlation combining all inclinations (a) Shah (1981), (b) Knott *et al.* (1959), (c) Bhagwat *et al.* (2012), (d) Tang & Ghajar (2007)..... 83

Figure 4.13 Flow pattern factor (Adapted from Tang (2011))..... 86

Figure 4.14 Performance of the proposed correlation combining all inclinations..... 89

NOMENCLATURE

A	cross sectional Area, m^2
C	constant leading coefficient, dimensionless
c_p	specific heat at constant pressure, kJ/kg-K
D	diameter of pipe, m
D_i	inside diameter of pipe, m
D_o	outside diameter of pipe, m
dz	differential change in axial direction, m
F_p	flow pattern factor, dimensionless
F_s	shape factor, dimensionless
Fr	Froude number ($=u^2/gD$)
f_b	bubble, plug, or slug frequency, s^{-1}
G	mass flux or mass velocity, kg/m^2s
Gr	Grashof Number, dimensionless
g	gravitational acceleration, m/s^2
I	inclination factor, dimensionless from Tang and Ghajar (2007)
I	electric current, A
h	heat transfer coefficient, $W/m^2.K$

$\bar{h}$	circumferentially averaged heat transfer coefficient
K	slip ratio, dimensionless
k	thermal conductivity, W/m.K
L	length of test section, m
L_b	bubble, plug, or slug length, m
$\dot{m}$	mass flow rate, kg/s
N	Number of data points
N_{ST}	no. of thermocouple stations
Nu	Nusselt number (= hD/k), dimensionless
Pr	Prandtl number (= $c\mu/k$), dimensionless
p	pressure, Pa
p_a	atmospheric pressure, Pa
$\frac{dp}{dz}$	pressure drop per unit length, Pa/m
Q	volumetric flow rate, m^3/s
$\dot{q}$	heat transfer rate, W
$\dot{q}''$	heat flux, W/m^2
R	electrical resistance, Ω
R_L	liquid fraction or liquid holdup, dimensionless
R_t	thermal resistance, m^2K/W
Re	Reynolds number (= $\rho VD/\mu$), dimensionless
S_L	wetted-perimeter, m
St	Stanton Number

T temperature, °C

$\bar{T}$ average temperature, °C

u axial velocity, m/s

u_b bubble, plug, or slug velocity, m/s

V Average velocity, m/s

V_D Voltage drop, V

w uncertainty, dimension varies with measured parameter

X Lockhart-Martinelli parameter $\sqrt{(\frac{dp}{dz})_{f,SL}/(\frac{dp}{dz})_{f,SG}}$, dimensionless

x flow quality $\dot{m}_G/\dot{m}$, dimensionless

Greek Symbols

α void fraction, dimensionless

μ dynamic viscosity, N.m/s^2

v kinematic viscosity, m^2/s

ϑ slug frequency in Deshpande *et al.* (1991) correlation, s^{-1}

φ two-phase multipliers, dimensionless

φ angle from the circumferential top from Hetsroni *et al.* (1998 a,b), rad.

θ inclination angle of pipe or test section, deg. or rad.

ρ density, kg/m^3

σ surface tension, N/m

Δ differential operator

Subscripts

ATM	atmosphere
avg	average
B	bottom of the pipe
b	bulk
CAL	calculated
eff	effective
EXP	experimental
f	frictional component
G	gas phase
H	homogeneous
i	index for *ith* value in mean absolute error equation
in	inlet
L	liquid phase
out	outlet
m	mixture
SG	superficial gas
SL	superficial liquid
sn	thermocouple station number
SYS	system
T	top of pipe
TP	two-phase

w wall

wi inner wall

wo outer wall

Superscripts

p constant exponent, dimensionless

q constant exponent, dimensionless

r constant exponent, dimensionless

Abbreviations

B bubbly

S slug

SD Standard deviation

ST stratified

W wavy

CHAPTER I

INTRODUCTION

Multiphase flow is defined as the flow where more than one phase simultaneously exists, either of similar or different components, without chemically reacting with each other. Two-phase flow is the simplest case of multiphase flow which can be classified based on the state of the phases which are flowing in conjunction with each other; such as solid-solid, solid-liquid, liquid-liquid and liquid-gas flow. These flows can be divided in disperse or separated flow. In disperse flow, the particles or bubbles of the components are connected with each other and interact through a continuous flowing medium. On the other hand, separated flow consists of two distinct phases separated by a continuous interface where each phase possesses its own flow characteristics. There are several different approaches which have been adopted by the researchers over the years to predict the behavior of two-phase flow. These approaches involve theoretical attempt using mathematical models and equations, conducting experiment in controlled environment with appropriate test setup or performing flow simulation applying computational method with the help of highly sophisticated and powerful computers. The complexity of multiphase flow presents a major obstacle in providing a closed form solution through theoretical or computational process as it necessitates complete solution of Navier-Stokes equation for each

phase to describe the motion of the fluid flowing around each particle and the characteristics of the interface separating them. The computational power which is required for such solution becomes even more astronomical when turbulence is induced in the two-phase flow. Hence, experimental approach in two-phase flow is preferable whenever the scale of the test setup matches that of the prototype or at least possesses enough similarity so as to extrapolate the outcome of the experiment to the practical applications. The approach of the current research is an experimental one which investigates the heat transfer phenomena in two-phase gas-liquid flow, hence, from here and onwards the discussion will mainly evolve around the heat transfer in two-phase gas-liquid flow.

Boiling and non-boiling heat transfer in two-phase flow is a complex phenomenon with immense industrial and practical engineering applications. Two-phase flow heat transfer occurs in the solar collector, stream turbine, boiler, heat exchanger, refrigeration and air conditioning system, cooling process of the core reactor in nuclear power plant, fluid transportation in oil and geothermal well bore, oil and gas delivery pipelines, etc.

Petroleum and geothermal industries are major fields where prediction and calculation of two-phase heat transfer and pressure drop are tantamount to the proper and cost effective transportation of reservoir fluid to the ground. In geothermal plants and oil rigs, liquid flows from the reservoir to the ground and heat transfer takes place due to difference of temperature between the formation and the fluid or oil which is flowing through the well bore. For instance, according to Trevisan *et al.* (2006), in sub-sea oil and gas platforms, the surrounding temperature around the rigs is 4^{o}C while temperature of the extracted hydrocarbon from the reservoir is about 75^{o}C. This type of big temperature difference might cause solidification of the hydrocarbons to paraffin and cause blockage in the pipeline interrupting the flow (Furuholt, 1988). Moreover, during transportation, oil and gas often exist simultaneously and without accurate knowledge of pressure

drop and heat transfer in the pipeline gas hydrate formation might take place (Ghajar, 2005). Cost of repairing and replacing these blocked pipe lines, cost of downtime and abundance of oil rigs beyond repair could cost the industry millions of dollars (Fogler, 2008).

Electricity generation through solar power is one of the popular renewable energy sources around the globe which also observes two-phase heat transfer phenomena. In the solar collector, water is evaporated at 400^{o}C to steam which is used as the medium of heat transfer between the solar field and power block for utilizing the high thermal efficiency of the steam power cycle (Hetsroni *et al.*, 1998b). Calculation of two phase flow heat transfer is highly important in such solar assisted heat pump type evaporators (Soldo *et al.*, 2006).

Two phase heat transfer is found in the power stations where boilers are used to produce steam from pressurized water by heating through pipe. The stream is used for power generation in turbine which operates in steam power cycle. Designing such equipment requires detailed understanding and knowledge of heat transfer and pressure drop in two-phase flow to ensure appropriate supply and regulation of the generated steam to the turbine and maintain safety of the procedure by properly controlling the boiler pressure.

In nuclear reactor knowledge of two-phase heat transfer is highly important for safe design and avoidance of nuclear accidents. Due to high temperature, boiling two-phase flow occurs while removing heat from the reactor core. Knowledge of two-phase flow is required to ensure efficient heat transfer from the coolant to the reactor and maintaining a stable flow condition with appropriate high velocity (Nürnberg, 1970). During the cooling process, at critical heat flux, the value of heat transfer coefficient starts to decrease with increasing temperature resulting in unstable situation and decreased cooling rate (Rzehak and Krepper, 2013). Appreciating the mechanism of two-phase transient boiling which takes place during the cooling process along

with the nature of critical heat flux with increased heat input is highly important for avoiding severe accidents in water based nuclear cooling system (Park *et al.*, 2012).

One of the modern application of non-boiling two-phase heat transfer is in microgravity condition which prevails in the space and highly important in the design of thermal control system in the communication satellites and space stations. The behavior and mechanics of two-phase flow interaction in reduced gravity condition can be completely different from what is observed in terrestrial environment. Two-phase heat transfer is desirable in such conditions due to its higher heat transfer coefficient compared to single phase flow and can play a vital role in reduction of system size. Moreover, the ability of the process to transfer heat in isothermal surface condition is also vital for the advanced instrumentation system being used in the space stations (Gabriel, 2007).

Due to its immense practical value, boiling and non-boiling two-phase heat transfer researches are highly warranted to establish complete understanding of the complex mechanism of heat transfer processes in two phase mixture. The complexity of the process arises due to several key factors. The most important factor is the flow pattern. The physical structure of the flow pattern, which affects the heat transfer tremendously, varies significantly at different liquid and gas flow rates, direction and inclination of flow etc. Different flow patterns are associated with different heat transfer characteristics and mechanisms. Two-phase heat transfer is also influenced by relative velocity of the phases in the mixture. Knott *et al.* (1959) noticed that introducing gas phase in the liquid phase in small amount increased the heat transfer as much as two times in air-water mixture flow. The authors mentioned the increase in the mixture velocity as the reason for increased heat transfer. The orientation of the setup and direction of flow also plays significant role in the nature of heat transfer in two-phase flow by changing the flow patterns and direction of the buoyancy force of the liquid phase. In the literature, researchers worked mostly with

different fluid combination with either constant temperature or heat flux boundary condition at horizontal and vertical upward flow. Little work is available in the literature related to the effect of flow orientation to the heat transfer in two phase flow. Hestroni *et al.* (2003) and, Tang and Ghajar (2007) observed significant increase in the heat transfer for slightly inclined upward flow compared to horizontal using air-water mixture. However, any research work is yet to be conducted in near horizontal downward inclined flow condition, which can be highly important in projecting further light on the effect of inclination on flow pattern and two-phase heat transfer. The information gathered from such research can be made highly useful by contrasting it with that of the near horizontal upward inclined flow and establishing a clear understanding of the difference in physical mechanism of two phase heat transfer between upward and downward flow. The outcome of the research can be valuable in finding novel applications of downward two phase flow heat transfer in the power generation and processing industry. It will also provide the necessary data which can pave the way for attempting to propose a universal correlation for prediction of two phase heat transfer coefficient irrespective of flow orientation, flow pattern, fluid combination and pipe size.

1.1 Basic Definitions and Terminology

Some of the two-phase flow terms appear ubiquitously in the literature. Most of these terms have been defined by modifying some of the basic quantities which are regularly used in single phase fluid flow such as mass flow rate, mass flux, liquid and gas Reynolds number etc. There are other two phase flow definitions which are more relevant to the quality or properties of the flow and have been defined in a manner to represent the mean flow property combining both phases, such as mixture density, specific volume, viscosity, void fraction, quality of flow etc. These definitions along with some important dimensionless numbers relevant to this research are discussed below in detail:

Two-phase mass flow rate can be defined as the summation of the individual mass flow rates of each phase.

$$\dot{m} = \dot{m}_G + \dot{m}_L \tag{1.1}$$

The definition of liquid, gas and mixture mass flux

$$G_G = \frac{\dot{m}_G}{A} \tag{1.2a}$$

$$G_L = \frac{\dot{m}_L}{A} \tag{1.2b}$$

$$G = \frac{\dot{m}}{A} \tag{1.2c}$$

Cross sectional area is the summation of the cross sectional area occupied by both the liquid and gas phase.

$$A = A_G + A_L \tag{1.3}$$

Superficial gas and liquid velocity is defined as following

$$V_{SG} = \frac{x\dot{m}v_G}{A} \tag{1.4}$$

$$V_{SL} = \frac{(1-x)\dot{m}v_L}{A} \tag{1.5}$$

Slip ratio indicates the relative velocity of the gas phase with respect to the liquid phase. Homogeneous mixture density when slip ratio is 1.

$$K = \frac{V_G}{V_L} \tag{1.6}$$

Superficial gas and liquid Reynolds number are defined in terms of gas and liquid density, viscosity and superficial gas and liquid velocity as follows:

$$\mathrm{Re}_{SG} = \frac{\rho_G D V_{SG}}{\mu_G} = \frac{GxD}{\mu_G} \tag{1.7}$$

$$\mathrm{Re}_{SL} = \frac{\rho_L D V_{SL}}{\mu_L} = \frac{G(1-x)D}{\mu_L} \tag{1.8}$$

The quality of the flow shows the ratio of mass flux of gas to that of the total mass flow rate of the mixture.

$$x = \frac{\dot{m}_G}{\dot{m}} \tag{1.9}$$

The void fraction is the ratio of the cross-sectional area occupied by the gas phase to that of the entire cross section.

$$\alpha = \frac{A_G}{A} \tag{1.10}$$

The liquid hold up is defined as

$$R_L = 1 - \alpha = \frac{A_L}{A} \tag{1.11}$$

Mixture density is defined as follows:

$$\rho_m = \alpha\rho_G + (1-\alpha)\rho_L \tag{1.12}$$

For homogeneous mixture, the mixture density is defined as

$$\rho_H = \frac{1}{x/\rho_G + (1-x)/\rho_L} \tag{1.13}$$

Specific volume of the mixture can be defined as

$$v_m = \frac{xv_G + K(1-x)v_L}{x + K(1-x)} \tag{1.14}$$

The slip ratio, K is unity for homogeneous mixture and thus specific volume for the homogeneous mixture

$$v_H = xv_G + (1-x)v_L \tag{1.15}$$

Some of the relevant dimensionless numbers for heat transfer analysis are Nusselt number, Prandtl number and Stanton number which are described below:

Nusselt Number is the ratio of convective to conductive heat transfer

$$Nu = \frac{hD}{k} \tag{1.16}$$

Prandtl Number is the ratio of the momentum diffusivity to thermal diffusivity

$$\mathrm{Pr} = \frac{\mu c}{k} \tag{1.17}$$

Stanton number is the ratio of heat transferred to the fluid to its thermal capacity

$$St = \frac{h}{\rho c u} \tag{1.18}$$

1.2 Basic Flow Patterns

The following flow patterns are observed in horizontal and near horizontal flow orientation as shown in Figure 1.1:

***Bubbly*:** Bubbly flow contains small gaseous bubbles which are dispersed in continuous liquid medium. Bubbly flow occurs when small amount of gas is introduced in the liquid phase. For horizontal flow, bubbles flow at the top due to buoyancy and for vertical flow it's evenly distributed throughout the flow. Introduction of gas phase in bubbly region increases the bubble diameter where they interact and eventually form larger bubbles.

***Intermittent*:** Intermittent flow consists of mainly two transitional flow patterns, slug wavy and annular wavy region. When gas flow rate is increased in slug flow, the gas-liquid interface is induced with waves due to shear force of the gas over the liquid phase. This flow pattern is called slug wavy. When gas flow rate is further increased, gas phase starts to press the liquid phase to the circumference as it flows through the core with high velocity. As a result, liquid film starts to develop at the pipe wall. This flow pattern is called wavy annular which ultimately becomes annular flow at higher gas flow rates.

***Stratified*:** In stratified flow, two phases are in a state of complete separation by a continuous interface. The separation is caused by either density difference or low flow rate of the phases. For example, in horizontal liquid-gas two-phase stratified flow as shown in Figure 1.1, the liquid flows touching the bottom of the pipe wall due to higher density and gas phase flows over the liquid phase making contact with the top pipe wall surface. Heat transfer coefficient is reduced in the stratified region and induced with higher degree of uncertainty.

***Slug*:** Slug flow is observed in gas-liquid two-phase flow where pockets of gases (formed due to coalescence of consecutive gas bubbles) flow through the liquid phase in intermittent manner at certain frequency. The length of the slug and frequency depends on the flow rate of the gas. Frequency of slug flow is greatly affected by the resistance of buoyancy force. It can be observed from Figure 1.1 that in horizontal flow, slugs flow touching the top of the pipe. However, in vertical upward flow, slugs stay at the centre and make a bullet shape nose due to buoyancy force. Gas slugs have lower heat transfer coefficient than liquid and hence the temperature at the top surface in contact with the slugs is more compared to the bottom in horizontal flow.

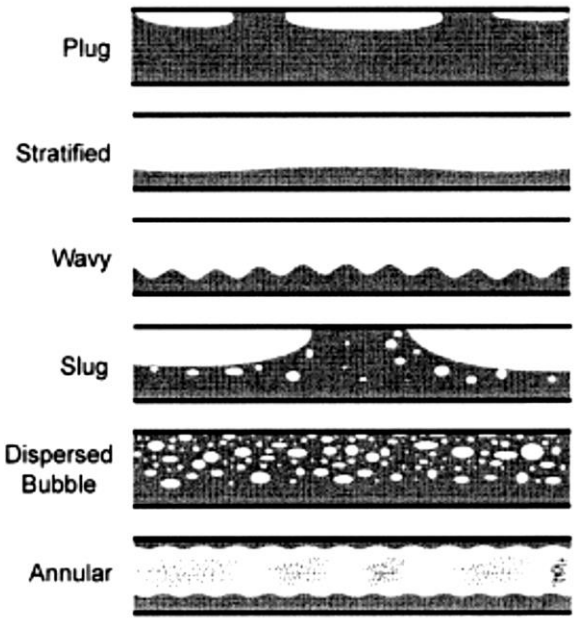

Figure 1.1 Different flow regimes in horizontal gas-liquid flow (Adapted from Tang (2011))

***Annular*:** Annular flow occurs in high liquid and gas flow rate where the momentum of the gas phase flowing at the core pushes the liquid phase to the wall and it forms liquid film at the pipe wall surface. Annular flow is dominated by gas phase and it's a shear driven flow. In industrial application, annular flow occurs in steam generator, condenser and evaporator. Annular flow is conducive for heat transfer as liquid film has greater heat transfer coefficient than gas phase which maintains permanent contact with the pipe surface.

1.3 Research Objectives

The main objective of this research is to investigate two-phase heat transfer in air-water mixture in horizontal and slightly horizontal downward flow to establish a basic understanding of the mechanism of heat transfer in downward flow. As previous researches in this field don't shed any light in slightly inclined downward flow, the purpose of the work is to utilize the flow pattern observation data, average and local heat transfer coefficient measurement to establish the trends which exist in such cases and provide a physical explanation of the heat transfer variation at different liquid and gas flow rates and, orientation of the flow. After examining the qualitative aspect of the heat transfer, a quantitative analysis will be performed to examine the performance of the existing heat transfer correlations in predicting slightly inclined downward flow heat transfer. Based on the outcome of the performance test, a recommendation will be made on the best correlation which is applicable for such case. After such analysis, a new correlation can be proposed which can predict two-phase heat transfer coefficient for downward flow with better accuracy and standard deviation by taking in account the effect of orientation on flow pattern.

For achieving the objectives, following tasks need to be done:

(1) Literature review of the existing works on prediction of non-boiling two-phase heat transfer in horizontal, vertical and inclined flow by different authors along with their experimental condition, test setup and methodologies.

(2) Measurement of two-phase heat transfer coefficient horizontal and near horizontal (-5^{o}, -10^{o} and -20^{o}) downward flow.

(3) Plotting the measurements and establishing a trend of heat transfer at different liquid and gas flow rates and, inclination angles.

(4) Analysing the established trend using the information obtained from flow pattern observation and inspection of local heat transfer coefficient at circumferential location for further in depth analysis of the trends.

(5) Performance analysis of the existing general and Reynolds analogy (isothermal pressure drop data) based two-phase heat transfer correlations proposed in the literature for horizontal, vertical and near horizontal upward flow and recommend the best correlations for the downward flow.

(6) Propose a new correlation with better accuracy and standard deviation for the prediction of heat transfer in horizontal and near horizontal downward flow.

1.4 Brief Outline

For accomplishing the research objectives, first a comprehensive literature survey will be performed to discuss the related research works by the previous authors in the field of two-phase flow heat transfer. This literature survey will be documented in Chapter II titled 'Literature Review'. After literature survey, two-phase heat transfer coefficient measurement will be made for air-water mixture by using the experimental setup with good number of representative points from each flow pattern. The details of the experimental setup which is going to be used for such measurements will be discussed in Chapter III titled 'Experimental Setup'. After collection of the data, plotting and analysis of the data points will be performed to establish the trend of heat transfer with flow pattern and inclination. After establishing the trend, flow pattern map and analysis of the local heat transfer coefficients will be utilized to propose a physical explanation of the observed trend. The experimental data and collected isothermal pressure drop data will be used to test the available correlations in the literature proposed by the previous authors based on specific inclination and combined data. Recommendations will be made on the best suitable correlations at each inclination and flow pattern separately and also for combined data. New

correlation will be proposed to improve the accuracy and robustness of the prediction of the heat transfer in the horizontal and slightly inclined downward flow. This analysis of the experimental data, performance test of correlations and new correlation development will be discussed in Chapter IV tilted ‘Results and Discussion’. Finally, in Chapter V, a summary of the research findings will be presented along with some recommendations for future work.

CHAPTER II

LITERATURE REVIEW

Significant amount of research have been conducted in the field of heat transfer in two-phase gas-liquid mixture in horizontal tubes. Researchers have addressed the subject from different perspectives; some researches were particularly interested in some specific flow regime and some adopted more robust approach. Mainly two different boundary conditions can be observed in the literature, constant temperature (Johnson and Abou-Sabe, 1952; Fried, 1954; Lunde, 1961; Oliver and Wright, 1964; Hughmark, 1965; Fedotkin and Zarudnev, 1970) and constant heat flux (Knott *et al.*, 1959; Davis and David, 1964; Pletcher and McManus, 1968; Martin and Sims, 1971; Aggour, 1978; Shah, 1981; Shoham *et al.*, 1982; Kago *et al.*, 1986; Deshpande *et al.*, 1991; Hestroni *et al.*, 2003; Kim and Ghajar, 2006; Tang and Ghajar, 2007). Some researchers experimented with different combination of fluid and gas (Aggour, 1978; Ravipudi and Godbold, 1978; Shah, 1981) and orientation of flow (Hestroni *et al.*, 2003; Tang and Ghajar, 2011) In order to establish a concrete understanding of the mechanism of two-phase flow heat transfer, researchers generally performed measurement of the circumferential temperature variation, two-phase heat transfer coefficient (both mean and local) at different combination of liquid and gas flow rates. These measurements ultimately helped to develop appropriate correlations for

predicting two-phase heat transfer coefficient by identifying the specific factors that play significant role in the phenomena. All of these researches paved way to better understanding of heat transfer by providing valuable insights. However, compared to horizontal flow, heat transfer in inclined two-phase gas-liquid flow has received little attention.

Aggour (1978), Oshinowo *et al.* (1984), Chu and Jones (1980), Kim *et al.* (2000) and Mollamahmutoglu (2012) were few researchers who paid attention in their research about inclined flow. Many of the inclined flow work only involve vertical orientation. Tang (2011) worked in horizontal, near horizontal flow (2^o, 5^o and 7^o) and vertical orientations, however, his work concentrated on the upward flow. Chu and Jones (1980), Oshinowo *et al.* (1984) and Mollamahmutoglu (2012) worked in vertical downward flow. Research on near horizontal downward flow is non-existent in the literature. Hence, further investigation is necessary in near horizontal downward flow to establish a better understanding of the effect of downward orientation in heat transfer.

Correlations were proposed by many authors based on their experimental data to predict heat transfer coefficient in two-phase flow. Some of these correlations are flow pattern specific and some are more robust which can predict heat transfer coefficient in different flow patterns and pipe orientations. Among these correlations mainly two different theme can be observed, a group of authors provided general correlations which focused on taking in account the average mixture properties, variation of properties with temperature, relative velocity of liquid and gas phase, flow pattern and inclination effect. Another group of authors used the isothermal two-phase frictional pressure drop data and attempted to correlate it with two-phase heat transfer coefficient with relatively simple structured correlation adopting Reynolds analogy. Hence, the ongoing literature review will be presented in two parts, in first part the authors who worked on establishing general correlations for two-phase heat transfer coefficient through experiment will be discussed and the

later part will focus on the works involving frictional pressure drop and heat transfer coefficient based relationship.

2.1 General Heat Transfer Correlations

Initial works in the literature involved an attempt to find the relationship between heat transfer and gas and liquid velocity ratio to understand how introduction of gas phase affects the heat transfer in two-phase gas-liquid flow. Knott *et al.* (1959) conducted one of the earliest works in the literature regarding establishment of a deeper understanding of such phenomena and proposed a simple correlation based on their heat transfer data. Experiments were performed in uniform heat flux condition with Nitrogen-Oil mixture. The work focuses on bubbly flow regime in two-phase flow. The authors show the effect of introduction of gas phase in liquid flow by plotting h_{TP}/h_L ratio against V_{SG}/V_{SL} and observed the heat transfer rate doubling at velocity ratio 10. The work concluded that introduction of gas phase increases heat transfer by increasing the mean velocity of the flow. The proposed correlation was:

$$\frac{h_{TP}}{h_L} = (1 + \frac{V_{SG}}{V_{SL}})^{\frac{1}{3}} \tag{2.1}$$

where h_L is calculated from Sieder & Tate (1936) given by:

$$h_L = 1.86(\frac{k}{D})(Re_{SL}Pr_L\ \frac{D}{L})^{\frac{1}{3}}\left(\frac{\mu_b}{\mu_w}\right)^{0.14} \qquad \text{(Laminar)}$$

$$h_L = 0.023(\frac{\mathrm{k}}{\mathrm{D}})Re_{SL}^{\ 0.8}Pr_L^{\ 0.4}(\frac{\mu_b}{\mu_w})^{0.14} \qquad \text{(Turbulent)}$$

Shah (1981) expanded the work on relationship between heat transfer and velocity ratio by conducting experiments in both vertical and horizontal set-up in circular and non-circular channels with gas-liquid combination. He proposed a correlation based on his experiment and tested the accuracy of the correlation with data collected from the literature with 10 different gas-liquid combinations including air-water, oil, nitrogen, glycol and channel hydrodynamic diameter

ranging from 4 to 70 mm. The correlation predicted 96% of the data within ±30% with root-mean square error of 15.5% among 672 data points. The proposed correlation for $Re_{SL} < 170$ was:

$$\frac{h_{TP}}{h_L} = (1 + \frac{V_{SG}}{V_{SL}})^{\frac{1}{4}} \tag{2.2}$$

where h_L is calculated from Sieder and Tate (1936).

For $Re_{SL} > 170$, the author presented the correlation graphically due to the complex nature of the relationship between the parameters. Elamvaluthi and Srinivas (1984) performed experiments to further quantify and predict the effect of velocity ratio on heat transfer in non-boiling two-phase flow with air-water mixture. The test section was 860 mm long and electrically heated. 10 mm internal diameter brass tube was used in the experiments. The authors reported sharp increase in the heat transfer coefficient value with the introduction of the gas phase for V_{SG}/V_{SL} less than 1 and marginal increase for greater than 1. Introducing small amount of air in the flow doubled the value of two phase heat transfer coefficient. Based on the data collected, authors proposed the following correlation for a range of 300-16500 for Re_{SL} and 0.3-4.6 for V_{SG}/V_{SL}:

$$Nu_{TP} = 0.5 {Re_M}^{0.7} {Pr_L}^{0.33} (\frac{\mu_b}{\mu_w})^{0.14} (\frac{\mu_G}{\mu_L})^{0.25} \tag{2.3}$$

$$Re_m = \frac{DV_{SL}\rho_L}{\mu_L} + \frac{DV_{SG}\rho_L}{\mu_L} \tag{2.4}$$

The correlation predicted about 90% of the data points collected from the literature within ±25% error.

In the literature several works can be found on two-phase heat transfer using different fluid combinations. Khoze *et al.* (1976) conducted experiments on heat transfer measurements in air-water, air-diphenyl oxide, and air-polymethylsiloxane flowing through rectangular channels. The liquids used in the experiment had wide range of viscosity. The following correlation was

proposed by the authors for two-phase heat transfer coefficient measurements which predicted 100% of the collected data points within ±20%:

$$Nu_{TP} = 0.26\ Re_{SG}{}^{0.2} Re_{SL}{}^{0.55} Pr_L{}^{0.4} \tag{2.5}$$

Aggour (1978) performed measurements of two-phase heat transfer coefficient for vertical upward flow for three different fluid combinations (water-air, water- helium, water-Freon 12). The tube was 1.168 cm in internal diameter and the electrically heated test section had *L/D* ratio of 130. The author reported that the effect of gas-phase density on heat transfer was found more prominent on low liquid flow rates and moderate to high superficial gas velocities. A simple correlation was proposed which is:

$$\frac{h_{TP}}{h_L} = (1-\alpha)^{-n} \tag{2.6}$$

where *n* is 0.33 for laminar flow and 0.83 for turbulent flow. α is calculated from Chisholm (1973). Single phase heat transfer coefficient number can be found from the following equations:

$$h_L = 1.615\ (\frac{\mathrm{k}}{\mathrm{D}})(Re_{SL} Pr_L \frac{D}{L})^{\frac{1}{3}} (\frac{\mu_b}{\mu_w})^{0.14} \qquad \text{(Laminar)} \tag{2.7}$$

$$h_L = 0.0155 (\frac{k}{D}) Re_{SL}{}^{0.83} Pr_L{}^{0.5} (\frac{\mu_b}{\mu_w})^{0.33} \qquad \text{(Turbulent)} \tag{2.8}$$

The correlation predicted 91% of the 338 data points within ±50% with 32.8 rms deviation. Ravipudi and Godbold (1978) also performed measurement of two phase heat transfer coefficients in vertical steam condenser with four different liquid-gas combinations (air-water, air-toluene, air-benzene, air-methanol) and superficial Reynolds number range of about 3500-82000 for gas and about 8500-90000 for liquid. The experiments were mainly performed in froth flow regime. The effect of mass transfer on heat transfer rates was investigated and for such case the heat transfer coefficients were found to be a function of liquid and gas mass flux densities,

vapor pressure of the liquid and the total pressure of the system. For cases without mass transfer, it was reported that the introduction of the gas phase in the flow increased the heat transfer rate substantially. Based on dimensional analysis a correlation was proposed for predicting heat transfer coefficient:

$$h_{TP} = 0.56\left(\frac{k}{D}\right)Re_{SL}^{0.6}Pr_L^{0.33}\left(\frac{\mu_b}{\mu_w}\right)^{0.14}\left(\frac{\mu_b}{\mu_G}\right)^{0.2}\left(\frac{V_{SG}}{V_{SL}}\right)^{0.3} \quad (2.9)$$

Several authors also compared the upward and downward heat transfer occurring in two-phase flow. Dorresteijn (1970) investigated forced convection heat transfer for both upward and downward flow in bubbly and froth flow pattern in two-phase gas-liquid mixture using oil-air as the working fluid. Electrical heating with 70 mm diameter coil was applied. The range of the liquid velocities was 0.02 to 4.64 m/s corresponding to Reynolds number range of 300 to 66000. For liquid velocity above 1 m/s slight increase in the heat transfer was observed by the author. However, no difference in heat transfer was observed while comparing upward and downward flow. The author proposed the following correlation:

$$\frac{h_{TP}}{h_L} = (1-\alpha)^{-0.33} \quad \text{(Laminar)} \quad (2.10)$$

$$\frac{h_{TP}}{h_L} = (1-\alpha)^{-0.8} \quad \text{(Turbulent)} \quad (2.11)$$

where, $h_L = 0.0123\, Re_{SL}^{0.9} Pr_L^{0.33}\left(\frac{\mu_b}{\mu_w}\right)^{0.14}\left(\frac{k}{D}\right)$

Chu and Jones (1980) performed heat transfer measurements for upward and downward flow in two phase air-water mixture. The internal tube diameter was 2.67 cm with *L/D* = 34. The setup was electrically heated with a V_{SG}/V_{SL} ratio range of 0.12 – 2.14. The authors reported vertical upward flow had a higher heat transfer rate than vertical downward flow in the laminar flow region; however, in the turbulent flow region downward heat transfer can be more. They

introduced the ratio of the system pressure and atmospheric pressure to take in account the effect of pressure change in heat transfer. The proposed correlation was:

$$h_{TP} = 0.43(\frac{k}{D})Re_{SL}^{0.55}Pr_L^{0.33}(\frac{\mu_b}{\mu_w})^{0.14}(\frac{Pa}{P})^{0.17} \quad (2.12)$$

Oshinowo *et al.* (1984) also performed experiments on the measurements of two phase heat transfer coefficient in vertical upward and downward air-water mixture flow with 25.8 mm internal diameter tube at 172.3 kPa pressure. The water and gas flow rates were varied from 54 to 172 kg/m^{2}s and 0 to 1.322×10^{-2} m^3/s. The authors reported that for similar liquid and gas flow rates heat transfer coefficients for upward flow is generally higher than the downward flow. The authors proposed a correlation based on dimensional analysis for both vertical upward and downward flow:

$$h_{TP} = 1.2(\frac{k}{D})Re_{SL}^{0.6}Pr_L^{0.33}(\frac{\mu_b}{\mu_w})^{0.14}(\frac{\mu_G}{\mu_L})^{0.2}(\frac{V_{SG}}{V_{SL}})^{0.1} \quad (2.13)$$

Drucker *et al.* (1984) conducted experiments on two phase heat transfer for vertical air-water flow inside tube and over rod bundles with blockage. For air-water flow inside tube, liquid Reynolds number range was 2000 to 150,000 and void fraction was varied between 0.01-0.40. Following correlation was proposed based on their work for air-water flow inside vertical tube:

$$\frac{h_{TP}}{h_L} = 1 + 2.5\,(\frac{\alpha Gr}{Re_{TP}^2})^{0.5} \quad (2.14)$$

where, $Gr = \frac{(\rho_L - \rho_G)gD^3}{\rho_L v_L^2}$

and h_L is from Sieder and Tate (1936).

The authors also observed considerable amount of heat transfer enhancement for flow over rod bundles at the downstream of the blockages and a modified correlation was proposed for such cases by changing the empirical constant value. Rezkallah and Sims (1987) tested eleven existing

vertical two phase flow heat transfer correlations using selected data sets collected from the literature with thirteen different gas liquid combinations with varying pipe dimensions and flow patterns. The authors reported good agreement for most of the correlations for air-water data. For high Prandtl number fluid like glycerin, where existing correlations failed to perform reasonably, the authors proposed the following correlation:

$$\frac{h_{TP}}{h_L} = (1-\alpha)^{-0.9} \tag{2.15}$$

where, h_L is from Sieder and Tate (1936)

Some of the experimental work in the literature focused on specific flow regime to provide better physical understanding of heat transfer in two-phase flow. Shoham *et al.* (1982) experimented on the heat transfer characteristics of the two-phase gas-liquid horizontal slug flow by observing the time variation of temperature, heat transfer coefficient and peripheral heat flux. The test section was electrically heated and the flow rates were varied between 0.45 to 1.6 kg/s for liquid and 0.0023 to 0.01 kg/s for gas. The study was qualitative in nature and focused on the effect of slug flow on the local heat transfer coefficient at the top and bottom. The authors reported heat transfer coefficient at the top was always less than the bottom in the slug flow and in some cases values at the bottom was twice as much as the top. At high liquid and low gas flow rates the ratio of heat transfer coefficients at the top and bottom is small, however, with the increase of gas flow rate the ratio goes up. They also observed that contact of gas with the pipe surface reduced the heat transfer coefficient value significantly. This research demonstrated the dominant effect of liquid phase in the two-phase gas-liquid flow. Despande *et al.* (1991) experimented on heat transfer in two-phase air-water mixture in horizontal pipes concentrating on plug-slug flow. Tubes with two different inside diameter were employed (0.028 and 0.057 m) and the test section was electrically heated. Velocity range was 0.2 -1.11 m/s for water and 0-3.6 m/s for air and the flow regime was plug-slug flow. Two-phase heat transfer coefficient was measured at the top and

bottom of the pipe and it was observed that the value of h_{TP} at the top was always greater than the bottom. It was reported that the velocity of the mixture and the slug flow hydrodynamic parameters such as frequency and liquid slug to total slug length ratio were important factors in heat transfer. Increasing liquid velocity increased both h_{TPT} and h_{TPB}, increasing gas velocity increased h_{TPB} but had little impact on h_{TPT}. The authors also reported increase in the slug frequency with the increase of superficial liquid velocity (V_{SL}) and initial decrease and subsequent increase in slug frequency with increase of superficial gas velocity (V_{SG}). Increase in the tube diameter decreased slug frequency for similar flow condition. The authors proposed three separate correlations for predicting h_{TPT}, h_{TPB} and mean h_{TP}. The correlation predicted 93.5% of the data points within ±10% for h_{TPB} and mean h_{TP}, while 90% within ±15%. The proposed correlations are:

$$h_{TPB} = 0.023(\frac{k}{D})Re_L{}^{0.83}Pr_L{}^{0.4}(\frac{V_{SL}}{V_m} - 0.1)^{0.3} \tag{2.16}$$

$$h_{TPT} = 1.93(\frac{k}{D})Re_m{}^{0.44}Pr_m{}^{0.4}(\frac{V_{SL}}{V_m})^{0.21}(\frac{V_{SL}v}{g})^{0.53} \tag{2.17}$$

$$h_{TP} = 0.023(\frac{k}{D})Re_m{}^{0.83}Pr_m{}^{0.4}(\frac{V_{SL}}{V_m})^{0.76} \tag{2.18}$$

where,

$$Re_L = \frac{DV_m\rho_L}{\mu_L}, Re_m = \frac{DV_m\rho_m}{\mu_m}, V_m = V_{SL} + V_{SG}$$

$$and, \vartheta = 0.0434[\left(\frac{V_{SL}}{V_m}\right)\left(\frac{2.02}{D} + \frac{V_m{}^2}{gD}\right)]^{1.02}$$

Hetsroni *et al.* (1998 a,b) performed experiment on horizontal and near horizontal flow (2^o and 5^o) with air-water mixture in the intermittent flow regime and developed a physical model to predict heat transfer in inclined flow by relating flow parameters such as superficial liquid velocity (u_{SL}), bubble length (L_b), bubble velocity (u_b) and bubble frequency (f_b). The setup was

heated electrically and the infrared thermographs were used to obtain thermal pattern on the heated wall and heat transfer coefficient. The tube had an inner diameter of 49.2 mm and *L/D* ratio of 3.6. Hestroni *et al.* (2003) reported as much as 10 times increase in the heat transfer coefficient in annular regime at 8^o inclination compared to single phase air flow. The following heat transfer correlation was proposed:

$$h_{TP} = 0.15\ (h_{TP})_{\varphi} + 0.85 h_L \tag{2.19}$$

where φ <0.3, for 0.9<Fr_L<2.0 and 0.03 < Fr_G<0.43 and $(h_{TP})_{\varphi}$ and h_L are determined using

$$(h_{TP})_{\varphi} = h_L[\ 0.40 + 0.54 {Fr_L}^{1.2} \exp\left(-\frac{f_b L_b}{u_b}\right)]$$

$$h_L = 0.0155\ (k/D) Re^{0.83} {Pr_L}^{0.5}$$

Some authors adopted a more robust approach and proposed correlation for prediction of heat transfer which can also take in account the effect of flow pattern and inclination for different gas-liquid combination. Kim and Ghajar (2002) performed experiments on two-phase heat transfer coefficient in horizontal tube with air-water mixture in uniform heat flux condition and based on the 150 two-phase heat transfer measurements proposed a general form of a correlation which can predict heat transfer at different flow regime with root mean square error of 12%. The correlation comes with different sets of exponent value for each flow regime. The range of the superficial gas and liquid Reynolds number is 640 to 35,500 and 40 to 21,200, respectively. The proposed correlation is:

$$\frac{h_{TP}}{h_L} = (1-\alpha)\left\{1 + C\left[\left(\frac{x}{1-x}\right)^m \left(\frac{\alpha}{1-\alpha}\right)^n \left(\frac{Pr_G}{Pr_L}\right)^p \left(\frac{\mu_G}{\mu_w}\right)^q\right]\right\} \tag{2.20}$$

The value of the exponents for slug and slug transition flow C = 2.86, m = 0.42, n = 0.35, p = 0.66, and q = −0.72,

For wavy-annular flow C = 1.58, m = 1.40, n = 0.54, p = −1.93, and q = −0.09,

For wavy flow, C = 27.89, m = 3.10, n = −4.44, p = −9.65, and q = 1.56.

h_L is determined by the Sieder and Tate (1936) equation.

Tang and Ghajar (2007) performed two-phase heat transfer measurement for air-water mixture in horizontal and near horizontal upward flow (2°, 5°, and 7°) with uniform heat flux condition with *L/D* ratio of 95. This is one of the important works in the literature which focuses on the inclined flow and its effect on the heat transfer. The range of the superficial liquid and gas Reynolds number were 740 to 26000 and 560 to 48000, respectively. The authors reported the heat transfer coefficient in air-water mixture increased when the pipe is inclined from horizontal to 5^o. Within Re_{SL} range of 800 to 5000, 33-38% increase in mean h_{TP} was observed in the slug, slug way and wavy annular region. When the pipe is inclined more the effect is reduced. Based on the 763 data points collected Tang and Ghajar (2007) proposed a robust correlation which can predict heat transfer for different flow regime and at different inclination. The correlation used two important factors, inclination factor (I) and flow pattern factor (F_p) (introduced by Ghajar and Kim (2005)), to take in account the effect of flow pattern and inclination. The proposed correlation:

$$\frac{h_{TP}}{h_L} = F_P\left\{1 + 0.55\left[\left(\frac{x}{1-x}\right)^{0.1}\left(\frac{1-F_P}{F_P}\right)^{0.4}\left(\frac{Pr_G}{Pr_L}\right)^{0.25}\left(\frac{\mu_L}{\mu_w}\right)^{0.25} I^{0.25}\right]\right\} \tag{2.21}$$

where,

$$F_P = (1-\alpha) + \alpha\left[\frac{2}{\pi}\left(\tan^{-1}\sqrt{\left(\frac{\rho_G\,(V_G - V_L)^2}{gD(\rho_L - \rho_G)}\right)}\right)\right]^2$$

$$I = 1 + \frac{[(\rho_L - \rho_G)gD^2|\sin\theta|]}{\sigma}$$

and, h_L is from Sieder and Tate (1936).

The correlation predicted 100% of the data within ±30% when Spedding and Chen (1984) correlation was used for measuring void fraction.

2.2 Pressure Drop and Heat Transfer Relationship Based Correlations

Johson and Abou-Sabe (1952) performed one of the earlier investigations on isothermal pressure drop and heat transfer coefficient relationship in two-phase air-water mixture flow in horizontal pipe. Experimental setup consisted of brass pipe of 25.4 mm inner diameter and 4.57 m length with uniform wall temperature condition designed by stream heating. Several thermocouples were used to monitor variation of tube wall temperature and despite the steam heating system the authors reported variation in the wall temperature. Considerable increase in the heat transfer was observed by the authors when gas phase was introduced in the flow. Based on their experimental measurement Johnson and Abou-Sabe (1952) formulated a correlation using the liquid pressure drop multiplier (φ_L):

$$\frac{h_{TP}}{h_L} = \frac{{Re_L}^{-0.5}}{1+0.006{Re_{SG}}^{0.5}}({\varphi_L}^2)^{0.33} \tag{2.22}$$

where h_L can be determined using

$$h_L = 0.023(k/D){Re_{SG}}^{0.8}{Pr_L}^{0.4}$$

King (1952) expanded the work of Johnson and Abou-Sabe (1952) and focused on the relationship between non-isothermal pressure drop and heat transfer by experimentation and proposed a correlation for predicting heat transfer data which was an improved modified version of Johnson and Abou-Sabe (1952) correlation. The author used air-water mixture as two-phase flow in a horizontal setup with copper tube with inner diameter 18.7 mm. The proposed correlation was:

$$\frac{h_{TP}}{h_L} = \frac{{Re_L}^{-0.52}}{1+0.025{Re_{SG}}^{0.5}}({\varphi_L}^2)^{0.32} \tag{2.23}$$

where h_L can be determined using

$$h_L=0.023(k/D)Re_{SG}^{0.8}Pr_L^{0.4}$$

Some of the authors focused more on particular flow regime like Fried (1954), Oliver and Wright (1964), Pletcher and McManus (1968) etc. Fried (1954) performed heat transfer and pressure drop experiments for air-water mixture flow in horizontal plug-slug flow regime with 0.019 m diameter pipe and 4.72 m length in constant temperature condition with stream heating system. The range of flow rates were 0.126 – 1.64 kg/s for water and 0.0012 to 0.026 kg/s for air. Fried (1954) also reported variation in circumferential temperature like Johnson and Abou-Sabe (1952). The author correlated the heat transfer data within ±30% by plotting the ratio of two-phase heat transfer coefficient (h_{TP}) and single phase heat transfer coefficient (h_L) against the ratio of two-phase frictional pressure drop ($(\frac{dp}{dz})_{f,TP}$) and single liquid phase pressure drop($\left(\frac{dp}{dz}\right)_{f,L}$). Oliver and Wright (1964) studied heat transfer and pressure drop in two phase gas-liquid flow in horizontal tubes with two different lengths (1.22 and 1.31 m) and similar diameter (12.7 mm) at constant temperature using water jacket. The authors observed higher heat transfer rate in the two-phase slug flow compared to single-phase flow. The maximum heat transfer was obtained when the liquid hold up was in the range of 0.3-0.5. The authors proposed a correlation for Newtonian fluid which was

$$Nu_{TP} = Nu_L(\frac{1.2}{Re_L^{0.36}} - \frac{0.2}{Re_L}) \quad (2.24)$$

where Nu_L is determined by

$$Nu_L = 1.615[\frac{(Q_G+Q_L)\rho D}{A\mu} Pr_L \frac{D}{L}]^{0.33} \left(\frac{\mu_b}{\mu_w}\right)^{0.14}$$

Pletcher and McManus (1968) studied plug-slug and annular flow heat transfer and pressure drop in constant heat flux two-phase air-water flow in horizontal setup with 0.025 m pipe diameter and 1.52 m pipe length and electrical heating. The flow rate range was 1.94 to 10.4 kg/min for water and 0.816 to 7 kg/min for air. Measurements were made for circumferential temperature variation and, both local and mean two-phase heat transfer coefficient. In the given condition, the authors observed substantial variation in the circumferential temperature at low air flow rate creating difference in the heat transfer coefficient value at top and bottom. The measured heat transfer coefficient values agreed within ±20% by correlating with Lockhart-Martinelli parameter (X) (introduced by Lockhart and Martinelli (1949)) through $X\,(\dot{m}_G/\dot{m}_L)^{0.4}$

One of the most effective and simple correlation relating heat transfer and isothermal pressure drop was proposed by Vijay (1978) who performed experiments in a vertical tube and proposed a correlation based on relationship between mean two phase heat transfer coefficient and frictional coefficient by adopting the same principle as applied by Fried (1954) to establish relationship between local heat transfer coefficient and frictional pressure drop in horizontal air-water flow through Spalding (l964) theory. The proposed correlation was:

$$\frac{h_{TP}}{h_L} = p(\varphi_L{}^2)^q . Re_{SL}{}^r \tag{2.25}$$

where, p = 1.811, q = 0.385, r = -0.05.

Later, a modified version of the correlation was proposed by Vijay *et al.* (1982)

$$\frac{h_{TP}}{h_L} = \left(\frac{(\frac{dp}{dz})_{f,TP}}{(\frac{dp}{dz})_{f,L}}\right)^{0.451} \tag{2.26}$$

$$h_L = 1.615\left(\frac{k}{D}\right)\left(Re_{SL}Pr_L\ \frac{D}{L}\right)^{\frac{1}{3}}\left(\frac{\mu_b}{\mu_w}\right)^{0.14} \qquad \text{(Laminar)}$$

$$h_L = 0.0155\ \left(\frac{k}{D}\right)Re_{SL}{}^{0.83}\,Pr_L{}^{0.5}\left(\frac{\mu_b}{\mu_w}\right)^{0.33} \qquad \text{(Turbulent)}$$

The correlation predicted 84% of the total 2275 data points within ±50%. However, he mentioned that the accuracy of the correlation for other fluid combinations except for glycerin-air data suffers significantly at low flow rates due to error related with the measurement of two-phase frictional pressure drop. Tang and Ghajar (2011) proposed a more robust and mechanistic heat transfer correlation based on the relationship between heat transfer and friction factor by applying Reynolds analogy. The experiment was conducted with air-water mixture in horizontal, near horizontal (2^o, 5^o and 7^o) and vertical upward flow. The stainless steel test section had 27.9 mm length with *L/D* = 95. Both pressure drop and two-phase heat transfer coefficient was measured. The correlation was derived by taking in account the flow pattern factor. The proposed correlation was of the following form:

$$\frac{h_{TP}}{h_L} = (\varphi_L)^{0.20}\ {F_P}^{0.5}(\frac{\rho_L}{\rho_{TP}})^{0.5}(\frac{\dot{m}_L}{\dot{m}}) \tag{2.27}$$

where flow pattern factor is given by

$$F_P = (1-\alpha) + \ \alpha[\frac{2}{\pi}(\tan^{-1}\sqrt{(\frac{\rho_G\,(V_G-V_L)^2}{gD(\rho_L-\rho_G)})}]^2$$

and h_L is calculated using Sieder and Tate (1936).

Among total 637 points the correlation predicted 87% within ±30% agreement.

In downward inclination, very few works are available in the literature for such cases. Mollamahmutoglu (2012) investigated two-phase non-boiling heat transfer in air-water mixture for vertical downward flow through circular tube with 0.01252 m diameter. The author reported an increase in the heat transfer in the downward two-phase flow compared to single phase flow. Comparison was also drawn between vertical upward and downward inclination and heat transfer in upward flow is found to be more than downward flow, especially at low flow rates of gas and liquid. Based on this work, Bhagwat *et al.* (2012) proposed a simple correlation based on

Reynolds analogy for predicting heat transfer in vertical downward flow. The proposed correlation was:

$$\frac{h_{TP}}{h_L} = \left(\frac{\left(\frac{dp}{dz}\right)_{f,TP}}{\left(\frac{dp}{dz}\right)_{f,L}}\right)^{0.55} \tag{2.28}$$

where h_L is from Sieder and Tate (1936).

The proposed correlation predicted 100% of the collected 47, 36 and 25 data points within ±30% in bubbly, annular and froth flow pattern, respectively and 94% of the 38 data points within ±30% in slug flow regime. They reported that the accuracy of the correlation suffers in the slug flow regime due to its pulsating nature. Overall, the prediction had mean error of 11.4% and standard deviation of 17.

The selected correlations which are going to be used for the performance evaluation of the current research are tabulated in Table 2.1.

Table 2.1 List of selected correlations for the heat transfer data analysis

Source	Correlations
Aggour *et al.* (1978)	$\frac{h_{TP}}{h_L} = (1-\alpha)^{-\frac{1}{3}}$ $h_L = 1.615\left(\frac{\mathrm{k}}{\mathrm{D}}\right)(Re_{SL}Pr_L\ \frac{D}{L})^{\frac{1}{3}}\left(\frac{\mu_b}{\mu_w}\right)^{0.14}$ (L) $\frac{h_{TP}}{h_L} = (1-\alpha)^{-0.83}$ $h_L = 0.0155\left(\frac{k}{D}\right)Re_{SL}^{0.83}Pr_L^{0.5}\left(\frac{\mu_b}{\mu_w}\right)^{0.33}$ (T)
Bhagwat *et al.* (2013)	$\frac{h_{TP}}{h_L} = \left(\frac{\left(\frac{dp}{dz}\right)_{f,TP}}{\left(\frac{dp}{dz}\right)_{f,L}}\right)^{0.55}$ h_L is from Sieder & Tate (1936)

Chu and Jones (1980)	$Nu_{TP} = 0.43 {Re_{SL}}^{0.55} {Pr_L}^{0.33} (\frac{\mu_b}{\mu_w})^{0.14} (\frac{Pa}{P})^{0.17}$
Dorresteijn (1970)	$\frac{h_{TP}}{h_L} = (1-\alpha)^{-0.33}$ (L) $\frac{h_{TP}}{h_L} = (1-\alpha)^{-0.8}$ $h_L = 0.0123\, {Re_{SL}}^{0.9} {Pr_L}^{0.33} \left(\frac{\mu_b}{\mu_w}\right)^{0.14} (\frac{k}{D})$ (T)
Drucker *et al.* (1984)	$\frac{h_{TP}}{h_L} = 1 + 2.5\, (\frac{\alpha Gr}{{Re_{TP}}^2})^{0.5}$ $Gr = \frac{(\rho_L - \rho_G) g D^3}{\rho_L {v_L}^2}$
Khoze *et al.* (1976)	$Nu_{TP} = 0.26\, {Re_{SG}}^{0.2} {Re_{SL}}^{0.55} {Pr_L}^{0.4}$
Kim *et al.* (2000)	$\frac{h_{TP}}{h_L} = (1-\alpha)\left\{1 + 0.27\left[\left(\frac{x}{1-x}\right)^{-0.04} \left(\frac{\alpha}{1-\alpha}\right)^{1.21} \left(\frac{Pr_G}{Pr_L}\right)^{0.66} (\frac{\mu_G}{\mu_w})^{-0.72}\right]\right\}$
Knott *et al.* (1959)	$\frac{h_{TP}}{h_L} = (1 + \frac{V_{SG}}{V_{SL}})^{\frac{1}{3}}$ $h_L = 1.86(\frac{\mathrm{k}}{\mathrm{D}})(Re_{SL} Pr_L \frac{D}{L})^{\frac{1}{3}} (\frac{\mu_b}{\mu_w})^{0.14}$
Martin and Sims (1971)	$\frac{h_{TP}}{h_L} = 1 + 0.64(\frac{V_{SG}}{V_{SL}})^{\frac{1}{2}}$ where h_L is from Sieder and Tate (1936)
Oshinowo *et al.* (1984)	$Nu_{TP} = 1.2 {Re_{SL}}^{0.6} {Pr_L}^{0.33} (\frac{\mu_b}{\mu_w})^{0.14} (\frac{\mu_G}{\mu_L})^{0.2} (\frac{V_{SG}}{V_{SL}})^{0.1}$
Ravipudi and Godbold (1978)	$Nu_{TP} = 0.56 {Re_{SL}}^{0.6} {Pr_L}^{0.33} (\frac{\mu_b}{\mu_w})^{0.14} (\frac{\mu_G}{\mu_w})^{0.2} (\frac{V_{SG}}{V_{SL}})^{0.3}$

Rezkallah and Sims (1987)	$\frac{h_{TP}}{h_L} = (1-\alpha)^{-0.9}$ where h_L is from Sieder and Tate (1936)
Shah(1981)	$\frac{h_{TP}}{h_L} = (1+\frac{V_{SG}}{V_{SL}})^{\frac{1}{4}}$ $h_L = 1.86(\frac{k}{D})(Re_{SL}Pr_L\ \frac{D}{L})^{\frac{1}{3}}(\frac{\mu_b}{\mu_w})^{0.14}$ (L) $h_L = 0.023(\frac{k}{D})Re_{SL}^{0.8}\ Pr_L^{0.4}(\frac{\mu_b}{\mu_w})^{0.14}$ (T)
Tang and Ghajar (2007)	$\frac{h_{TP}}{h_L} = F_P\left\{1+0.55\left[\left(\frac{x}{1-x}\right)^{0.1}\left(\frac{1-F_P}{F_P}\right)^{0.4}\left(\frac{Pr_G}{Pr_L}\right)^{0.25}(\frac{\mu_L}{\mu_w})^{0.25}I^{0.25}\right]\right\}$ $F_P = (1-\alpha) + \alpha[\frac{2}{\pi}(\tan^{-1}\sqrt{(\frac{\rho_{G\,(V_G-V_L)^2}}{gD(\rho_L-\rho_G)})}]^2$ $I = 1+\frac{[(\rho_L-\rho_G)gD^2\lvert\sin\theta\rvert]}{\sigma}$ where h_L is from Sieder and Tate (1936)
Tang and Ghajar (2011)	$\frac{h_{TP}}{h_L} = (\varphi_L)^{0.20}F_P^{0.5}(\frac{\rho_L}{\rho_{TP}})^{0.5}(\frac{\dot{m}_L}{\dot{m}})$ $F_P = (1-\alpha) + \alpha[\frac{2}{\pi}(\tan^{-1}\sqrt{(\frac{\rho_{G\,(V_G-V_L)^2}}{gD(\rho_L-\rho_G)})}]^2$ where h_L is from Sieder and Tate (1936)
Vijay *et al.* (1982)	$\frac{h_{TP}}{h_L} = (\frac{(\frac{dp}{dz})_{f,TP}}{(\frac{dp}{dz})_{f,L}})^{0.451}$ $h_L = 1.615(\frac{k}{D})(Re_{SL}Pr_L\ \frac{D}{L})^{\frac{1}{3}}(\frac{\mu_b}{\mu_w})^{0.14}$ (L) $h_L = 0.0155(\frac{k}{D})Re_{SL}^{0.83}\ Pr_L^{0.5}(\frac{\mu_b}{\mu_w})^{0.33}$ (T)

CHAPTER III

EXPERIMENTAL SETUP

In this section, different parts of the test setup including the flow connections and instrumentations are going to be discussed in details along with the test procedures which are required to ensure the repeatability from the experiment. The current experimental has been designed originally by Cook (2008). The test section consists of two branches, one for the measurement of heat transfer and non-isothermal pressure drop using rough pipe and the other section for the measurement of pressure drop, flow visualization and void fraction in smooth pipe. As this experiment involves mainly heat transfer, main components which are relevant to the heated test section will be primarily discussed in the following sections.

3.1 Details of Experimental Setup

The circuit diagram of the experimental setup is illustrated with its different components and connections in Figure 3.1 and photograph of the heat transfer test section is presented in Figure 3.2. The main parts of the setup are discussed below.

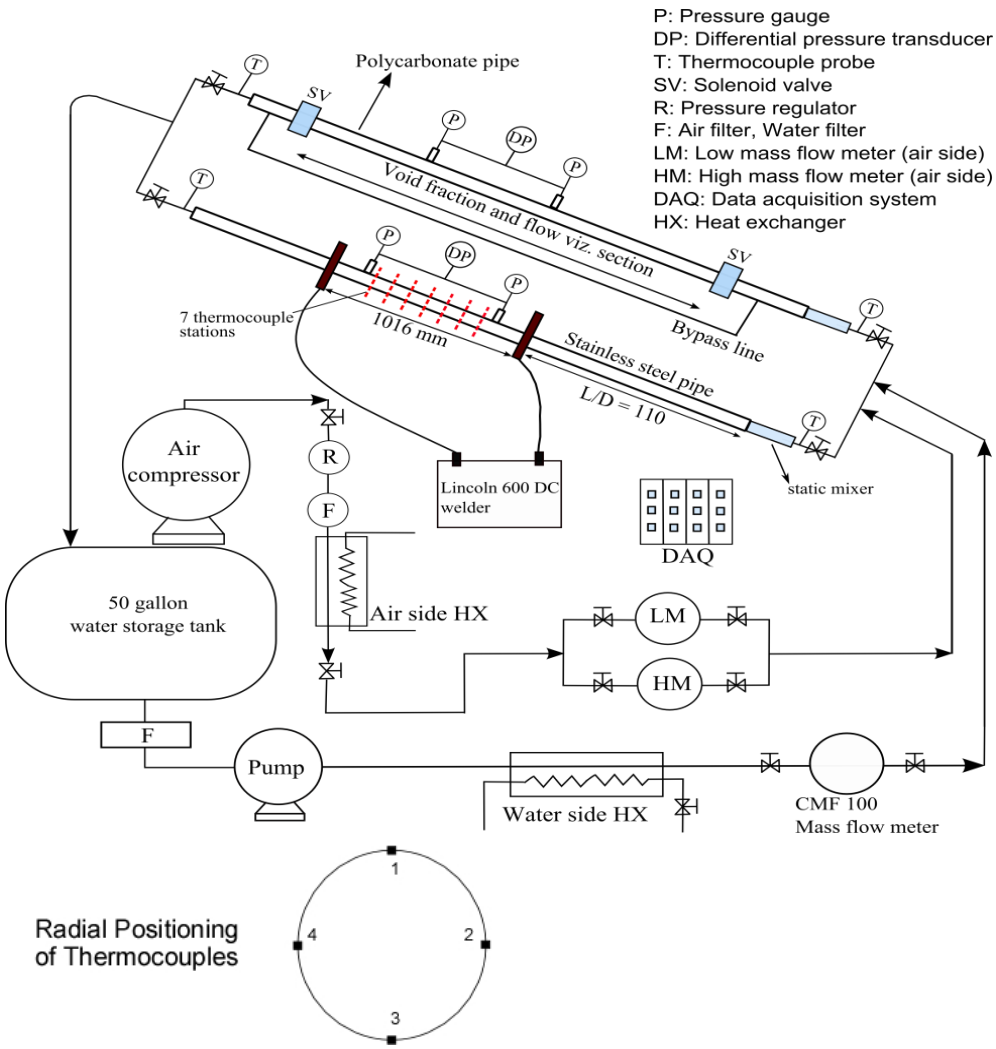

Figure 3.1 Experimental setup circuit diagram

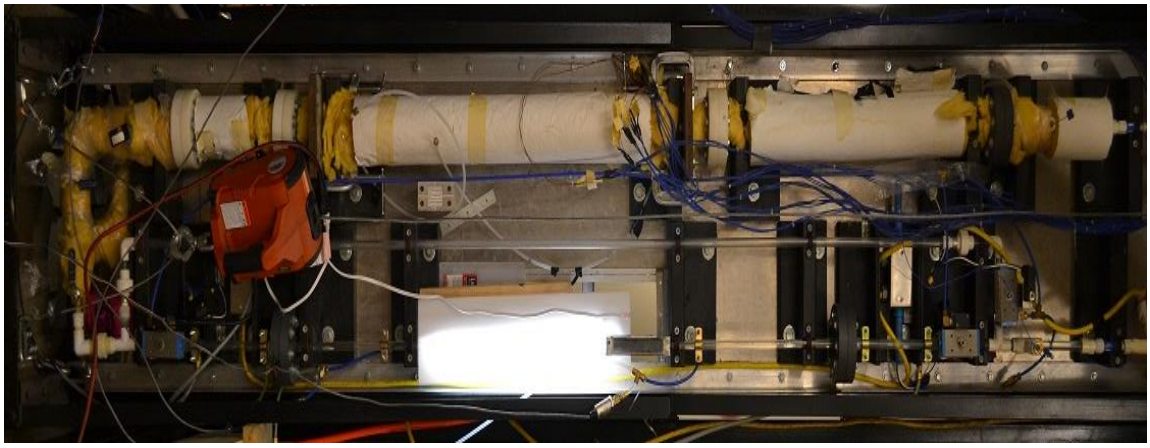

Figure 3.2 Experimental setup

***Mixing Section*:** The purpose of the mixing section is to agitate the air-water mixture so that the mixture temperature is uniform and an accurate measurement of the mixture temperature can be performed by the thermocouple probe. Two mixers are installed at the entry and exit of the test section. The inlet mixer is Koflo 3-vane static mixer Model 3/8-40C-4-3V-2 which makes sure air-water is mixed well before temperature measurement takes place. The outlet mixer is a Koflo ½-80-4C-3-2 which mixes the hot outlet water exiting the test section to prevent loss of integrity of the experiment.

Heated Test Section: A schematic of the heated test section is provided in Figure 3.1. The test section consists of a 12.5 mm I.D. schedule 10 S steel pipe with a length of 1.016 m with 0.0152 mm roughness. The setup also consists of a 12.67 mm I.D. transparent polycarbonate pipe that can be used for flow visualization and measurement of void fraction and pressure drop. *L/D* ratio of the heated section is 110. High amperage current (*I*) is passed through the test section to heat it which is supplied by Lincoln DC-600 welder. Uniform heat flux ($\dot{q}''$) which can be provided by the welder is in a range of 7500 W/m^2 to 57,000 W/m^2 with highest current supply capability of 750 Amp. 17.8 cm by 17.8 cm Copper plates with 6.35 mm thickness is soldered at both end of the test section for the purpose of heating. The plates encircle the test section and make sure even distribution of current is achieved around the circumference. Plates are attached with 1.27 cm thick phenolic resin board at the end in order to prevent heat loss from the heated to unheated section of the setup. Current is supplied from the welder to the plate through 4/0 AWG welding cable. In order to prevent heat loss to the surrounding a 0.076 m (3 in.) thick Micro-Lok Fiber Glass insulation with thermal conductivity of 0.042 W/m^{o}C is used as insulation. The remaining test section is insulated with three layers of Thermwell Fiber-Glass Pipe Insulation Wrap with each layer with *R*-value of 1.6. Pressure taps are installed at both end of the test section to measure non-isothermal pressure drop. The distance between the pressure taps is 88.9 cm and they are placed 12.7 cm (5 in.) from the inlet and outlet of the test section. Pressure taps are kept

in relatively large gap to produce large pressure drops. Pressure taps are connected with the Validyne pressure transducer through ¼ inch nominal Teflon tubing.

Thermocouple Array: Thermocouple probes and thermocouples are used at the inlet, exit and along the length of the pipe at particular interval to measure the temperature. The accuracy of the thermocouple is greater of either $\pm 1^{o}$C or ±0.75% of the measured temperature with a range of -250^{o}C to 350^{o}C. The CO1-T type thermocouples are used to measure wall temperatures at seven different stations spaced 127 mm apart along the pipe length. These thermocouples are protected by two thin layers of phenolic resin providing protection from outside disturbance.

The arrangement of the thermocouples along the circumference is shown in Figure 3.1. The thermocouple probes (TMQSS-06U-6) which are used to measure temperature at the pipe inlet ($T_{in,b}$) and outlet ($T_{out,b}$) are inserted inside through pipe wall till it almost touched the other end of the pipe wall in order to ensure that the probes are always in contact with the two phase mixture. Thermocouples and thermocouple probes are connected with the data acquisition system through 6.1 m lengths of Omega 24 gauge Type T thermocouple wire (EXIT-T-24-SLE).

Water Transport System: Water and air is used as the working fluid in the current experiment. Reverse osmosis process is used to filter the water by the Chemistry Department at Oklahoma State University. In the laboratory, the water is stored in a 208.2 L (55 gal) polyethylene cylindrical reservoir. Water is transported in the system through a closed system. A Bell and Gosset series Coupled Centrifugal Pump (Model 3545 D10) is used for pumping the water from the reservoir to the system. The pump can achieve as much as 0.226 kg/s (30 lbm/min) mass flow rate when supplying water to individual test section. After pumping, the water is purified by an Aqua-Pure AP12T water purification system. The purifier helps to separate any unwanted object or prevent growth of organics which might be introduced into the system. The paper filters can trap objects as small as 20μm (7.87E-04 in). The maximum operating temperature and pressure

are 38^{o}C (100^{o}F) and 862 kPa (125psi), respectively. In order to remove organic impurities the water is filtered through a bypass line with small Oberdorfer Model 600 F13 pump and Bio Logic-1.5 UV filter once a week. An ITT Standard model BCF 4063 one shell and two-tube pass heat exchanger is used in the water cycle in order to maintain the desired temperature required for the experiments. It has an area of 1.97 m^2 (12.2 ft^3) and a maximum duty of 19.7 kW (18.67 Btu/s). In heat transfer experiment, the heat exchanger helps to regulate the temperature of the water which gets heated up every time it passes through the system. It's also very useful during summer season to cool down the inlet temperature which gets too high due to ambient temperature. The temperature of the cooling water, which is collected from the tap, might show seasonal variation between 18^{o}C (64.4^{o}F) and 26^{o}C (78.8^{o}F). After passing through the heat exchanger, the water flows through one of the two Coriolis flow meters before it reaches the gate valve which regulates the flow rate to the system. After that, the water is mixed with the air and returns to the 208.2 L (55 gal) reservoir after it passes through the test section through return line. Air is released from the reservoir through a curved vent on its upper surface.

Air Transport System: The air is supplied to the system by a large industrial compressor (Ingersoll-Rand T30 Model 2545) located in outbuilding adjacent to the lab. Due to high noise and heat generation it was necessary to install it outside. The compressor has maximum pressure and flow rate capacity of 862 kPa (125 psi) and 0.25 kg/min (0.55 lbm/min), respectively. The air from compressor goes through a 1379 kPa (200 psi) regulator/filter-drier assembly. The air pressure can be regulated from this point before it goes to the flow meter. The filter-drier removes unwanted objects and condensed water which might be produced by the compressor. The filtered air then passes through copper coil submerged in a pool of running water supplied from the tap which cools the air due to compression and outside temperature. After passing through the simple heat exchanger the air achieves almost similar temperature as the inlet water. This air is again passed through a filter-drier assembly before it reaches the Parker Model 24NS 82(A)-V8LN-SS

Needle valve, used for controlling the flow rate. The metering valve provides fine air mass flow rate adjustment through system of ¼ inch turn ball valves. After passing through one of the Coriolis flow meters the air is mixed with water in static mixture and enters the test section. After it exits the test section, it is carried back to the water reservoir and removed from the system.

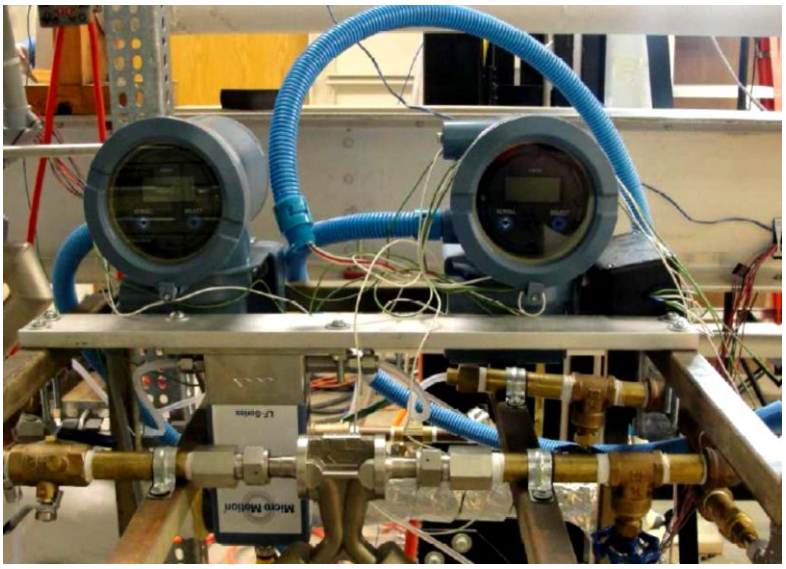

Figure 3.3 Coriolis flow meters

Coriolis Flow Meters: Two Micro Motion meters with accuracy of ±0.05% liquid flow rate and ±0.20% of the gas flow rate which is shown in Figure 3.3. The liquid flow meter (Model CMF100) can measure water flow rate ranging from 1360 kg/hr (2998 lbm/hr) to 27,200 kg/hr (59,966 lbm/hr). It uses a Micro Motion Model RFT9739 Field-Mount Transmitter to display the flow rate readings and properties and transmit the flow rate data to the data acquisition system. The other flow meter (Model CMF025) is utilized to monitor air mass flow rate. It has the capability to measure either liquid or gas flow ranging from 54 kg/hr (119 lbm/hr) to 2180 kg/hr (4806 lbm/hr). It uses Micro Motion Model 1700 transmitter to display mass flow rate readings and physical property and transmit the information to the data acquisition system.

Pressure Transducer: Pressure drop across the test section is measured using a Validyne model DP-15 pressure transducer along with a CD15 carrier demodulator. A high range of pressure drop ranging from 0.862 kPa (0.125 psi) to 1379 kPa (200 psi) can be measured by using interchangeable diaphragms with accuracies of ±0.25%. Both branches of the test section have the pressure drop measurement, in the heated section non-isothermal and in non-heated section isothermal pressure drop can be measured.

Connections to the Test Area: Air and water are transported to the testing area through flexible tubing. Standard $^{3}/_{8}$ inch nominal air compressor hose is used for air and $1^{1}/_{8}$ inch Nylon reinforced flexible clear PVC tubing is used for water transport. The same piping system is used for the return line. The air-water mixture enters the test area through ½ inch IPS plastic tee and gets divided in two branches, one leads to the void fraction / flow visualization section and other leads to the heated section. ½ inch quarter turn valves are used for controlling the flow rate to the test section. Except for a small portion at the exit area (which is made of ½ inch CPVC Schedule 80 to protect it from high heat), the rest of the piping system is constructed from ½ inch and $^{3}/_{8}$ inch PVC schedule 40.

3.2 Data Acquisition System

The data is acquired from the setup by National Instruments Data Acquisition system and saved in a CPU. There are three parts of the data acquisition system: chassis, modules and terminal blocks. All the components of the data acquisition system is housed in the chassis. The purpose of the chassis is to provide a low noise environment for the purpose of signal conditioning, power supply and circuitry control. It's AC powered and the model of the chassis is SCXI 1000. It consists of four slots for modules and accompanying terminal blocks.

Modules are connected directly with the chassis. The purpose of the module is to condition the signal. Terminal blocks are attached with the modules. Two 32 channel analog modules (SCXI 1102s) and one eight channel analog module (Model SCXI 1125) are used for taking data from the test section. The 32 channel module performs high accuracy signal conditioning of the thermocouples. They can also acquire data through millivolt, 0 to 20 mA, and 4 to 20 mA current signals. A 2 Hz low pass filter is used by each channel for the reduction of noise from the 60 Hz power source. An amplifier which is connected with each channel serves to vary the gain from 1 to 100.

The eight channel analog module is also used to gather data from the thermocouples. The module is used for isolated signal condition through its eight channels. Each channel is equipped with a low pass filter which can be fixed for either 4 Hz or 10 kHz. Each of these channels has 12 programmable gain settings with a range of 1 to 2000.

The terminal blocks provide connection between various devices which are being monitored. For the heat transfer test section, thermocouples, pressure transducer and the Coriolis flow meters are connected to the terminal blocks. The model of the 32 channel terminal block is SCXI 1303. Terminal blocks are connected with the modules. The blocks have isothermal construction which is required for high accuracy thermocouple measurement. In addition, a temperature sensor mounted on the board ensures further increase in the accuracy by cold junction compensation.

The 8 Channel module is connected through a SCXI 1313 8 Channel High Voltage Attenuator Terminal Block. This enables the terminal block to take voltage inputs up to 300 V_{rms} or ±300 VDC when used along with the SCXI 1125 module. This block is used for reading voltage and current passing through the test section.

A CPU is used for data recording and storage. A LABVIEW program, designed by National Instruments, is used for the purpose. A data acquisition program has been originally written and later modified by former PhD candidates Jae-young Kim and Clement Tang, respectively.

3.3 Experimental Procedure

Start-up procedure: Start up procedure should be followed so that the experimental setup is steady and safe before performing experiment. The first step of experimental procedure is to turn on all the electrical instruments: the National Instruments data acquisition system, the Coriolis flow meters, and Validyne CD15 carrier demodulator for the pressure transducer. After turning on the data acquisition system, the LABVIEW software is executed which displays the inlet and exit temperature along with the temperature at every thermocouple station. Comparing these initial readings with the surrounding temperature can serve as an indication of whether the thermocouples are working properly or not. In the next step, the air and water filters are checked to ensure they are working properly. After that, the water tap is turned on which is used in both water and air heat exchanger to stabilize the reservoir water and air temperature to same temperature which are going to be used for the experimental purpose in the test section. After that the centrifugal pump and air compressor are turned on to supply air-water mixture in the test section. Before data taking, the test section, delivery and return lines should checked for any leakage.

Measurement Procedure: The measurement procedure consists of a set of steps which should be followed for the purpose of properly acquiring experimental data. The steps should ensure that the collected data is reliable and repeatable. The first step is to check the electrical connections between the copper plates and, DC welder machine and data acquisition system. The wires and cables used for connection should be in proper condition. Burned cable and improper connection could create short circuit causing overheating and damage of valuable equipment. Next step is to

adjust the water and air flow rate to the desired level. The water and air flow rate can be controlled by the gate valve and needle valve respectively which has been described previously. Flow rate can be observed in the Coriolis flow meters and also in the data acquisition system. After the flow rate is fixed, the DC welder machine is turned on and the amperage is fixed at the desired level by turning the knob. The DC current passes through the test section providing the necessary heat flux to the air-water mixture.

In the next step, the water and air temperature should be allowed to reach steady state. This step is very important to obtain correct value of heat transfer coefficient. The steady state can be assumed to be achieved once the temperature measured by the inlet and exit thermocouple probe doesn't show more than $0.5^{o}C$ variation within 5 minutes. The temperature at the thermocouple stations can be monitored virtually in the LABVIEW Virtual Instrument (VI) program. It is important to ensure that temperature at none of the temperature stations achieve more than $60^{o}C$. Otherwise, the flow might not be non-boiling or local boiling can cause dry spot during experiment.

After the temperature reaches steady state, the data can be recorded by pressing 'Run' button on the LabVIEW software. The program records the water and air flow rates, inlet and outlet mixture temperature, surface temperatures at each thermocouple station, pressure drop and supplier heat flux. For each measurement, usually about thousand samples are collected.

After recording the data, the DC welder machine is turned off and the system is allowed to cool down to ambient temperature. After the test section cools down, the next reading can be taken. The heat transfer data and non-isothermal pressure drop readings are taken simultaneously in the same data file.

Data Reduction: The experimental setup measures the outside wall temperature at definite interval (as shown in Figure 3.1) in the four circumferential locations separated by $\pi/2$ radian along with the inlet and outlet bulk temperatures of the air-water mixture. The inside wall temperature which is required for the measurement of the heat transfer coefficient is not measured directly due to difficulty of measurement, rather it is calculated from the outside wall temperature and wall heat flux by using a data reduction program which has been developed by Ghajar and Kim (2006). With the help of the program, the local inside wall temperature, wall heat flux and circumferential convective heat transfer coefficient is calculated using a finite difference formulation. The two phase convective heat transfer coefficient is represented by the average of the measured local values at each station as shown in Eq. (3.1).

$$h_{TP} = \frac{1}{L}\int \bar{h}\, dz = \frac{1}{L}\sum_{j=1}^{N_{ST}} \bar{h}_j \Delta z_j \tag{3.1}$$

3.4 Validation of the Experimental Setup

Validation of the experimental setup is performed by calculating the uncertainty of single and two phase heat transfer measurements for the current experimental setup and, then comparing the single phase heat transfer coefficient measurements with several widely accepted single phase heat transfer correlations such as Sieder and Tate (1936), Gnielinski (1976) and Ghajar and Tam (1994). In this section, heat transfer uncertainties of the single phase and two phase, and comparison of heat transfer coefficients with correlations will be presented in consecutive sections.

3.4.1 Single Phase Heat Transfer Uncertainty

The uncertainties of the experimental data for single phase heat transfer coefficient are calculated using Kline and McClintock (1953) uncertainty analysis formula which is provided in Appendix

A. A Total of 19 data points are collected in single phase heat transfer in Re_L range of 1300 and 26,000. The maximum and minimum uncertainties for the data points are found to be ±12.08% and ±5.31%, respectively. At low liquid flow rates heat transfer uncertainty of single phase flow becomes maximum. The sample calculations of the best and worst run in terms of uncertainties are presented in Table A.1 and A.2, respectively in Appendix A.

3.4.2 Two Phase Heat Transfer Uncertainty

The uncertainties of the experimental data for two phase heat transfer coefficient are calculated using the same equation of Kline and McClintock (1953) as used for single phase heat transfer coefficient. Minimum and maximum uncertainty in measurements of two phase heat transfer coefficient at different pipe inclinations and for each observed flow pattern are presented in Table 3.1. Maximum uncertainties are observed for stratified flow pattern with 31.54%, 31.09% and 27.42% at -5^0, -10^0 and -20^0, respectively. Interestingly, the minimum values of uncertainties are also observed in the same flow pattern with 7.1%, 7.42% and 6.26% at -5^0, -10^0 and -20^0, respectively.

Table 3.1 Two phase heat transfer uncertainties at different flow patterns

Flow Pattern		0^0	-5^0	-10^0	-20^0
Bubbly	Max. %	12	11.3	10.7	11.1
	Min. %	10	10.3	10.3	10.8
Slug	Max. %	13	12.4	10.5	11.5
	Min. %	9	8.6	8.6	7.8
Stratified	Max. %	27	31.5	31.1	27.4
	Min. %	10	7.1	7.4	6.3
Intermittent/ Annular	Max. %	25	17.3	28.6	29
	Min. %	11	9.2	10.3	11.1

One of the probable reasons for very high values of percentage uncertainty in stratified flow might be the higher heat balance error compared to other flow patterns. In stratified flow, the heat balance error is between 8% to 16% compared to intermittent and slug region where it is around 1% to 7%. No clear trend can be established on the effect of pipe inclination on uncertainty in

measurement of two phase heat transfer coefficient. However, for slug and stratified flow, the minimum percentage uncertainty is observed to decrease with increase in the downward pipe orientation.

The sample calculations for the best and worst case of heat transfer uncertainties are presented in Table A.3 and A.4, respectively in the Appendix A.

3.4.3 Comparison of Single Phase Heat Transfer Measurements with Correlations

The validity of the single phase heat transfer data is also confirmed by comparing it against three correlations, Gnielinski (1976), Ghajar and Tam (1994) and, Sieder and Tate (1936) which are described in Table 3.2. 11 data points in the Re_L range of 6000 to 23,000 are compared with these correlations. As shown in Figure 3.4, the measured single phase heat transfer coefficients are found to be within ±10% of the predicted values by Sieder and Tate (1936). The average and maximum deviation in measurement of single phase heat transfer coefficient with respect to the correlations of Gnielinski (1976) and Ghajar and Tam (1994) is found to be 4.8%, 14.82% and 0.86%, 3.7%, respectively.

Table 3.2 Single phase heat transfer correlations

Author	Single phase heat transfer correlations
Sieder and Tate (1936)	$Nu_L = 1.86(Re_{SL}Pr_L \frac{D}{L})^{\frac{1}{3}}$ (L) $Nu_L = 0.023Re_{SL}^{0.8}Pr_L^{0.4}(\frac{\mu_b}{\mu_W})^{0.14}$ (T)
Gnielinski (1976)	$Nu_L = \frac{\left(\frac{f}{8}\right)(Re-1000)Pr}{1+12.7(\frac{f}{8})^{0.5}(Pr^{\frac{2}{3}}-1)}$ where, $f = (0.79\ln(Re) - 1.64)^{-2}$
Ghajar and Tam (1994)	$Nu_L = 0.023Re^{0.8}Pr^{0.385}(L/D)^{-0.0054}(\mu_b/\mu_W)^{0.14}$

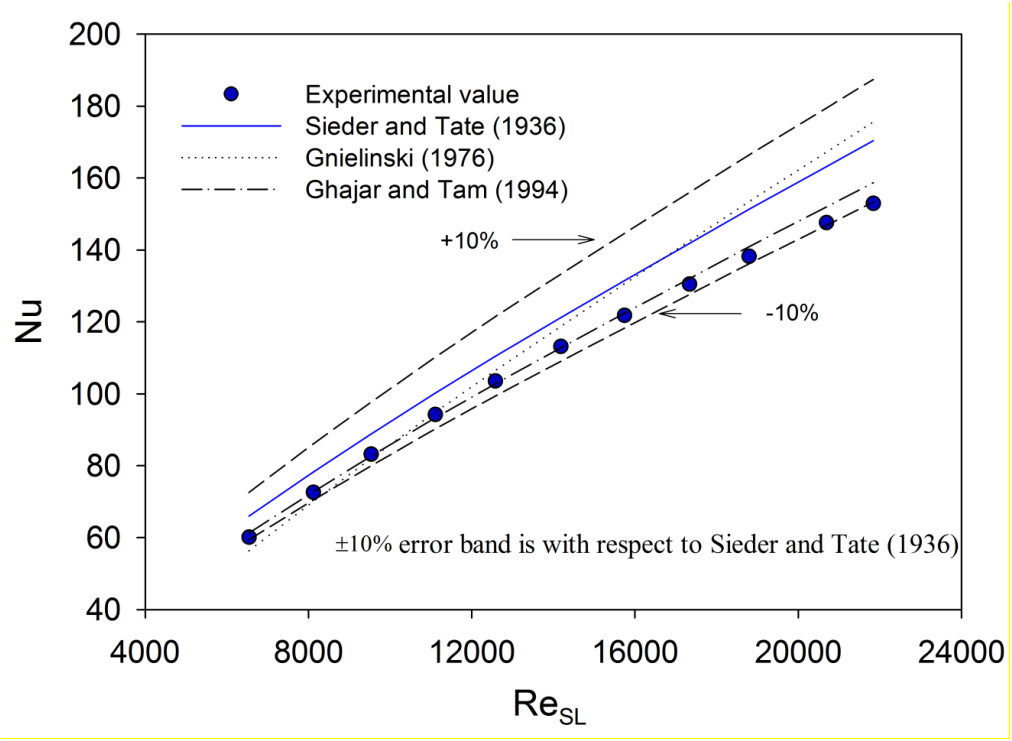

Figure 3.4 Experimental setup validation with single phase heat transfer correlation

The errors associated with the prediction of single phase heat transfer with these correlations fall well within the acceptable range of error for the measurement of single phase heat transfer data with the given range of uncertainties of the system. Hence, the comparison validates the experimental setup which is going to be used for the measurement of two phase heat transfer coefficients in the current research.

CHAPTER IV

RESULTS AND DISCUSSION

In this chapter, a detailed analysis and discussion will be performed for the experimental measurements of heat transfer coefficients which are collected at different pipe orientations. In the first section, the flow patterns which are observed in horizontal and inclined downward flow at -5^o, -10^o and -20^o are going to be discussed in details along with the flow visualization images and a combined flow map for all orientations. Then, the effect of these observed flow patterns on heat transfer will be discussed by plotting the h_{TP} values against the superficial liquid (Re_{SL}) and gas (Re_{SG}) Reynolds numbers. After that, the effect of pipe inclination on heat transfer at different downward inclinations will be discussed. Analysis of the trends of the local heat transfer coefficients at circumferential locations will also be performed for establishing deeper understanding of the physical mechanism of heat transfer at inclined flow. In the second section, the performance of the correlations which have been selected in Chapter II (Table 2.1) will be tested against the collected experimental data and recommendations will be made on the best performing correlations based on both general and Reynolds analogy based

correlations. In the final section, development of a Reynolds analogy based correlation will be performed and its performance against the collected experimental measurements will be discussed to highlight the comparative improvement of the performance of heat transfer prediction by the proposed correlation.

4.1 Flow Patterns and Flow Pattern Maps

The two phase flow literature reports that the physical structure of flow patterns is significantly influenced by the pipe orientation which further significantly affects the two phase heat transfer coefficient in gas-liquid two phase flow. The flow pattern maps are essential for the estimation of the sequence of appearance of different flow patterns with change in the gas and liquid flow rates. The definitions of flow patterns and their transitions are highly qualitative in nature and are mostly based on the individual's perception. The flow pattern map which is used for this research was constructed by Bhagwat, S. M., a PhD candidate in Dr. Ghajar's Two-phase Flow Laboratory which has also been referred by Hossainy *et al.* (2014). The key flow patterns observed in horizontal and downward inclined two phase flow are bubbly, slug, intermittent, stratified and annular flow regimes as shown in Figure 4.1. These flow patterns are generated by changing the gas and liquid flow rates (superficial gas and liquid Reynolds numbers) in a range of 0.001 kg/min to 0.2 kg/min (Re_{SG} = 200 to 19,000) and 1.5 kg/min to 12.5 kg/min (Re_{SL} = 2000 to 18,000), respectively. The superficial gas and liquid Reynolds number is defined in terms of superficial phase velocity, phase density and viscosity and pipe diameter as represented in Eq. (4.1) and Eq. (4.2). The flow visualization is carried out in transparent polycarbonate pipe using Nikon D3100 camera and 200 mm f/5.6 lens with a exposure time of 1/4000 s.

$$\mathrm{Re}_{SG} = \frac{\rho_G D V_{SG}}{\mu_G} = \frac{GxD}{\mu_G} \tag{4. 1}$$

$$\mathrm{Re}_{SL} = \frac{\rho_L D V_{SL}}{\mu_L} = \frac{G(1-x)D}{\mu_L} \qquad (4.2)$$

The bubbly flow regime is characterized by the dispersion of small bubbles in the continuous liquid medium while the slug flow is identified as a flow structure consisting of elongated gas slugs that flow alternate to a liquid plug. The stratified flow is featured by the flow of liquid film parallel to the gas phase. The annular flow is observed in form of liquid film flowing in contact with the pipe wall that surrounds a fast moving gas core. The definition of intermittent flow is vague since there is no particular way in which gas and liquid phases are aligned across the pipe cross section. In the present study, the intermittent flow pattern is identified based on the pulsating and chaotic nature of the two phase flow. Thus the flow structure tagged as intermittent flow in the present study consists of slug-wavy, stratified-wavy and annular-wavy flow patterns for moderate liquid and moderate gas flow rates, low liquid and moderate gas flow rates and low to moderate liquid and high gas flow rates, respectively.

As shown in Figure 4.1 , for all pipe orientations considered in this study, the bubbly flow exists for low gas and high liquid flow rates. At low liquid flow rates, increase in the gas flow rate causes the flow pattern to shift from stratified to intermittent and finally to annular flow. Whereas, for moderate liquid flow rates, the flow pattern shifts from slug to intermittent to annular flow as the gas flow rate is increased from low to moderate to high flow rates. It is also evident from this flow pattern map that the transition boundaries between different flow patterns with the exception of boundary between intermittent and annular flow are significantly influenced by the change in pipe orientation. It should be noted that for horizontal flow, there is no stratified flow pattern for gas mass flow rates lower than 0.01 kg/min. In Figures 4.2, 4.3 and 4.4 comparative flow visualization images of stratified, slug and intermittent regime have been presented for each inclination, respectively.

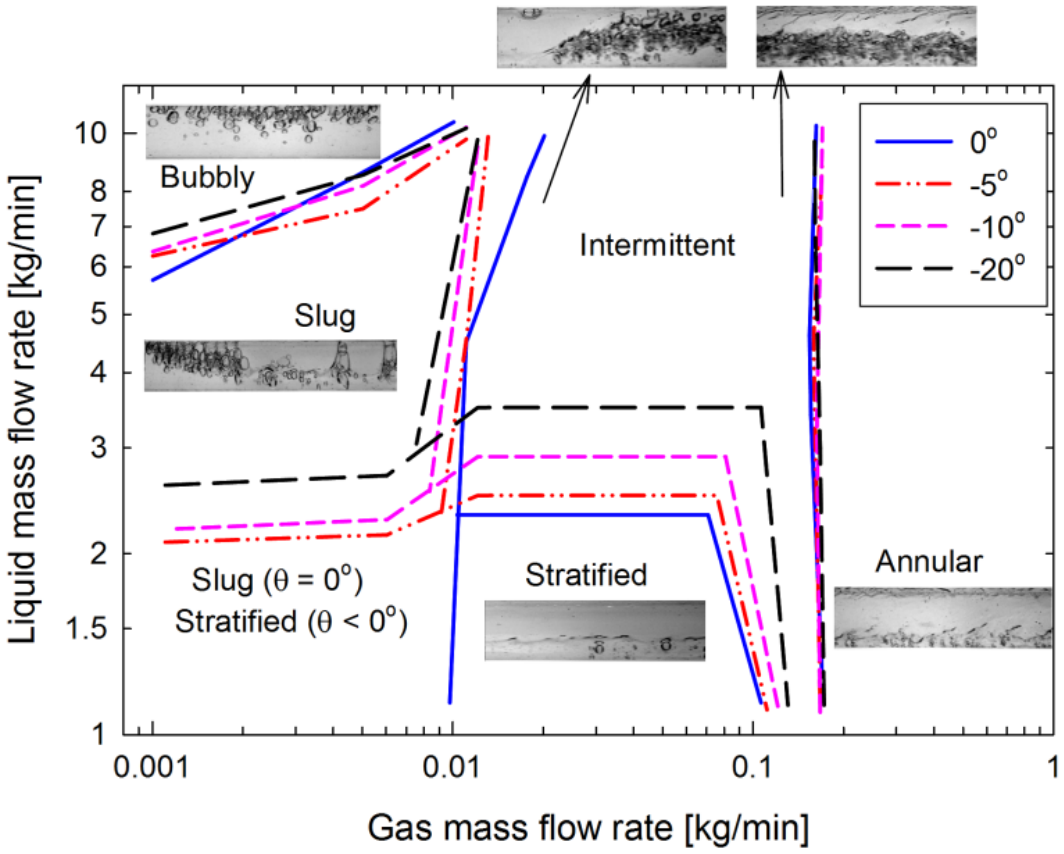

Figure 4.1 Flow regime map for horizontal and downward inclined two phase flow (Adapted from Hossainy *et al.* (2014))

In the present study, majority of the data points for the two phase heat transfer coefficient have been collected for slug, stratified and intermittent flow regimes. Although the flow patterns for similar gas and liquid superficial Reynolds number might be identical, it is important to acknowledge that the physical characteristics of these similar flow patterns may not completely be identical. For instance, the translational velocity of the slug through pipe, the thickness of liquid layer at the bottom of the pipe in the stratified flow regime, frequency of the disturbance waves in annular flow regime and intensity of turbulent mixing in the intermittent flow pattern varies as the pipe orientation is taken from horizontal to downward inclinations.

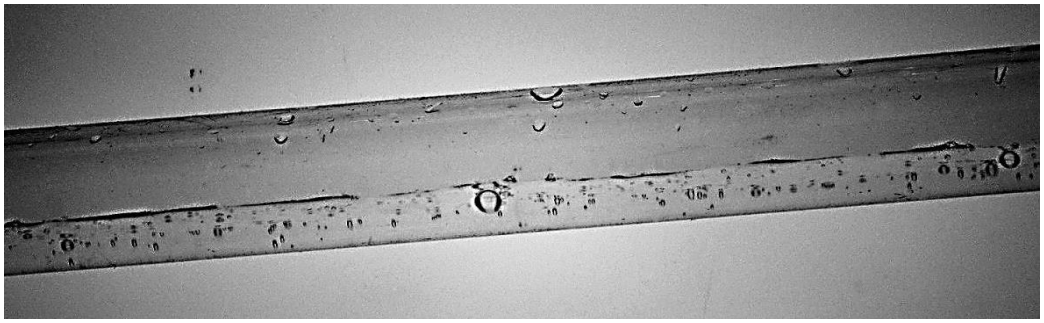

(a) -5^{o} inclined flow

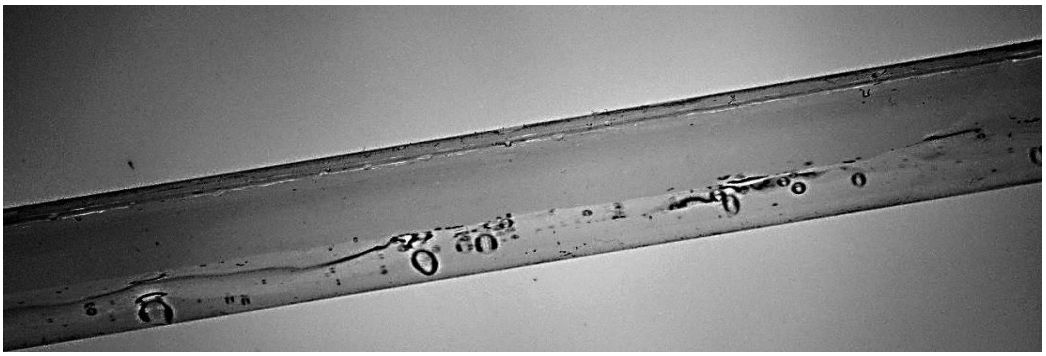

(b) -10^{o} inclined flow

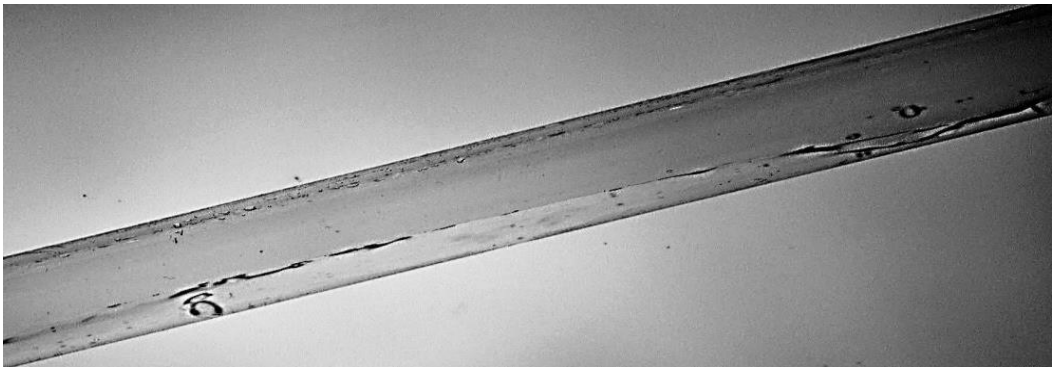

(c) -20^{o} inclined flow

Figure 4.2 Representative photographs of stratified flow for horizontal, -5^{o}, -10^{o} and-20^{o} at Re_{SL}=2600, Re_{SG}=700

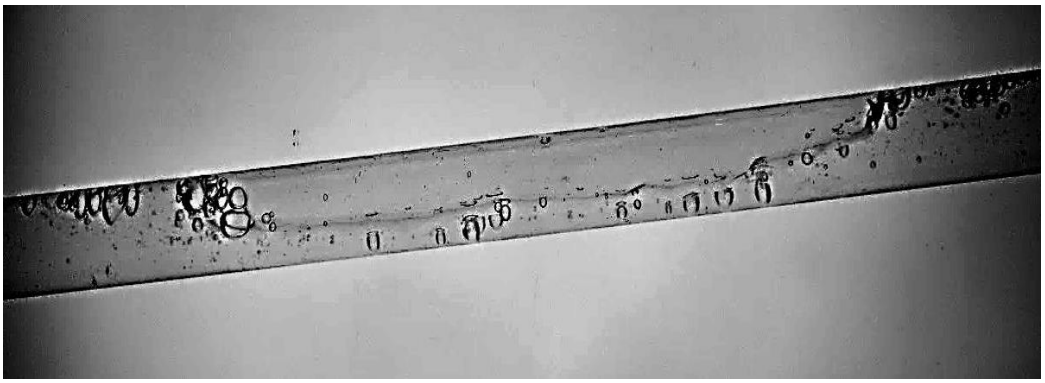

(a) -5^{o} inclined flow

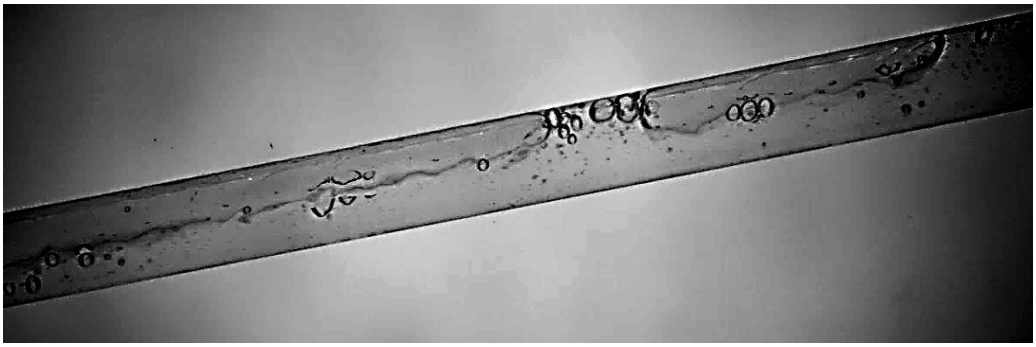

(b) -10^{o} inclined flow

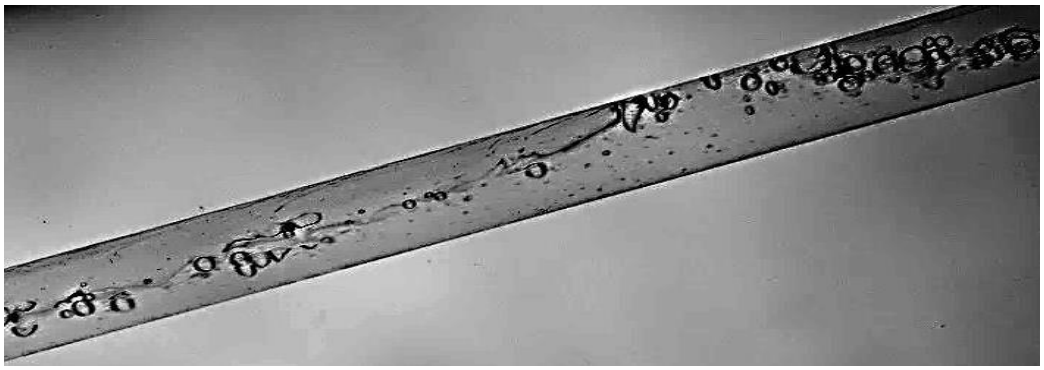

(c) -20^{o} inclined flow

Figure 4.3 Representative photographs of slug flow for horizontal, -5^{o}, -10^{o} and-20^{o} at Re_{SL}=7400, Re_{SG}=700

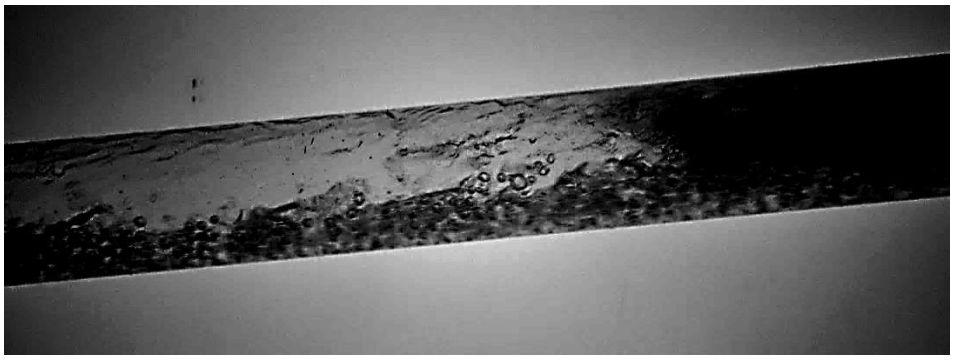

(a) -5^{o} inclined flow

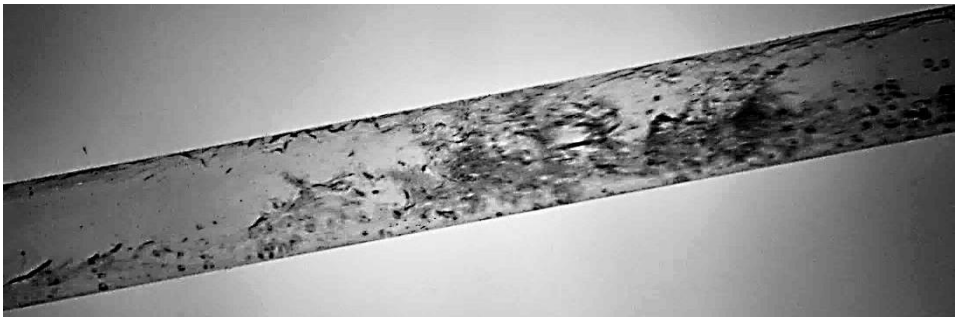

(b) -10^{o} inclined flow

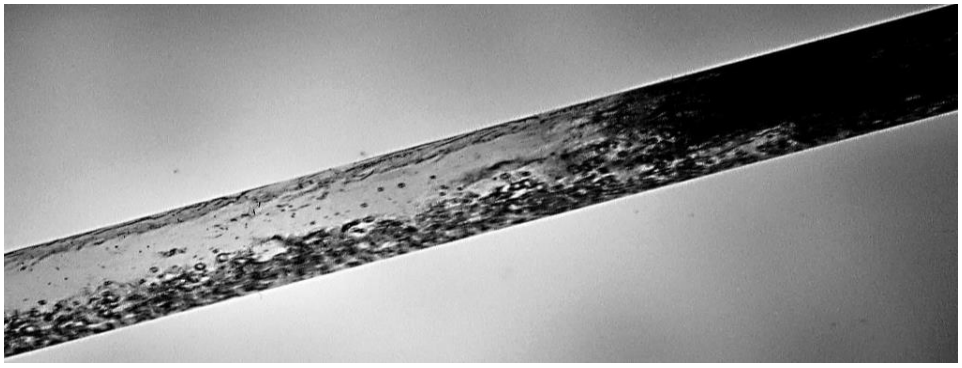

(c) -20^{o} inclined flow

Figure 4.4 Representative photographs of intermittent flow for horizontal, -5^{o}, -10^{o} and-20^{o} at Re_{SL}=12000, Re_{SG}=14000

In total 400 two phase heat transfer measurements are made at different inclinations with about 100 data points in each inclination. The number of data points for different flow patterns in each orientation is tabulated in Table 4.1. Majority of the data points are taken in the stratified, intermittent and slug flow regions. Due to limitations on the range of mass flow meters and difficulty in generating a sufficient enough temperature difference across pipe inlet and outlet, only few data points could be measured in bubbly and annular flow regimes.

Table 4.1 Number of data points in different flow patterns at different pipe inclinations

Flow pattern	**0^o**	**-5^o**	**-10^o**	**-20^o**
Stratified	5	10	17	17
Slug	30	25	13	15
Intermittent/Annular	57	59	66	65
Bubbly	4	9	6	2

4.2 Heat Transfer

4.2.1 Effect of Flow Patterns and Pipe Orientation on Two Phase Heat Transfer Coefficient

Since the two phase heat transfer coefficient is affected by the change in physical structure of flow patterns which is in turn a function of pipe orientation; it is interesting to take a look at the combined effect of phase flow rates (or alternatively the flow patterns) and the pipe orientation on the two phase heat transfer coefficient.

The effect of pipe inclination on the two phase heat transfer coefficient is investigated by comparing its magnitude at different pipe inclinations and similar liquid and gas flow rates (or alternatively superficial Reynolds numbers). Figure 4.5 represents the change of two phase heat transfer coefficient (h_{TP}) with superficial gas Reynolds number Re_{SG} measured at constant Re_{SL}. The flow pattern corresponding to combination of each Re_{SL} and Re_{SG} is also identified in the figure. It is observed that the two phase heat transfer coefficient increases with the increase of

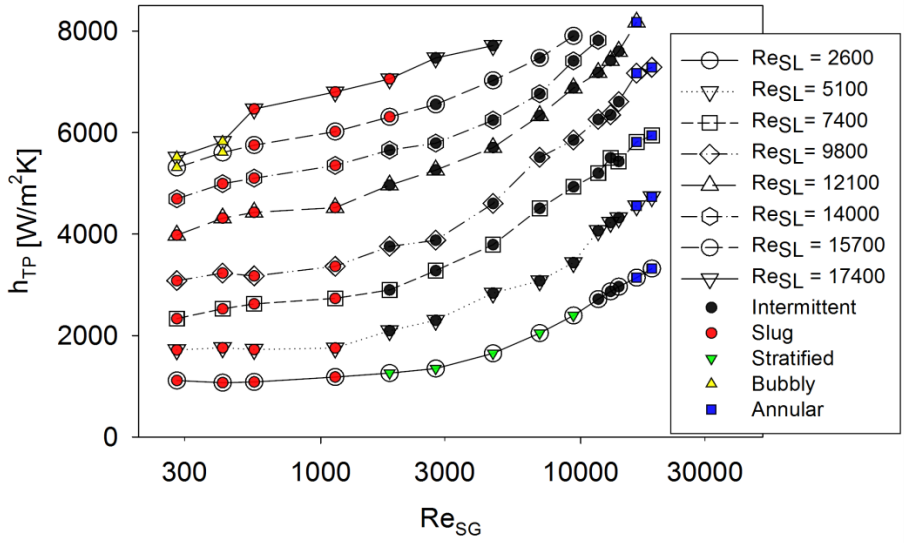
8000
6000
4000
2000
0
h_{TP} [W/m^{2}K]
300
1000
3000
10000
30000
Re_{SG}
Re_{SL} = 2600
Re_{SL}= 5100
Re_{SL}= 7400
Re_{SL}= 9800
Re_{SL}= 12100
Re_{SL}= 14000
Re_{SL} = 15700
Re_{SL} = 17400
Intermittent
Slug
Stratified
Bubbly
Annular

(a)

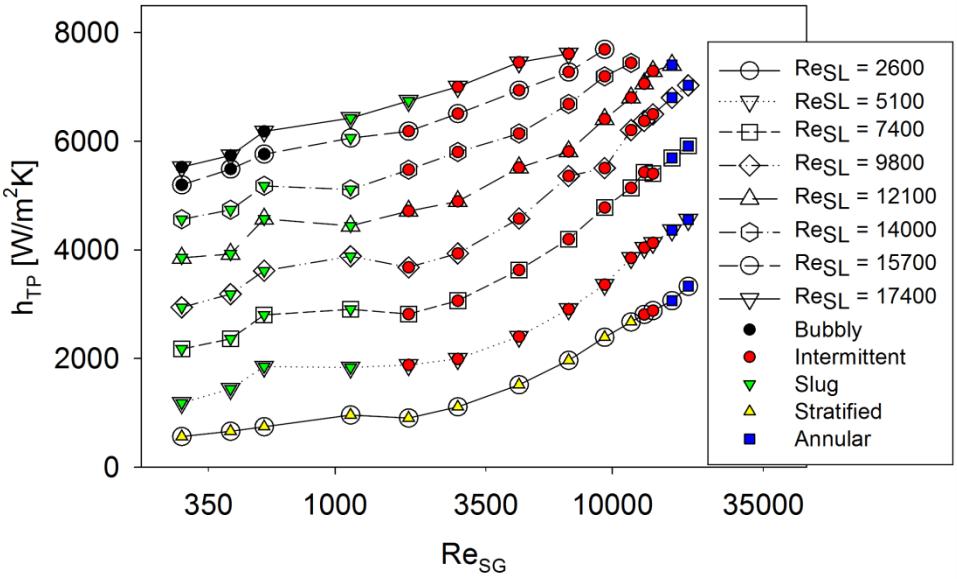
8000
6000
4000
2000
0
h_{TP} [W/m^{2}K]
350
1000
3500
10000
35000
Re_{SG}
Re_{SL} = 2600
ReSL = 5100
Re_{SL} = 7400
Re_{SL} = 9800
Re_{SL} = 12100
Re_{SL} = 14000
Re_{SL} = 15700
Re_{SL} = 17400
Bubbly
Intermittent
Slug
Stratified
Annular

(b)

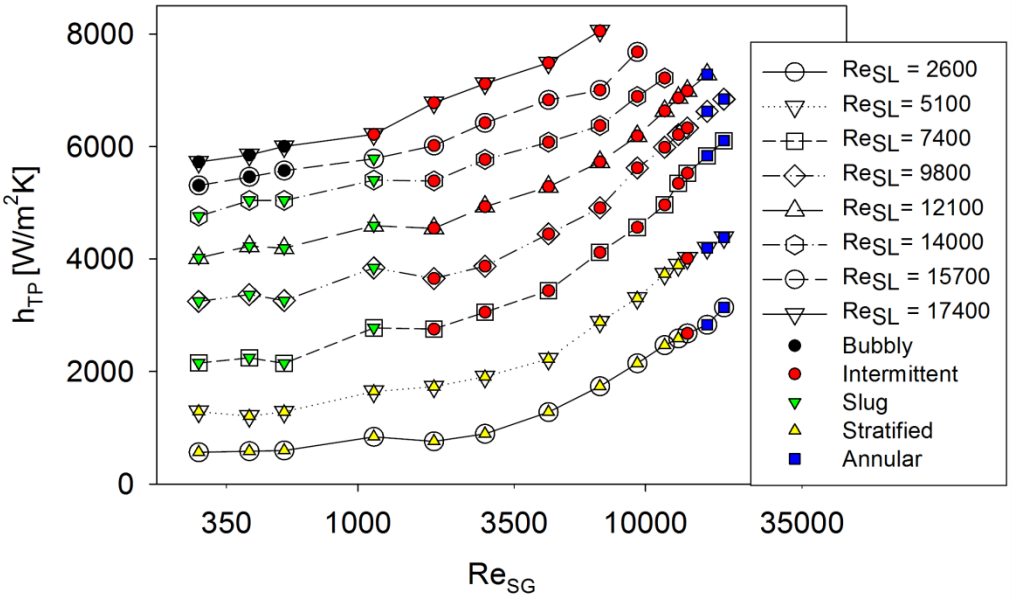

(c)

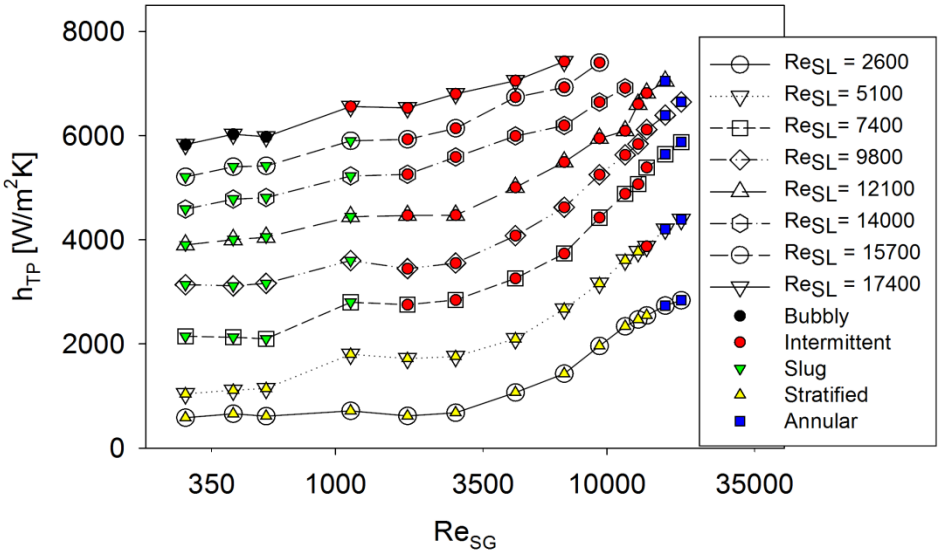

(d)

Figure 4.5 Variation of two phase heat transfer coefficient at fixed Re_{SL} and increasing Re_{SG}

(a) 0 degree, (b) -5 degree, (c) -10 degree, (d) -20 degree.

Re_{SG} and Re_{SL}. Overall it is observed that the two phase heat transfer increases at low Re_{SG} (stratified and slug flow patterns), then it remains virtually unchanged at the middle range of Re_{SG} (intermittent flow) and then increases in the higher range of Re_{SG} (transitional intermittent flow approaching annular flow). In stratified flow, Re_{SG} < 3000 and Re_{SL} < 2600 the heat transfer coefficient value increases slowly with the increase in Re_{SG}. For similar Re_{SL} and 2600 < Re_{SG} < 10,000, the flow is still stratified but the h_{TP} indicates steeper slope. This is probably due to shear driven nature of the stratified flow compared to low inertia stratified flow occurring at Re_{SG} < 2600. In this range of Re_{SG} (2600 to 1000) corresponding to the stratified flow, disturbance waves are frequently observed that locally accelerates the two phase flow mixture resulting into increase in the heat transfer coefficient.

When Re_{SG} <1200 and the liquid superficial Reynolds number is increased beyond 6000, the stratified flow in the downward inclined orientations transits to slug flow. The value of h_{TP} increases with higher Re_{SL} in the slug flow regime. This is consistent with the observation made by Bhagwat *et al.* (2012) and Oliver and Wright (1964). The reason for such increase is the length of slugs traversing through the pipe. Slug length and slug frequency are one of the main factors affecting the two phase heat transfer in slug flow regime.

An increase in the liquid flow rate for a fixed gas flow rate results into a short length slug that traverses with comparatively high frequency through the pipe causing increase in the two phase heat transfer. It can also be observed from Figure 4.5 that for all pipe orientations, initially at low Re_{SG} in slug flow regime heat transfer increases steadily, however, at higher Re_{SG} (approximately above 1200) which is the onset of the intermittent (slug-wavy) flow, the slope of h_{TP} becomes less steeper. With a further increase in Re_{SG}, the two phase heat transfer coefficient increases rapidly. Albeit, the flow pattern for these two cases i.e., 1200 < Re_{SG} ≤ 10,000 and Re_{SG} > 10,000 is intermittent, the physical structure of the intermittent flow is significantly different. For the low

values of Re_{SG}, the intermittent flow is essentially slug-wavy in nature while for high values of Re_{SG}, the intermittent flow is wavy-annular (shear driven) in nature. At this point, the intermittent flow starts to develop continuous thin liquid film that is in contact with the pipe top wall and is very conducive to heat transfer due to better contact with the liquid at the pipe upper surface.

Overall, in the intermittent flow region, the flow is induced with significant mixing and turbulence which contributes to the enhancement in two phase heat transfer. Pipe inclination plays a major role in heat transfer in two phase flow. As the pipe is inclined downward from horizontal to -5^o, -10^o and -20^o, the two phase heat transfer coefficient is found to decrease systematically.

This observation of reduction of heat transfer at downward inclination is consistent with the observations of Oshinowo *et al.* (1984). They found the two phase heat transfer coefficient to decrease when the pipe is oriented from vertical upward to vertical downward. It is also worthwhile to mention that the amount of decrease in two phase heat transfer depends on the flow pattern. As observed from Figure 4.6 the highest average percentage decrease in heat transfer from horizontal is observed in stratified flow with 15%, 22% and 27% reduction at -5^o, -10^o and -20^o, respectively. The effect of pipe orientation is also prominent for intermittent flow with an average reduction of 4%, 6% and 10% corresponding to -5^o, -10^o and -20^o inclinations, respectively. Slug flow region shows less sensitivity to the change in pipe inclination with around 2%, 2% and 5% reduction in two phase heat transfer coefficient at -5^o, -10^o and -20^o inclinations, respectively. However, it should be mentioned that due to highly random slug length and slug frequency at inclined flow in some instances, reduction in two phase heat transfer is much higher than the average values. For example, the highest percentage reduction obtained in slug flow is 31%, 17% and 20% at -5^o, -10^o and -20^o, respectively which is fairly high compared to its average reduction.

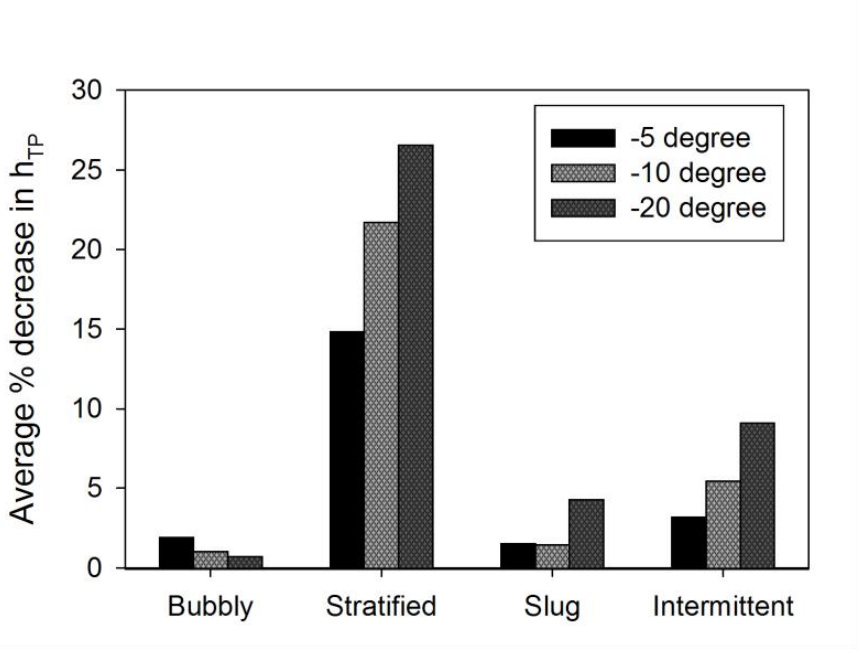

Figure 4.6 Average percentage decrease in h_{TP} for different inclinations with reference to horizontal orientation.

The comparisons of two phase heat transfer coefficient at different pipe inclinations with respect to horizontal are presented in Figures 4.7 and 4.8. In Figure 4.7, the ratio of two phase heat transfer coefficient at a fixed inclination to that of horizontal flow is plotted against $Re_{SL.}$ It shows how the effect of pipe orientation on heat transfer varies with Re_{SL}. In Figure 4.7 (a), at Re_{SG} = 279, the lines are very close to each other for the entire range of Re_{SL} which indicates that the effect of inclination and Re_{SL} change between -5^o and -20^o have minor effect on heat transfer at low gas flow rate. However, even at low Re_{SG}, there's a definite decrease in heat transfer from horizontal to inclined flow at low $Re_{SL,}$ as observed from Figure 4.7 (a), which can be attributed to the difference in flow pattern between the horizontal and inclined flow. Horizontal flow have slug flow pattern which possess better heat transfer characteristics compared to stratified flow which persists at inclined orientation. In Figure 4.7 (b) and (c), when Re_{SG} is in between 2500 and

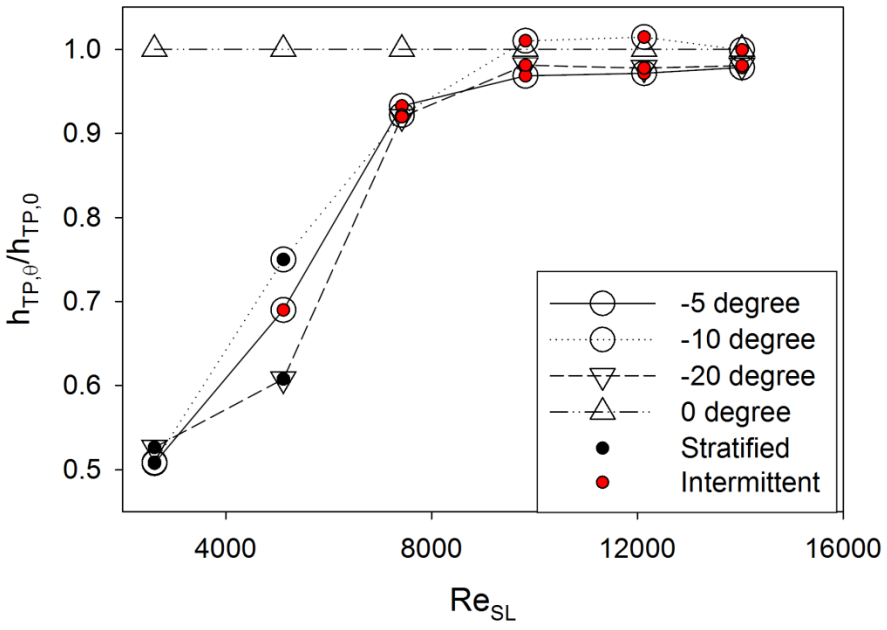
1.0
0.9
0.8
0.7
0.6
0.5
$h_{TP,\theta}/h_{TP,0}$
4000
8000
12000
16000
Re_{SL}
-5 degree
-10 degree
-20 degree
0 degree
Stratified
Intermittent

(a)

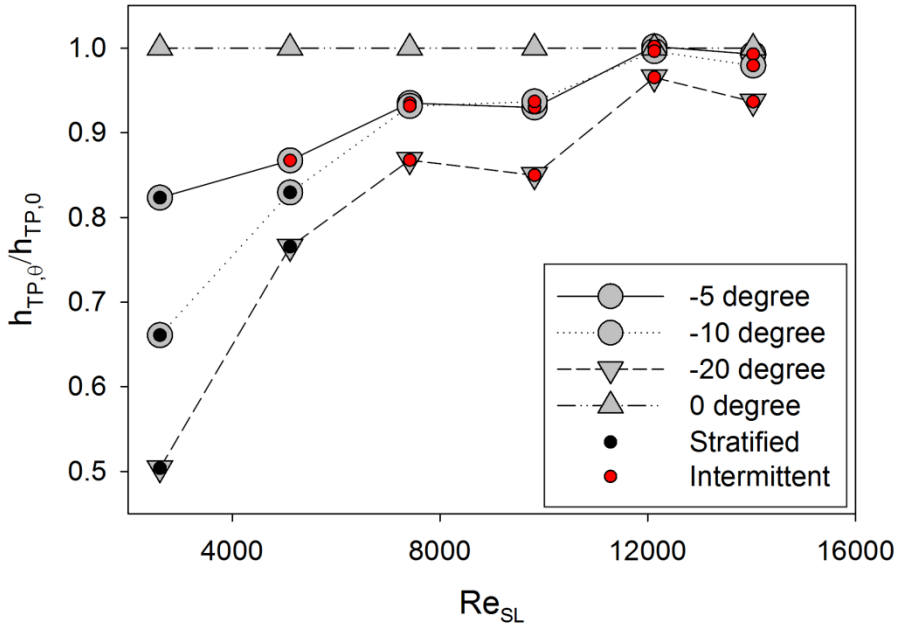
1.0
0.9
0.8
0.7
0.6
0.5
$h_{TP,\theta}/h_{TP,0}$
4000
8000
12000
16000
Re_{SL}
-5 degree
-10 degree
-20 degree
0 degree
Stratified
Intermittent

(b)

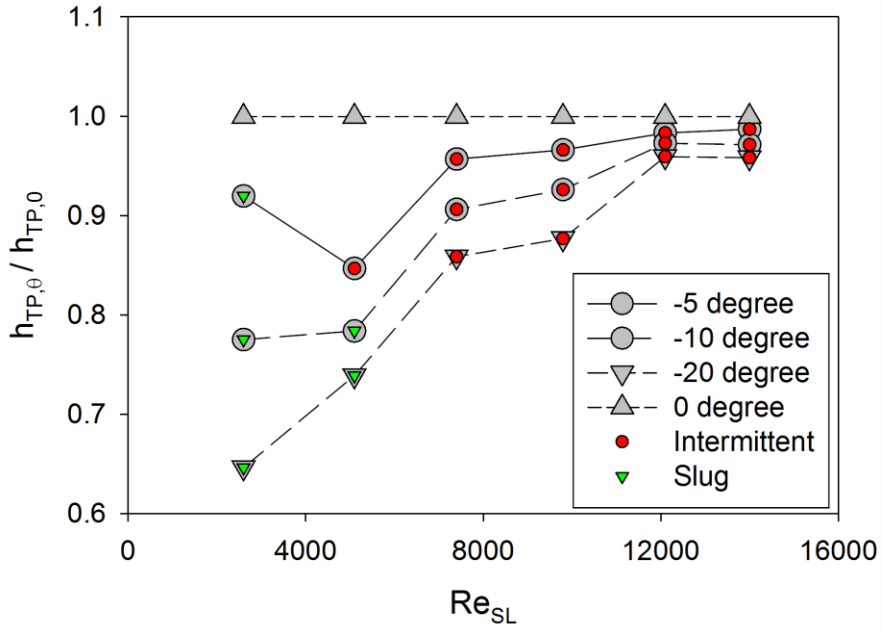
1.1
1.0
0.9
0.8
0.7
0.6
0
4000
8000
12000
16000
$h_{TP,\theta} / h_{TP,0}$
Re_{SL}
-5 degree
-10 degree
-20 degree
0 degree
Intermittent
Slug

(c)

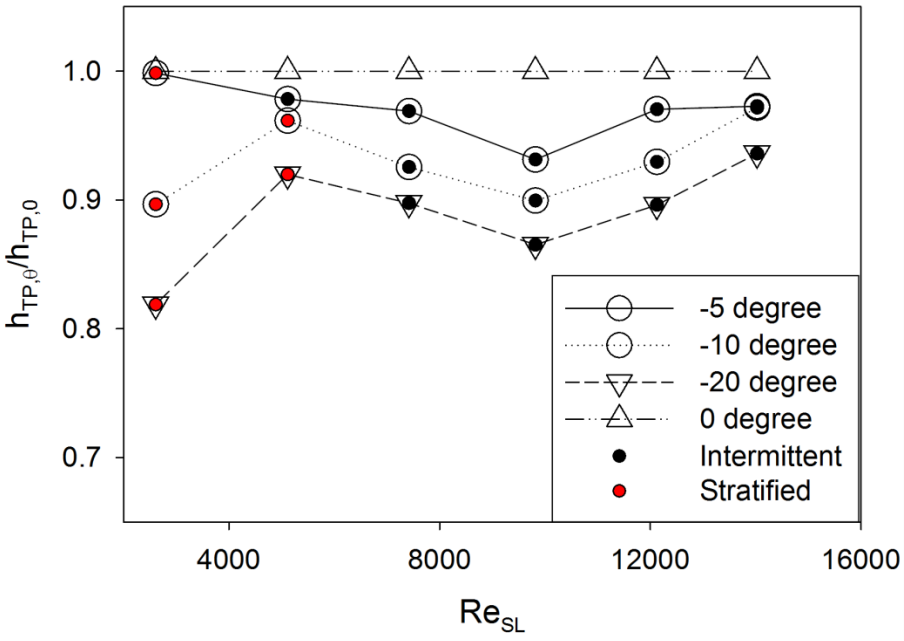
1.0
0.9
0.8
0.7
4000
8000
12000
16000
$h_{TP,\theta}/h_{TP,0}$
Re_{SL}
-5 degree
-10 degree
-20 degree
0 degree
Intermittent
Stratified

(d)

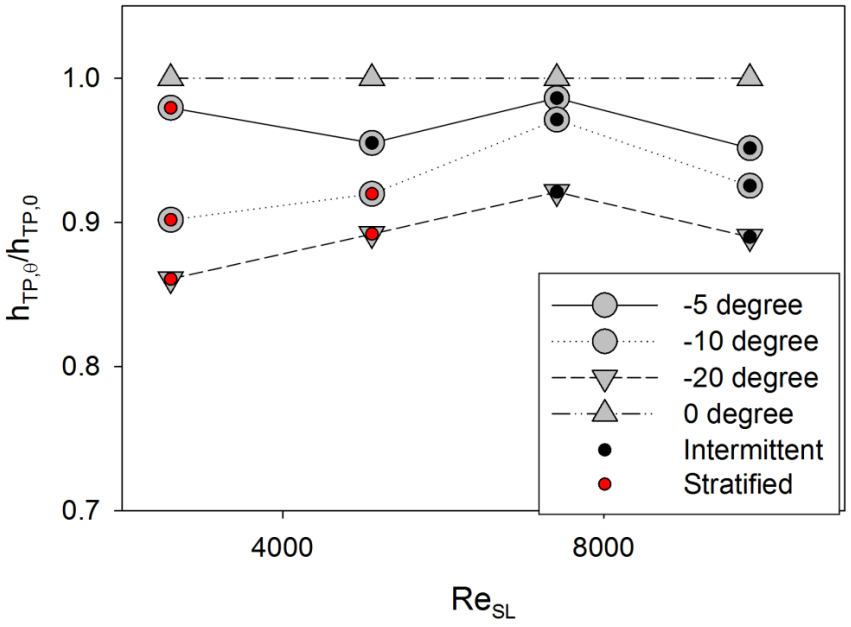

(e)

Figure 4.7 Comparison of $h_{TP,\theta}/h_{TP,0}$ at different inclinations at (a) Re_{SG} = 279, (b) Re_{SG} = 2800, (c) Re_{SG} = 4500, (d) Re_{SG} = 9000, (e) Re_{SG} = 13000

4500, initially, at low Re_{SL} the lines are more spread out indicating the effect pipe inclination on h_{TP}. At low Re_{SL} the ratio has a minimum value of about 0.67 at -20 degree. As the liquid flow rate is increased, for all orientations the ratio gradually approaches 1 and the curves start to converge indicating the effect of inclination on heat transfer is reduced at high Re_{SL}. Finally, in Figures 4.7 (d) and (e), at higher gas flow rates when Re_{SG} is in between 10,000 and 13,000, it can be observed that the ratio is almost insensitive to the change of liquid flow rate. For Re_{SG} = 13000, the ratios at -5^o, -10^o and -20^o are approximately 0.87, 0.90 and 0.96 at Re_{SL} = 2000 and maintains almost the same value when Re_{SL} = 14000. Hence, we can conclude that the effect of liquid flow rate on heat transfer is more prominent at low gas flow rates. However, at higher gas flow rates, the effect of changing the liquid flow rate diminishes.

In Figure 4.8, the h_{TP} values are plotted against Re_{SG} at horizontal, -5°,-10° and -20° in the same graph to show how the effect of inclination varies with Re_{SG}. A considerable decrease in the heat transfer is observed in Figure 4.8 (a) at Re_{SG} < 2200 from horizontal to the downward inclined flow with highest reduction of 49%, 50% and 51% at -5°,-10° and -20° pipe orientations, respectively. This greater reduction takes place due to the difference in flow pattern in the downward inclined flow compared to the horizontal flow. In the given range, the horizontal flow pattern is slug compared to stratified flow in downward inclinations. Slug flow has higher heat transfer than stratified flow due to greater contact between liquid surface and the pipe upper wall surface. In this range, -5°,-10° and -20° has similar flow pattern (stratified) with relatively similar heat transfer coefficient values at low Re_{SG}. However, higher difference in the two phase heat transfer coefficient is observed as the gas flow rate is increased in stratified flow pattern. It might

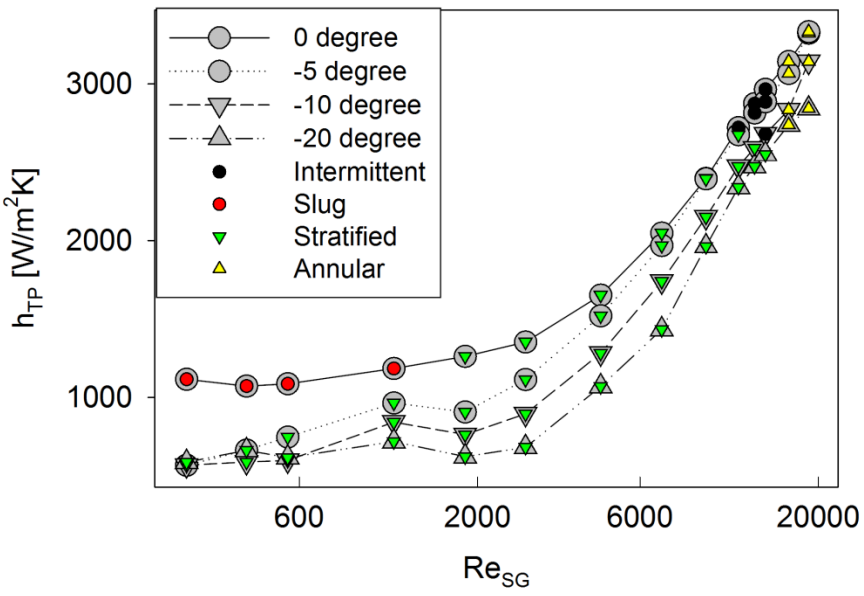

(a)

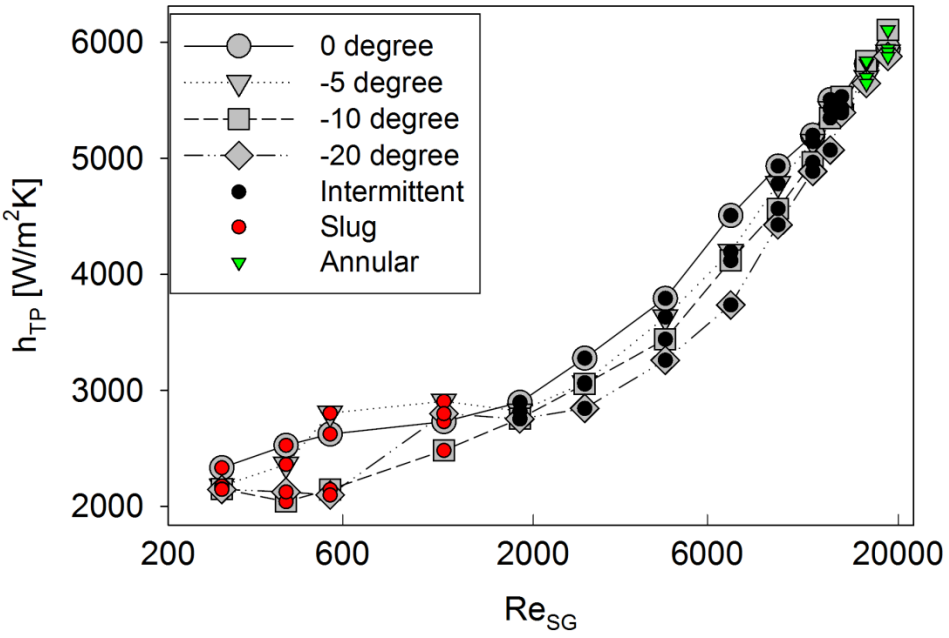
0 degree
-5 degree
-10 degree
-20 degree
Intermittent
Slug
Annular
6000
5000
4000
3000
2000
200
600
2000
6000
20000
h_{TP} [W/m^{2}K]
Re_{SG}

(b)

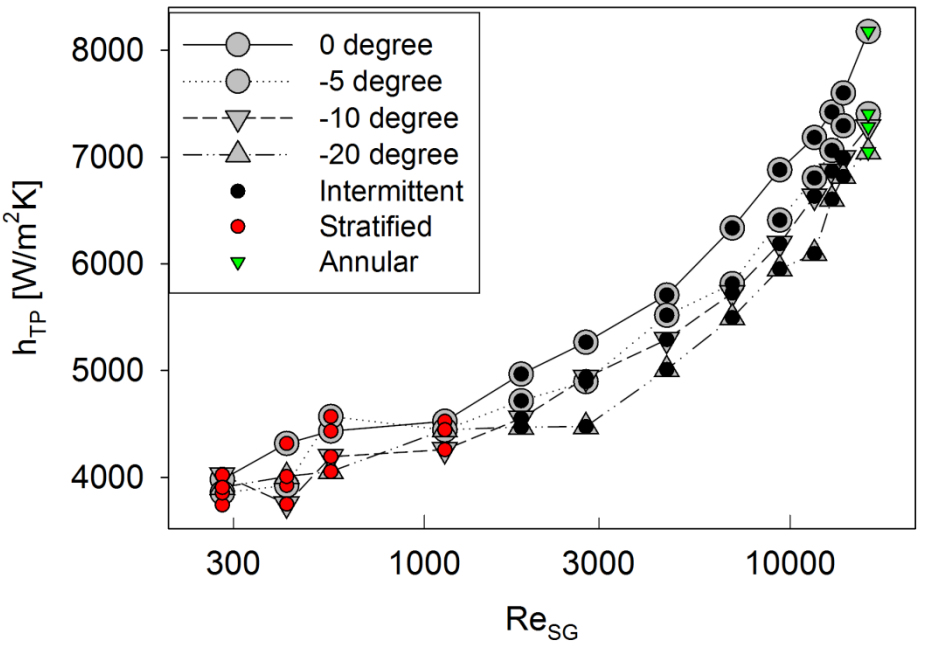
0 degree
-5 degree
-10 degree
-20 degree
Intermittent
Stratified
Annular
8000
7000
6000
5000
4000
300
1000
3000
10000
h_{TP} [W/m^{2}K]
Re_{SG}

(c)

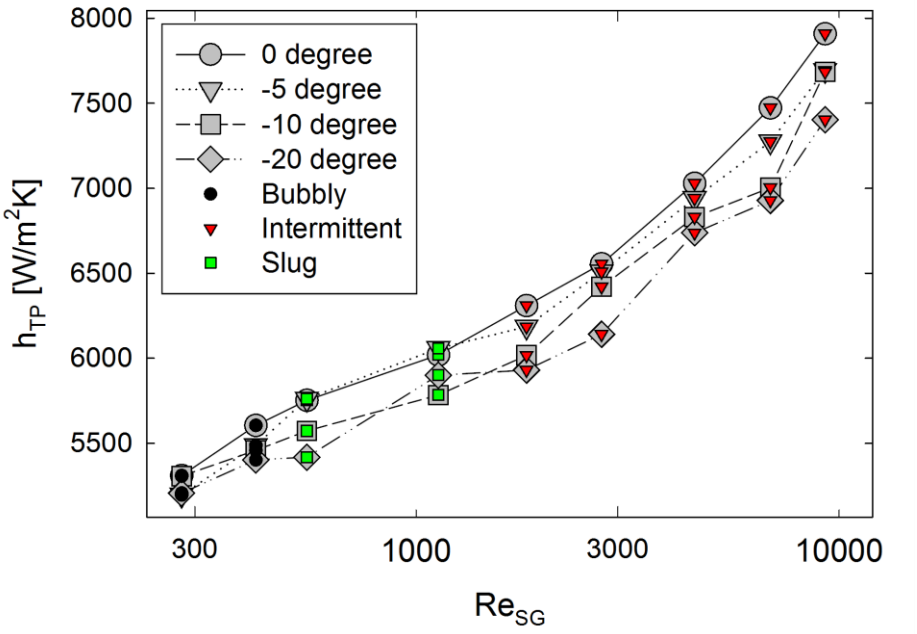

(d)

Figure 4.8 Comparison of two phase heat transfer coefficient h_{TP} at different liquid Re_{SL}, (a) Re_{SL} = 2600, (b) Re_{SL} = 5100, (c) Re_{SL} = 7400, (d) Re_{SL} = 9800.

be due to the fact that in this region the flow is induced with disturbance waves which are a decreasing function of pipe inclination. As mentioned earlier, the disturbance wave locally accelerates the two phase flow mixture that triggers the enhancement in the heat transfer. It is speculated that the flow through steeper pipe inclinations in downward direction causes the frequency of disturbance waves to reduce (due to opposite direction of buoyancy force) and hence results into reduction in two phase heat transfer coefficient. From Figures 4.8 (b), (c) and (d), it can be observed that for higher Re_{SL} the flow transits from stratified to slug region. Slug flow regime has highest percentage reduction of 31%, 18% and 20% at -5^o,-10^o and -20^o pipe orientations, respectively. In this region, the heat transfer trend becomes highly irregular making it difficult to establish a clear trend. With the increase of Re_{SG} the slug length increases which

contributes in making the h_{TP} less steeper. Initially at low Re_{SG} the effect is not very pronounced and a steady increase in the h_{TP} value is observed. However, as Re_{SG} increases the slug length increases considerably to adversely affect the heat transfer. This effect of retardation of heat transfer due increased slug length has been observed at a lower value of Re_{SG} (Re_{SG} = 400) for the 0^o and -5^o compared to -10^o and -20^o (Re_{SG} = 1200). Due to this reason, the trend of h_{TP} comparison between different inclinations becomes highly irregular in this region. The irregularity in the trend might also be attributed to the fact that in the inclined flow the slug traversing through the pipe faces resisting force due to buoyancy that increases its residence time in the test section. This resistance force causes the gas slugs to move in quite random and irregular manner while the liquid phase slips past the gas phase in downward direction. It is observed during flow visualization that slug moves very slowly and at times even appears stationary for an extended period due to its inability to overcome the shear due to dominant buoyant force acting opposite to the direction of two phase flow. These types of random events might cause the heat transfer coefficient to differ randomly from one orientation to the other. A more in depth analysis will be performed later in this section for the slug region by plotting and establishing the trend of local heat transfer coefficients at the top and bottom surface of the pipe which will shed more light on the reason for irregular trend in the slug flow pattern.

At Re_{SL} > 5000 (i.e., Figures 4.8 (b), (c) and (d)) the effect of inclination on heat transfer is more prominent at the mid-range of Re_{SG} (2000 < Re_{SG} < 10,000). In this range, the flow is in the intermittent region which mainly consists of slug-wavy, stratified-wavy and wavy-annular flow. The onset of the intermittent flow regime is slug-wavy in nature where the effect of buoyancy is pronounced and it can be observed from Figure 4.8 that in this region there is significant difference in heat transfer from one orientation to the other. The buoyancy force causes the gas phase in the slug to move slowly. This effect is enhanced as the setup is inclined more in downward orientation. Another reason for higher heat transfer at lower inclinations might be the

higher amount of turbulence and mixing at lower inclination compared to higher inclinations due to higher gas velocity and less resistance of buoyancy force. The highest percentage reductions observed in this region are 9%, 10% and 17% in -5^o, -10^o and -20^o, respectively compared to the horizontal two phase flow. As the Re_{SG} is further increased beyond 10,000, it is observed from the graph that the difference between the h_{TP} values is gradually reduced and the values at different inclination start to converge. This reduced effect of inclination on h_{TP} can be attributed to the fact that as the flow starts to approach the annular region, a more continuous and stable film of liquid (as observed in Figure 4.4) starts to develop at the top surface making the flow pattern almost similar in different inclinations and results in almost similar h_{TP} value. Furthermore, as the Re_{SG} value is increased, gas phase starts to accelerate further and the inertia force starts to dominate the buoyancy force of the liquid. At this point the nature of two phase flow is shear driven, the effect of buoyancy in reduction of heat transfer in downward inclination is diminished gradually and considerable difference in heat transfer between different inclinations is not found.

The reason for erratic trend of h_{TP} in slug flow regime is further investigated by examining the average heat transfer coefficient values at the top and bottom surface of the pipe. In Figures 4.9 (a), (b), (c) and (d) comparative plotting of the top and bottom surface h_{TP} has been presented for each orientation. It can be observed that the heat transfer coefficient at the top surface of the pipe in the slug flow is always greater than the bottom surface irrespective of the inclination. This can be explained by the fact that in the slug region the bottom surface is always in contact with liquid while the top surface makes frequent contact with gas phase due to slugs passing through the top of the pipe. Hence, it can be observed from the figure that at low Re_{SG} the difference between the top and bottom appears to be negligible. As the Re_{SG} increases the difference between the top and bottom surface h_{TP} increases significantly.

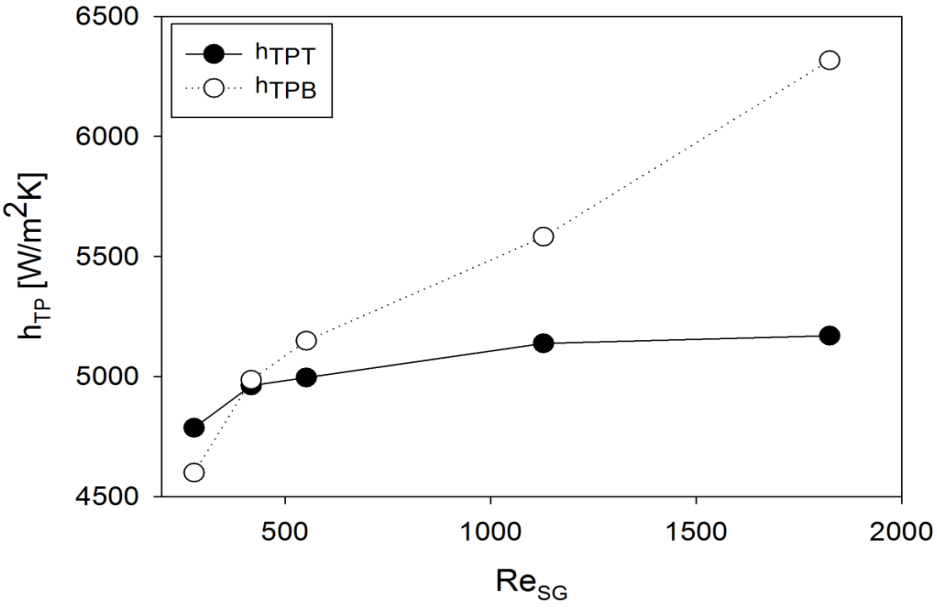
6500
6000
5500
5000
4500
500
1000
1500
2000
hTPT
hTPB
hTP [W/m2K]
ReSG

(a)

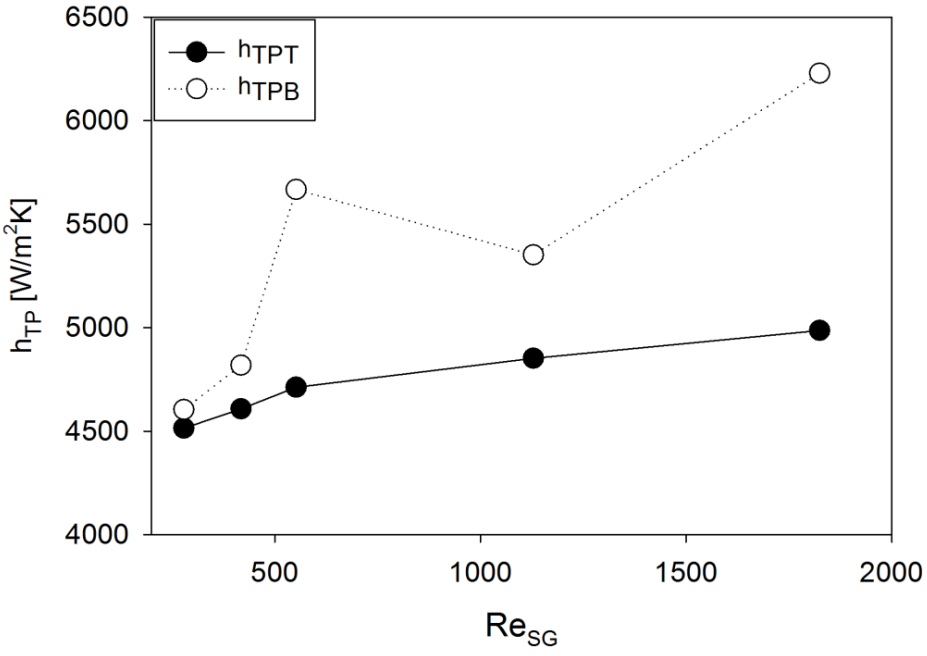
6500
6000
5500
5000
4500
4000
500
1000
1500
2000
hTPT
hTPB
hTP [W/m2K]
ReSG

(b)

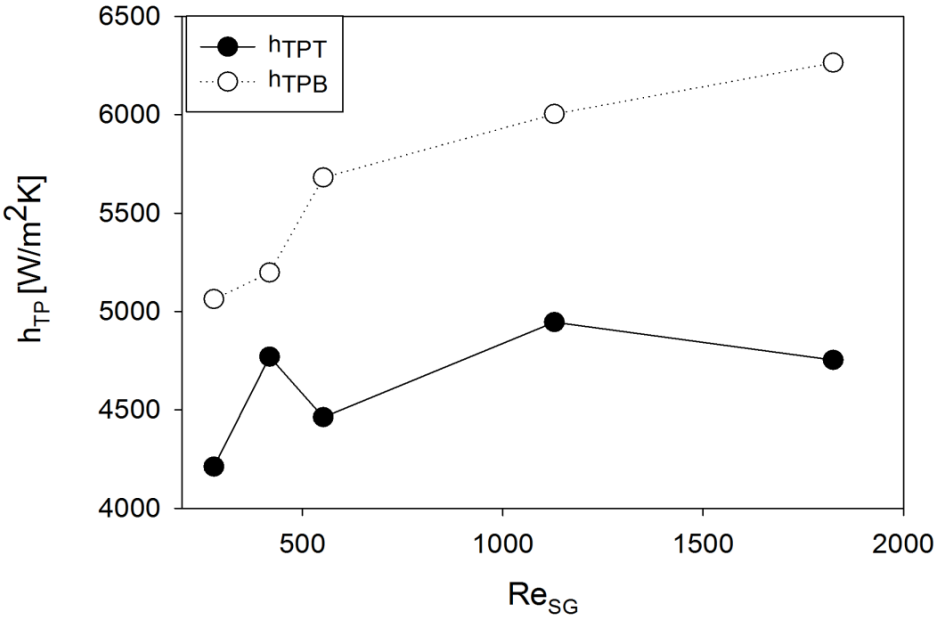

(c)

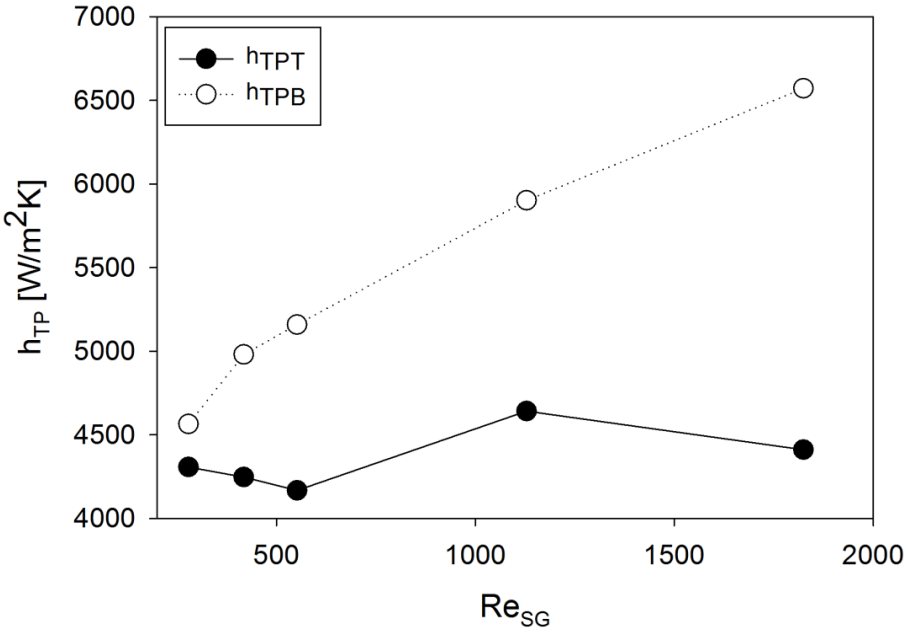

(d)

Figure 4.9 Comparison of top and bottom surface h_{TP} for (a) 0 degree, (b) -5 degree, (c) -10 degree, (d) -20 degree at Re_{SL} = 12,500

This observation is consistent with observation of Shoham *et al.* (1982) and Deshpande *et al.* (1991). Now it's imperative to check how the trend of top and bottom h_{TP} is affected by the inclination. In Figures 4.10 (a) and (b), h_{TP} values are plotted for top and bottom surface of the pipe at different inclinations for Re_{SL} = 12000 and Re_{SG} ranging from 279 to 1500 in the slug flow regime. It can be observed from Figure 4.10 (a) that in slug flow regime the heat transfer coefficient at the top surface (h_{TPT}) decreases systematically as the inclination is increased and in Figure 4.10 (b) for the bottom surface the trend appears to be exactly opposite which observes an increase in the two-phase heat transfer coefficient at the bottom surface (h_{TPB}) value with inclination. This comparison illustrates the opposing effect of buoyancy and momentum on heat

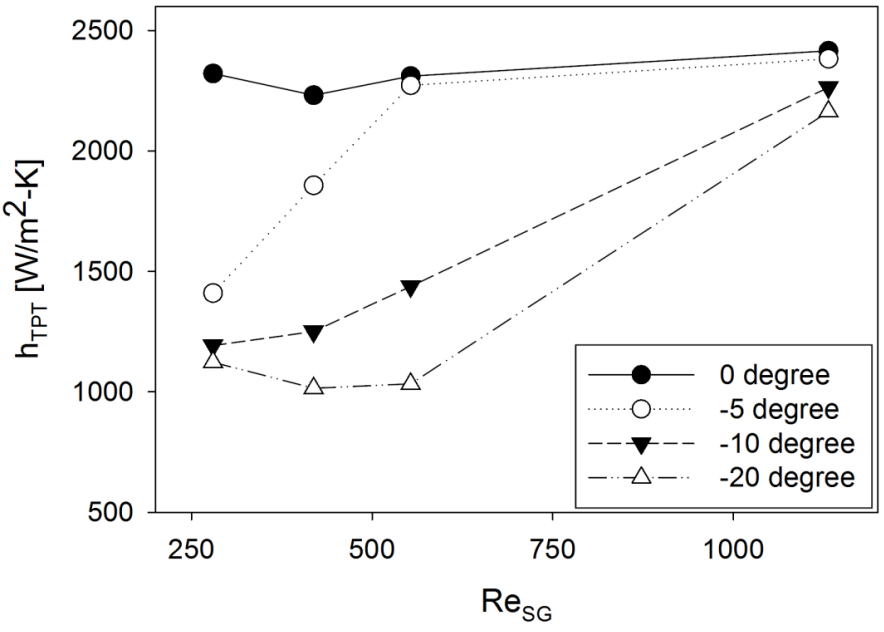

(a)

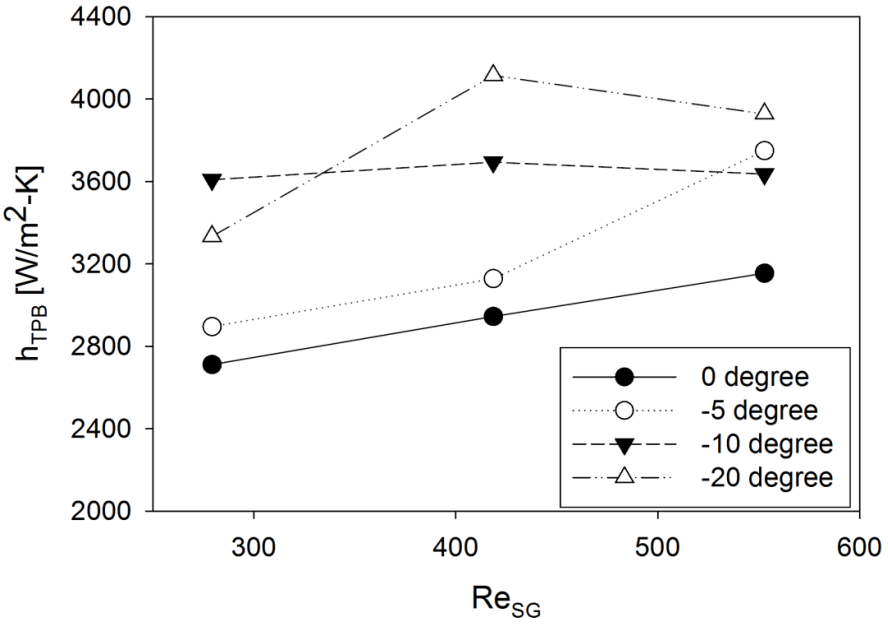

(b)

Figure 4.10 (a) Top surface, (b) Bottom surface h_{TP} comparison in slug flow regime Re_{SL} = 7400

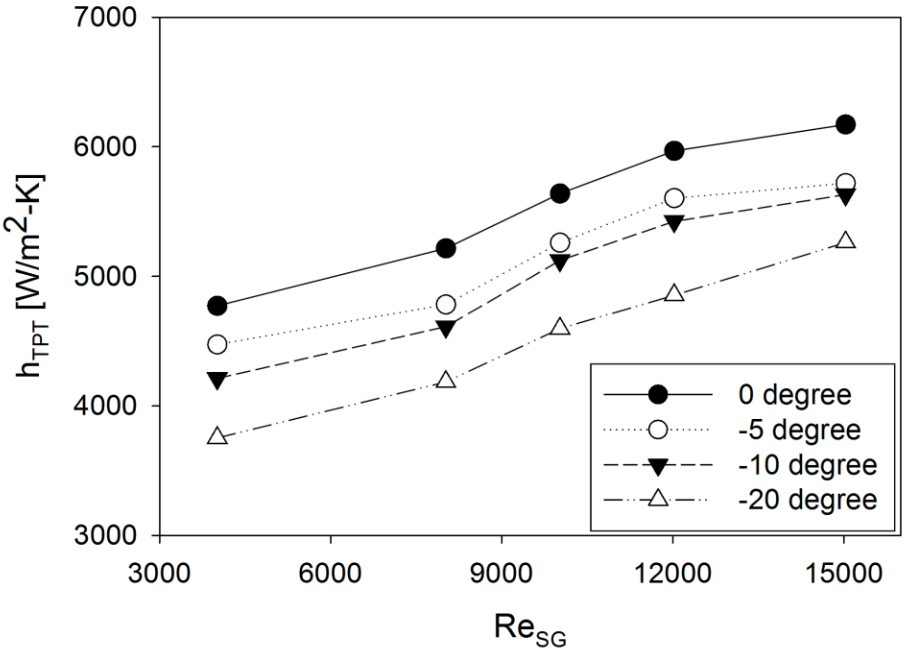

(a)

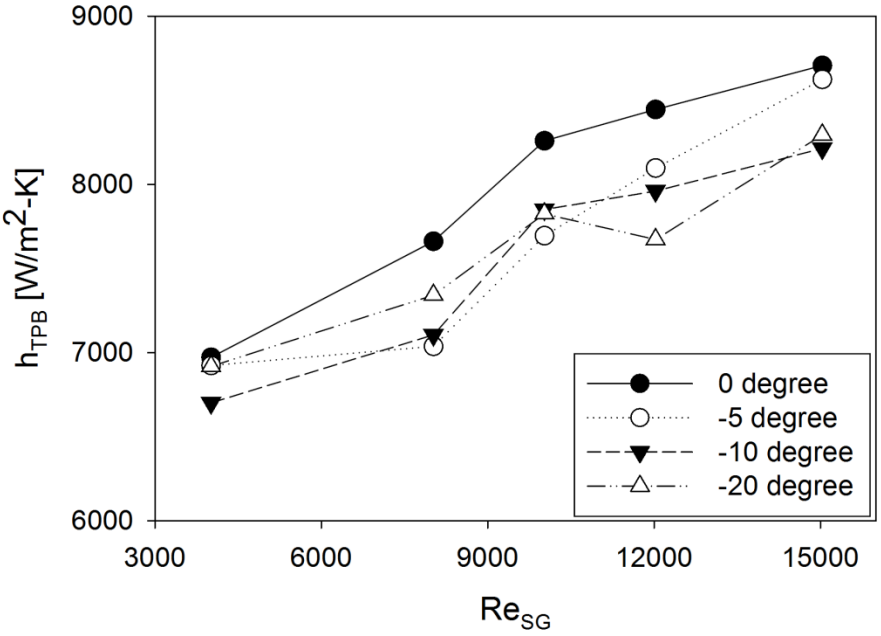

(b)

Figure 4.11(a) Top surface h_{TP} comparison, (b) Bottom surface h_{TP} comparison at Re_{SL} = 12,000 in the intermittent flow region

transfer for downward inclined flow. The decrease in h_{TPT} value with inclination can be attributed to the buoyancy force adversely affecting the heat transfer by slowing down the slugs which touches the top surface of the pipe by shear resistance and increasing their residence time. On the other hand, the accelerating liquid phase due to gravity at the bottom surface of the pipe assists the heat transfer as the inclination increases more. This combined effect of this opposing trend of h_{TP} at the top and bottom surface of the pipe makes the overall trend of average heat transfer coefficient (h_{TP}) erratic and makes it difficult to establish a clear trend.

Similar comparisons are also made for the intermittent flow where gas phase dominates the entire flow. In Figures 4.11 (a) and (b), average two-phase heat transfer coefficient (h_{TP}) at the top and bottom surface of the pipe have been plotted at different inclination for Re_{SG} ranging from 8000 to

15000. It can be observed from the figure that for both top and bottom surface, h_{TPT} and h_{TPB} values show a slight decrease with increase of inclination or remain almost similar. The similarity in the decreasing heat transfer trend for both top and bottom can be explained by the fact that the intermittent flow is dominated by the gas phase unlike slug flow which is dominated by liquid phase. The gas phase faces greater resistance due to shear force from the buoyancy of liquid which ultimately reduces the heat transfer for both top and bottom surface in the intermittent flow regime. Due to this reason, in intermittent flow, a clearer trend of decreasing average h_{TP} value with inclination is observed.

4.2.2 Heat Transfer Correlation Performance

Two heat transfer data collected in horizontal and near horizontal downward inclination (-5, -10, -20^{o}) are used to test the performance of the two phase heat transfer correlations which have been proposed by different authors in the literature as tabulated in Table 2.1. As discussed in Chapter II, two different kinds of correlations are going to be discussed for performance evaluation, general heat transfer correlations and Reynolds analogy based correlations. The required pressure drop data for the Reynolds analogy based correlation are collected from Ghajar and Bhagwat (2014). The authors performed isothermal pressure drop experiments in the same lab using the void fraction and pressure drop test branch of the same experimental setup. They mentioned that the uncertainties of the isothermal pressure drop were calculated by method of Kline and McClintock (1953) and the maximum uncertainty for the worst case scenario was 16% at very low values of pressure drop. Isothermal pressure drop data which are going to be used in the heat transfer correlations for performance evaluation are acquired at comparable liquid and gas flow rates. The performance of the correlations is evaluated based on the following parameters:

Error band: For each correlation, the accuracy is measured based on the calculation of percentage of points which falls in between a particular error band, such as ±25% and ±30%.

These values are tabulated and then represented graphically for each inclination separately and also in combined manner so that the strength of any correlation can be evaluated for any particular inclination along with the overall performance in all inclinations. In the graph, each point is also associated with their respective flow pattern which is helpful in understanding the strength of any correlation in any particular flow regime.

Percentage error: Percentage error is calculated with the following equation:

$$\text{Error } [\%] = \frac{h_{TP,CAL} - h_{TP,EXP}}{h_{TP,EXP}} \times 100\% \tag{4.3}$$

The sign of the error indicates whether the calculated value overestimate or underestimate the heat transfer coefficient value compared to the one measured by experiment.

Mean absolute error: Mean absolute error is calculated with the following equation:

$$Mean\ abs.error\ [\%] = \frac{1}{N}\sum_{i=1}^{N}\left|\frac{(h_{TP,CAL})_i - (h_{TP,EXP})_i}{(h_{TP,EXP})_i}\right| \times 100\% \tag{4.4}$$

Standard deviation: The standard deviation of the errors is calculated with following equation:

$$SD = \sqrt{\frac{1}{N}\sum_{i=1}^{N}((Abs.error)_i - Mean\ abs.error)^2} \tag{4.5}$$

For any particular correlation, it gives an idea about the spread of the error for a set of points.

Based on the criteria which are mentioned above the collected two-phase heat transfer data are used to test the correlations which are available in the literature. Very few correlations have been specifically proposed for downward flow in the literature, hence, correlations which are suggested for horizontal or upward inclined flow are also considered for testing the performance. 16 correlations are selected as listed in Table 2.1 and appraised based on the above mentioned performance criteria so that the best correlation can be recommended for horizontal and near

horizontal downward flow. First each orientation (0, -5^{o}, -10^{o},-20^{o}) is discussed below based on the tabulated outcome in Tables 4.2, 4.3, 4.4 and 4.5 and, then the overall performance is discussed based on all inclination based on Table 4.6.

Horizontal inclination: In horizontal inclination a total 96 points have been collected, 4 bubbly, 57 intermittent/annular, 30 slug and 5 stratified points. In bubbly flow regime, Shah (1981), Knott *et al.* (1959) and Tang and Ghajar (2007) predict 100% of the data points within ±20%. Among Reynolds analogy based correlations, Bhagwat *et al.* (2012) predicts 100% of the data points within ±30%. Rest of the correlations fail to perform satisfactorily but it's worthwhile to mention very few points were collected in bubbly region. In the intermittent/annular flow zone, Shah (1981) and Knott *et al.* (1959) predict 98% and 82% of the data points respectively within ±30%. Vijay *et al.* (1982) and Bhagwat *et al.* (2012) also predict 93% and 88% of the data points within ±30%. In the slug flow regime, Knott *et al.* (1959), Shah (1981) and Tang & Ghajar (2007) perform well by predicting 83%, 97% and 100% of the points respectively within ±30%. No Reynolds analogy based correlation performs satisfactorily in slug region in horizontal flow compared to the performance of the general correlations. In the stratified flow regime, Shah (1981) predicts 80% of the data points within ±30% error range. Combining all the flow patterns, Knott *et al.* (1959), Shah (1981) and Bhagwat *et al.* (2012) predict 80%, 97% and 79% of the data points between ±30%. Hence, these are the recommended heat transfer correlations for air-water mixture horizontal flow.

-5 degree inclination: Total of 105 data points have been collected in this inclination with 9 bubbly, 59 intermittent/annular, 25 slug and 10 stratified points. In bubbly flow regime, Shah (1981), Knott *et al.* (1959), Ghajar and Tang (2007), Vijay *et al.* (1982) and Bhagwat *et al.* (2012) predict 100% of the data points within ±30%. In the intermittent region, Shah (1981),

Table 4.2 Heat transfer coefficient performance for 0 degree

0 degree	96 points				Bubbly (4 points)		Intermittent/ Annular (57 points)		Slug (30 points)		Stratified (5 points)	
Correlation	1[1]	2	3	4	1	2	1	2	1	2	1	2
Knott *et al.* (1959)	69	80	16	9	100	100	72	82	70	83	0	20
Shah (1981)	69	97	16	8	100	100	60	98	83	97	60	80
Tang and Ghajar (2007)	44	56	31	20	100	100	16	32	93	100	20	40
Dorresteijn (1970)	26	43	36	21	0	25	19	35	50	63	0	20
Khoze *et al.* (1976)	0	0	302	77	0	0	0	0	0	0	0	0
Martin and Sims (1971)	29	40	46	32	50	50	26	39	36	47	0	0
Aggour (1978)	24	36	39	22	0	25	25	33	30	50	0	0
Chu and Jones (1980)	31	49	48	47	0	0	47	70	3	13	40	60
Drucker *et al.* (1984)	32	42	40	37	50	50	28	39	40	43	20	60
Oshinowo *et al.* (1984)	0	0	151	74	0	0	0	0	0	0	0	0
Ravipudi and Godbold (1978)	32	42	51	47	50	50	33	39	33	53	0	0
Rezkallah and Sims (1987)	12	16	82	61	50	50	0	3	16	37	0	0
Kim and Ghajar (2006)	11	22	42	15	0	50	9	14	20	33	0	20
Pressure drop based correlation												
	76 points				Bubbly (4 points)		Intermittent/ Annular (40 points)		Slug (28 points)		Stratified (4 points)	
Vijay *et al.* (1982)	57	73	20	17	50	50	70	93	46	54	0	0
Bhagwat *et al.* (2012)	66	79	20	27	50	100	78	88	54	64	50	75
Ghajar and Tang (2011)	25	47	47	39	100	100	5	54	46	61	0	0

[1] In Table 4.2, 1, 2, 3 and 4 refers to ±20% error band, ±30% error band, mean absolute error [%] and standard deviation respectively.

Table 4.3 Heat transfer coefficient performance for -5 degree

-5 degree	103 points				Bubbly (9 points)		Intermittent/ Annular (59points)		Slug (25 points)		Stratified (10 points)	
Correlation	1[2]	2	3	4	1	2	1	2	1	2	1	2
Knott *et al.* (1959)	53	73	28	37	100	100	51	76	60	76	0	10
Shah (1981)	81	88	18	29	100	100	92	100	72	80	20	30
Tang and Ghajar (2007)	38	51	33	27	100	100	20	37	68	80	10	10
Dorresteijn (1970)	30	47	39	32	0	11	36	49	32	64	20	20
Khoze *et al.* (1976)	0	0	333	154	0	0	0	0	0	0	0	0
Martin and Sims (1971)	11	25	67	54	22	22	5	25	24	36	0	0
Aggour (1978)	27	46	41	35	0	33	31	48	40	64	0	0
Chu and Jones (1980)	44	53	57	87	0	0	70	85	8	12	20	20
Drucker *et al.* (1984)	29	47	53	54	22	56	31	48	36	56	10	20
Oshinowo *et al.* (1984)	0	0	188	143	0	0	0	0	0	0	0	0
Ravipudi and Godbold (1978)	29	36	73	81	78	89	19	27	48	52	0	0
Rezkallah and Sims (1987)	7	19	105	82	22	100	0	3	16	36	0	0
Kim and Ghajar (2006)	14	33	36	15	11	8	2	12	40	68	20	30
Pressure drop based correlation												
	78 points				Bubbly (9 points)		Intermittent/ Annular (39 points)		Slug (23 points)		Stratified (7 points)	
Vijay *et al.* (1982)	59	74	30	45	100	100	87	94	35	52	0	0
Bhagwat *et al.* (2012)	59	78	29	47	100	100	67	95	44	61	25	25
Ghajar and Tang (2011)	22	32	62	57	100	100	2	10	30	52	0	0

[2] In Table 4.3, 1, 2, 3 and 4 refers to ±20% error band, ±30% error band, mean absolute error [%] and standard deviation respectively.

Table 4.4 Heat transfer coefficient performance for -10 degree

-10 degree	102 points				Bubbly (6 points)		Intermittent/ Annular (66 points)		Slug (13 points)		Stratified (17 points)	
Correlation	1[3]	2	3	4	1	2	1	2	1	2	1	2
Knott *et al.* (1959)	75	84	22	29	100	100	86	97	85	92	12	24
Shah (1981)	75	86	20	27	100	100	86	99	92	92	18	29
Tang and Ghajar (2007)	38	55	34	25	33	100	33	50	77	92	29	29
Dorresteijn (1970)	30	44	39	25	0	0	35	50	31	46	24	35
Khoze *et al.* (1976)	0	0	349	166	0	0	0	0	0	0	0	0
Martin and Sims (1971)	13	20	63	54	0	0	15	30	23	0	0	23
Aggour (1978)	28	45	36	24	0	0	35	50	46	46	0	41
Chu and Jones (1980)	37	50	61	91	0	0	55	74	15	15	0	0
Drucker *et al.* (1984)	27	43	53	77	0	0	35	53	15	39	18	24
Oshinowo *et al.* (1984)	0	0	185	134	0	0	0	0	0	0	0	0
Ravipudi and Godbold (1978)	30	39	69	81	83	100	30	38	46	69	0	0
Rezkallah and Sims (1987)	2	17	108	91	0	100	2	11	1	31	0	0
Kim and Ghajar (2006)	16	35	36	15	83	100	6	15	54	69	0	65
Pressure drop based correlation												
	77 points				Bubbly (6 points)		Intermittent/ Annular (45 points)		Slug (13 points)		Stratified (13 points)	
Vijay *et al.* (1982)	77	74	23	21	0	100	77	93	23	61	8	8
Bhagwat *et al.* (2012)	56	78	31	53	83	100	71	93	46	77	0	15
Ghajar and Tang (2011)	21	30	63	58	100	100	35	20	38	61	0	0

[3] In Table 4.4, 1, 2, 3 and 4 refers to ±20% error band, ±30% error band, mean absolute error [%] and standard deviation respectively.

Table 4.5 Heat transfer coefficient performance for -20 degree

-20 degree	99 points				Bubbly (2 points)		Intermittent/ Annular (65 points)		Slug (15 points)		Stratified (17 points)	
Correlation	1[4]	2	3	4	1	2	1	2	1	2	1	2
Knott *et al.* (1959)	67	78	26	46	100	100	23	89	87	100	6	12
Shah (1981)	74	83	26	41	100	100	85	95	83	100	12	18
Tang and Ghajar (2007)	50	61	32	34	100	100	46	60	80	87	29	35
Dorresteijn (1970)	21	58	34	27	50	100	3	62	60	60	53	35
Khoze *et al.* (1976)	0	0	381	204	0	0	0	0	0	0	0	0
Martin and Sims (1971)	16	20	79	80	100	100	8	11	60	73	0	0
Aggour (1978)	41	56	34	30	0	50	48	60	20	53	41	41
Chu and Jones (1980)	33	52	65	96	0	0	51	75	0	0	0	12
Drucker *et al.* (1984)	41	55	50	82	100	100	46	60	40	60	18	24
Oshinowo *et al.* (1984)	0	0	203	166	0	0	0	0	0	0	0	0
Ravipudi and Godbold (1978)	14	23	89	110	0	0	12	19	40	73	0	0
Rezkallah and Sims (1987)	14	16	127	121	100	100	5	6	60	67	0	0
Kim and Ghajar (2006)	26	42	36	24	0	0	26	42	13	27	41	65
Pressure drop based correlations												
	75 points				Bubbly (2 points)		Intermittent/ Annular (45 points)		Slug (15 points)		Stratified (13 points)	
Vijay *et al.* (1982)	49	68	27	32	100	100	53	75	66	80	8	23
Bhagwat *et al.* (2012)	52	68	40	66	100	100	53	78	87	87	0	8
Ghajar and Tang (2011)	24	27	77	71	100	100	9	11	80	87	0	0

[4] In Table 4.5, 1, 2, 3 and 4 refers to ±20% error band, ±30% error band, mean absolute error [%] and standard deviation respectively.

Table 4.6 Heat transfer coefficient performance for all inclinations

All orientation	400 points				Bubbly (11 points)		Intermittent/ Annular (247 points)		Slug (83 points)		Stratified (49 points)	
Correlation	1[5]	2	3	4	1	2	1	2	1	2	1	2
Knott *et al.* (1959)	73	85	26	32	100	100	60	76	76	90	14	25
Shah (1981)	75	89	20	29	100	100	81	98	83	96	20	31
Tang and Ghajar (2007)	43	56	32	27	81	100	30	45	81	90	25	29
Dorresteijn (1970)	32	47	37	28	0	14	36	49	36	59	20	31
Khoze *et al.* (1976)	0	0	347	158	0	0	0	0	0	0	0	0
Martin and Sims (1971)	17	26	65	60	29	29	13	26	35	45	0	0
Aggour (1978)	30	46	38	28	81	24	35	48	26	54	27	29
Chu and Jones (1980)	37	51	58	83	0	0	55	76	4	8	12	18
Drucker *et al.* (1984)	33	47	49	73	29	43	35	50	35	48	16	27
Oshinowo *et al.* (1984)	0	0	182	135	0	0	0	0	0	0	0	0
Ravipudi and Godbold (1978)	27	35	71	84	67	76	23	30	41	49	0	0
Rezkallah and Sims (1987)	9	17	109	91	29	91	2	6	41	41	0	0
Kim and Ghajar (2006)	17	33	38	18	5	71	11	21	27	48	33	53
Pressure drop based correlations												
	306 points				Bubbly (21 points)		Intermittent/ Annular (169 points)		Slug (79 points)		Stratified (37 points)	
Vijay *et al.* (1982)	54	73	25	31	38	90	72	89	43	60	5	10
Bhagwat *et al.* (2012)	58	76	30	51	85	100	67	89	55	74	11	21
Ghajar and Tang (2011)	17	28	49	29	100	100	7	20	41	54	0	0

[5] In Table 4.6, 1, 2, 3 and 4 refers to ±20% error band, ±30% error band, mean absolute error [%] and standard deviation respectively.

Vijay *et al.* (1982) and Bhagwat *et al.* (2012) perform better than the rest and predict 100%, 94% and 95% of the data points respectively within ±30%. In the slug region, no correlation performs exceedingly well. Only Shah (1981) and Tang and Ghajar (2007) predict 80% of the points within ±30% error. In the stratified region, all the correlations perform poorly. Overall, Shah (1981) and Bhagwat *et al.* (2012) are the best performing correlations in this orientation and predict 88% and 78% of the points within ±30% error. These are the two recommended correlations for -5^{o} inclination.

-10 degree: In -10 degree inclination, a total of 102 data points are collected with 6 bubbly, 66 intermittent/annular, 13 slug and 17 stratified points. In bubbly flow regime, 100% of the points are predicted within ±30% by Knott *et al.* (1959), Shah (1981) , Tang and Ghajar (2007), Rezkallah and Sims (1987), Vijay *et al.* (1982) and Bhagwat *et al.* (2012). In the intermittent/annular flow region, Shah (1981) and Knott *et al.* (1959) perform really well and predict 97% and 99% of the points respectively within ±30% error. Reynolds analogy based Vijay *et al.* (1982) and Bhagwat *et al.* (2012) also perform satisfactorily and predict 93% of the points within ±30%. In the slug region, Knott *et al.* (1959), Shah (1981) and Tang & Ghajar (2007) perform equally well with 92% of the points predicted within ±30%. Bhagwat *et al.* (2012) also predicts 77% of the points within ±30% in slug flow demonstrating the performance of the Reynolds analogy based correlation gets comparatively better at higher downward inclination in slug flow. In the stratified region, none of the correlations performs well. Combining all the flow patterns, Knott *et al.* (1959), Shah (1981) and Bhagwat *et al.* (2012) predict 84%, 86% and 78% of the points respectively within ±30%, hence, are the recommended correlations for -10^{o}.

-20 degree: In -20 degree inclination, a total of 99 points have been collected, 2 bubbly, 65 intermittent/annular, 15 slug and 17 stratified points. There are very few bubbly points collected

in this region and all of them are well predicted by most of the correlations within ±20% error as can be observed in Table 4.5. In the intermittent/annular region, only Knott *et al.* (1959), Shah (1981) and Bhagwat *et al.* (2012) perform well with 89%, 95% and 78% of the data points respectively predicted between ±30%. In the slug flow regime, Knott *et al.* (1959) and Shah (1981) perform exceedingly well and predict 100% of the points within ±30%. Tang and Ghajar (2007) and Bhagwat *et al.* (2012) also perform decently and all of them predict about 87% of the points within ±30%. None of the correlations perform well in the stratified region similar to the previous orientations. Combining all the flow patterns, in -20^{o} orientation, Shah (1981) and Bhagwat *et al.* (2012) perform well and predict 83% and 68% of the points within ±30%.

Horizontal, -5,-10 and -20^{o}: In total 400 points are collected, with 11 bubbly, 247 intermittent/annular, 83 slug and 49 stratified points. In the bubbly region, Knott *et al.* (1959), Shah (1981) and Bhagwat *et al.* (1982) predict 100% of the points within ±20% error. In the intermittent/annular flow, Shah (1981), Bhagwat *et al.* (2012) and Vijay *et al.* (1982) correlations perform exceptionally well and predict 98%, 89% and 89% of the points, respectively between ±30%. In the slug region, Knott *et al.* (1959), Shah (1981) and Tang and Ghajar (2007) correlations predict 90%, 92% and 90% of the points respectively within ±30%. None of the Reynolds analogy correlation performs satisfactorily in this region when compared to the performance of the general correlations. In the stratified region, all the correlations fail to predict the points with satisfactory accuracy. Combining all flow regimes, recommended correlations are Knott *et al.* (1959), Shah (1981) and Bhagwat *et al.* (2012) which predict 85%, 89% and 76% of the points respectively within ±30%. In Figures 4.12 (a), (b), (c) and (d), the performance of the Knott *et al.* (1959), Shah (1981), Bhagwat *et al.* (2012) and Tang and Ghajar (2007) are presented within ±25% and ±30% error band along with their respective flow patterns. It can be observed that Knott *et al.* (1959) and Shah (1981) predict most of the points within the error band

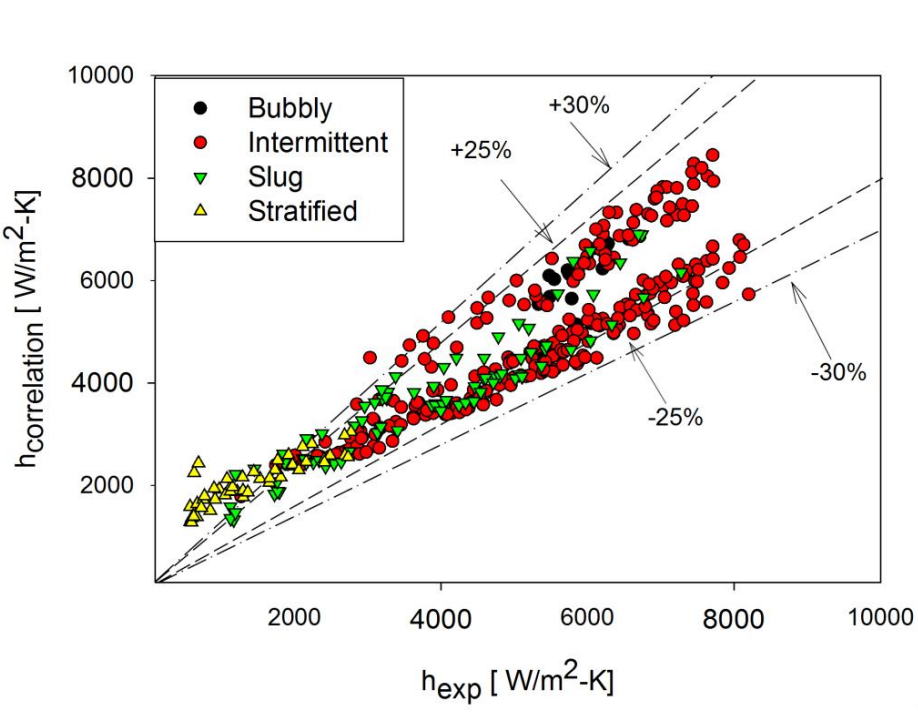
Bubbly
Intermittent
Slug
Stratified
+30%
+25%
-30%
-25%
10000
8000
6000
4000
2000
2000
4000
6000
8000
10000
$h_{correlation}$ [W/m^2-K]
h_{exp} [W/m^2-K]

(a)

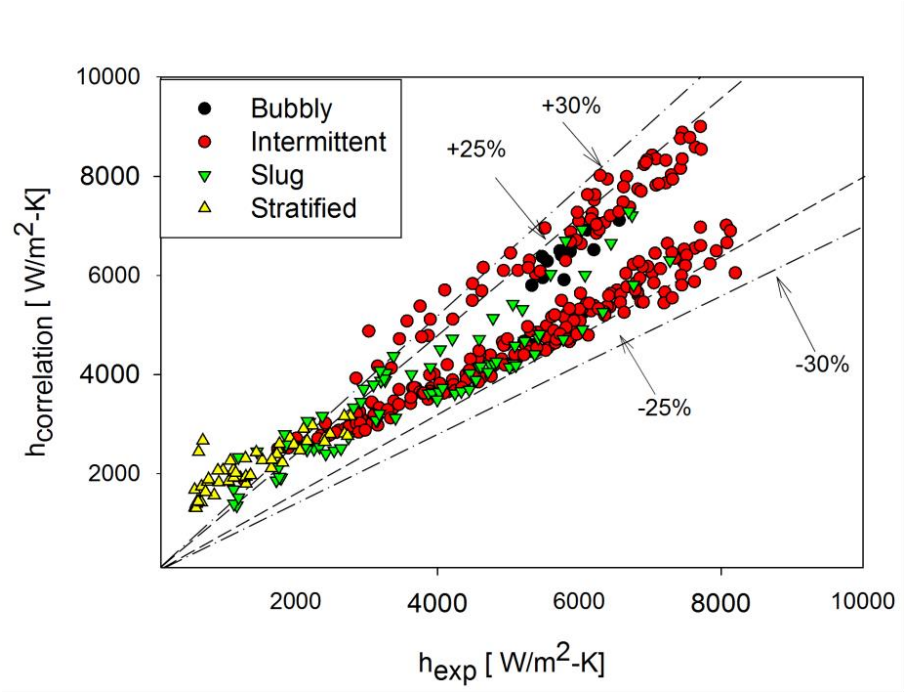
Bubbly
Intermittent
Slug
Stratified
+30%
+25%
-30%
-25%
10000
8000
6000
4000
2000
2000
4000
6000
8000
10000
$h_{correlation}$ [W/m^2-K]
h_{exp} [W/m^2-K]

(b)

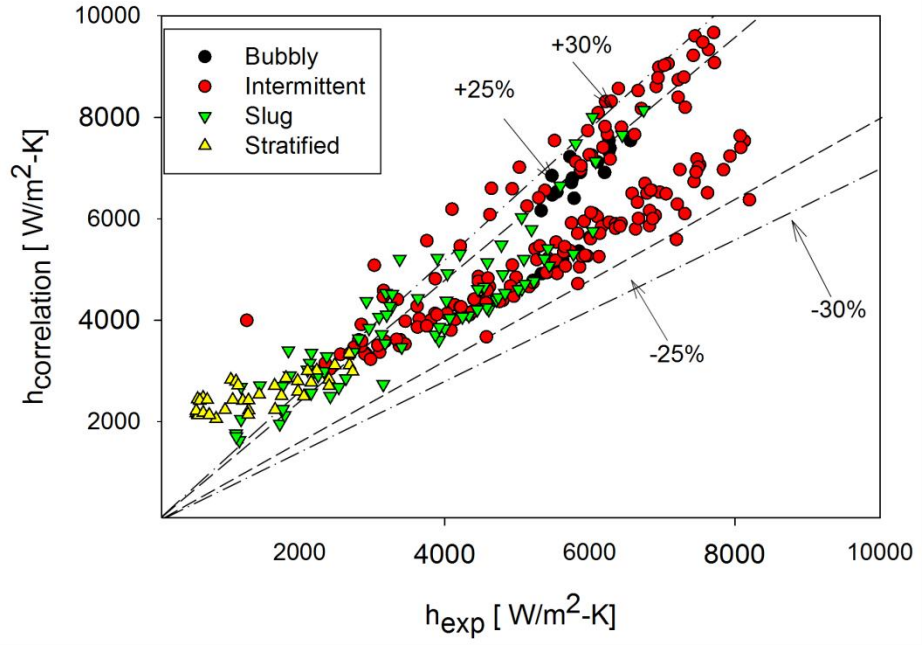

(c)

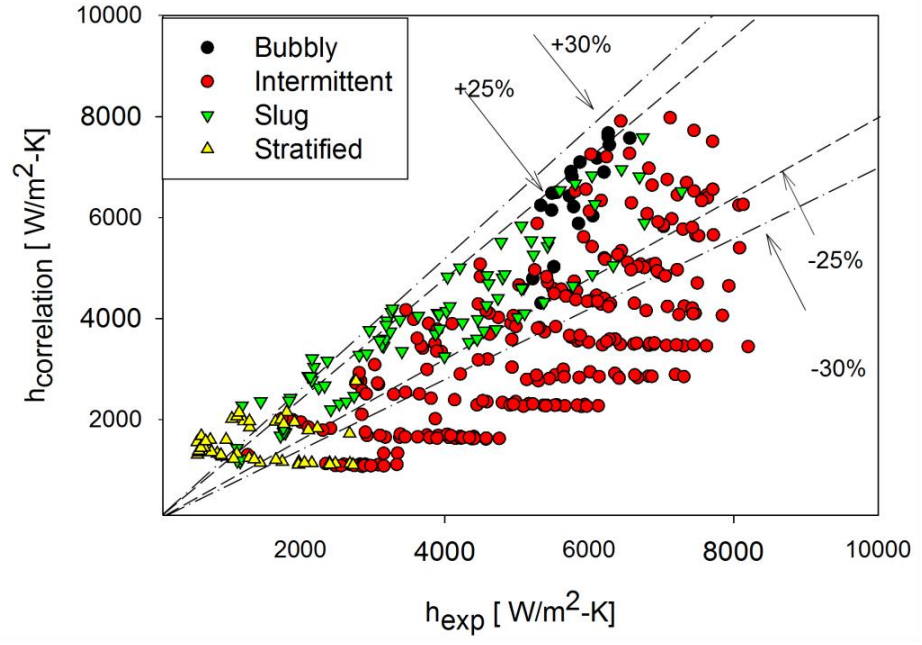

(d)

Figure 4.12 Performance of correlation combining all inclinations (a) Shah (1981), (b) Knott *et al.* (1959), (c) Bhagwat *et al.* (2012), (d) Tang & Ghajar (2007)

while Bhagwat *et al.* performs poorly in the slug region and Tang and Ghajar (2007) performs well only in the slug region. Among general correlations, Knott *et al.* (1959) and Shah (1981) are the recommended correlations. Although, the difference between the structures of these two correlations is merely the leading coefficient in the equation determination of single phase heat transfer (h_L) and the exponent of the term ($1+\frac{V_{SG}}{V_{SL}}$). Shah (1981) correlation performs comparatively better than Knott *et al.* (1959) and hence, should be the recommended general correlation for two phase heat transfer coefficient in air-water mixture flow in horizontal and near horizontal downward inclination. It predicts 89% of the points within ±30% with mean absolute error of 20% and standard deviation of 29%. The performance of this correlation is undermined due to the presence of the stratified flow points in the data set which are not well predicted by any of the correlations available in the existing literature. Without the stratified flow points, the accuracy of Shah (1981) correlation goes up significantly. It predicts 97% of the points within ±30% and 93% of the points within ±25% with mean absolute error of 13% with standard deviation of 9. This accuracy is exceptionally good considering it predicts points taken at 4 different orientations and three different flow regime, bubbly, slug and intermittent. Shah's correlation has also been validated in the near horizontal upward inclined (5^o, 10^o and 20^o) air-water mixture flow by the experiments conducted by Kalapatapu (2014). He reported that among general correlations, Shah (1981) performs best and among 371 data points 96% of the points are predicted within ±30% and 80% within ±20%. Moreover, previous study conducted by Mollamahmutoglu (2012) in the similar setup on vertical downward flow revealed among a total of 165 points 93% of the points are predicted within ±30% by Shah's correlation. Considering this results, it can be concluded that Shah's correlation is the best heat transfer correlation combining horizontal, vertical, near horizontal upward and downward inclined flow ($\pm5^o$, $\pm10^o$, $\pm20^o$ and 0^o) for at least air-water mixture. It is worth mentioning that Shah (1981) tested his correlation for 10 different gas-liquid combinations and channel hydrodynamic diameter ranging

from 4 to 70 mm with 96% of the data within ±30% with root-mean square error of 15.5% among 672 data points. Hence, even with different fluid combinations and diameter this correlation still have the potential to predict two-phase heat transfer coefficient with considerable accuracy which makes it the most likely candidate for qualifying as a universal two-phase heat transfer correlation. In practical cases, this correlation can also be recommended due to its simple structure and convenience of usage. In Figure 4.12 (a), it can be observed that for Shah (1981), most of the points which are out of the error band belong to stratified zone with very low liquid and gas flow rate. The restriction of $Re_{SL} > 2500$ can be put on Shah's correlation to improve the accuracy of the correlation.

Now, in practical circumstances, Reynolds analogy based correlations can be highly useful if the two-phase isothermal pressure drop data is available. Among the available Reynolds analogy correlation, Bhagwat *et al.* (1982) performs best with 76% of the points within ±30% with mean absolute error of 30% with standard deviation of 51. Without the stratified points, Bhagwat *et al.* predicts 84% of the data points within ±30% with mean absolute error of 18% and standard deviation of 20. With a closer look at flow regime specific performance, it can be observed that the accuracy of the correlation suffers largely in the slug region with only 74% of the points within ±30%.

4.2.3 Correlation Development

Based on the exceptional performance of Shah (1981) among general correlations, no modification is suggested for improving prediction using that correlation. However, as discussed in the previous section, the performance of Bhagwat *et al.* (2012) suffers significantly in the slug flow regime and an improvement in the prediction is necessary for this Reynolds analogy based correlation.

To improve the performance of the correlation in the slug region and bring an overall performance improvement, a modified correlation is required while utilizing the main skeleton of the correlation. Two ideas are put forward:

(1) The exponent of the pressure drop multiplier can be adjusted to better fit the data to the correlation.

(2) As the performance suffers in a particular flow pattern, a factor can be included in the correlation which can take in account the change in the physical shape of flow with the flow pattern to improve the correlation's performance. Flow pattern factor is included to take care of the change of the flow shape with the flow pattern.

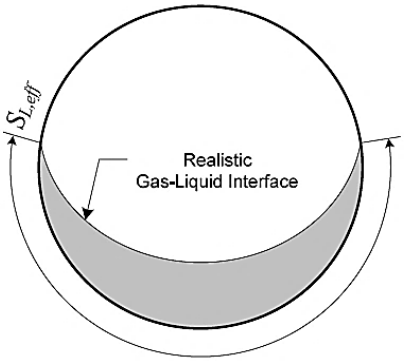

Figure 4.13 Flow pattern factor (Adapted from Tang (2011))

Flow pattern factor: Kim and Ghajar (2006) developed a parameter to represent flow patterns in two-phase flow which is the square of the ratio the effective wetted perimeter ($S_{L,eff}$) to the circumference of a circular pipe and named as flow pattern factor which is explained graphically in Figure 4.13. It is expressed as:

$$F_p = (\frac{S_{L,eff}}{\pi D})^2 = 1 - \alpha \tag{4.6}$$

Taking in account the effect of void fraction, inertia and gravity forces in the two phase flow, the flow pattern factor becomes:

$$F_p = (1-\alpha) + F_s^2\alpha \tag{4.7}$$

where,

$$F_s = \frac{2}{\pi}(\tan^{-1}\sqrt{\frac{\rho_G (V_G - V_L)^2}{gD(\rho_L - \rho_G)}}) \tag{4.8}$$

It's called shape factor and it's a normalized and modified Froude number (*Fr*).

This shape factor (F_s) represents the change in the shape of gas-liquid interface due to the effect of momentum and gravity force. For vertical two-phase flow the flow pattern factor becomes unity as the effective wetted perimeter ($S_{L,eff}$) equals the circumference due to the liquid surface effectively wetting the entire circumference of the pipe.

For the current research, this factor is being introduced in the proposed Reynolds analogy correlation in the following form:

$$\frac{h_{TP}}{h_L} = (\varphi_L)^p . F_P{}^q \tag{4.9}$$

p and q are the adjustable exponent of the correlation, φ_L is the pressure drop multiplier which can be defined as

$$\varphi_L{}^2 = \frac{(\frac{dp}{dz})_{f,TP}}{(\frac{dp}{dz})_{f,L}} \tag{4.10}$$

Single phase heat transfer coefficient (h_L) is from Seider & Tate (1936).

In Table 4.7, the best suitable exponents (p and q) for each orientation and all data points combined are presented in the tabular form for the suggested correlation. The inclination factor has an exponent of 0.48 for each individual orientation and 0.47 for the combined data. It shows very little variation with inclination. On the other hand, the exponent of φ shows variation

Table 4.7 Specific value of the exponents of the proposed correlation $h_{TP}/h_L = (\varphi_L)^p\ (F_p)^q$ in different inclinations

Data sets (without stratified points)	*p*	*q*	Percentage points within ±30%	Mean absolute error [%]	Standard deviation
Horizontal (Air-water) (72 points)	0.466	0.48	96%	19.43	18
-5 degree (Air-water) (71 points)	0.42	0.48	96%	13.12	13.32
-10 degree (Air-water) (64 points)	0.465	0.48	100%	11.23	6.95
-20 degree (Air-water) (62 points)	0.397	0.48	99%	16.90	8.40
All inclinations (269 points)	0.465	0.47	96%	16.1	13.69

Table 4. 8 Comparison of performance Bhagwat *et al.* (2012) and proposed correlation

	269 points				Bubbly (21 points)		Intermittent/ Annular (169 points)		Slug (79 points)	
Correlations	1[6]	2	3	4	1	2	1	2	1	2
Bhagwat *et al.* (2012)	74	84	18	20	91	100	79	88	61	74
Proposed Correlation	88	96	14	9	91	100	93	98	78	91

between 0.397 and 0.466 at different orientations and 0.465 provides the best fit with all the data points combined. No clear trend is observed in the change of exponent for φ at different orientations. In Table 4. 8, comparison is drawn between the performance of Bhagwat *et al.* (1982) and proposed correlation at different flow patterns based on ±30% and ±25% error band. Stratified flow points have not been considered for the performance evaluation as none of the

[6] In Table 4.8, 1, 2, 3 and 4 refers to ±25% error band, ±30% error band, mean absolute error [%] and standard deviation respectively.

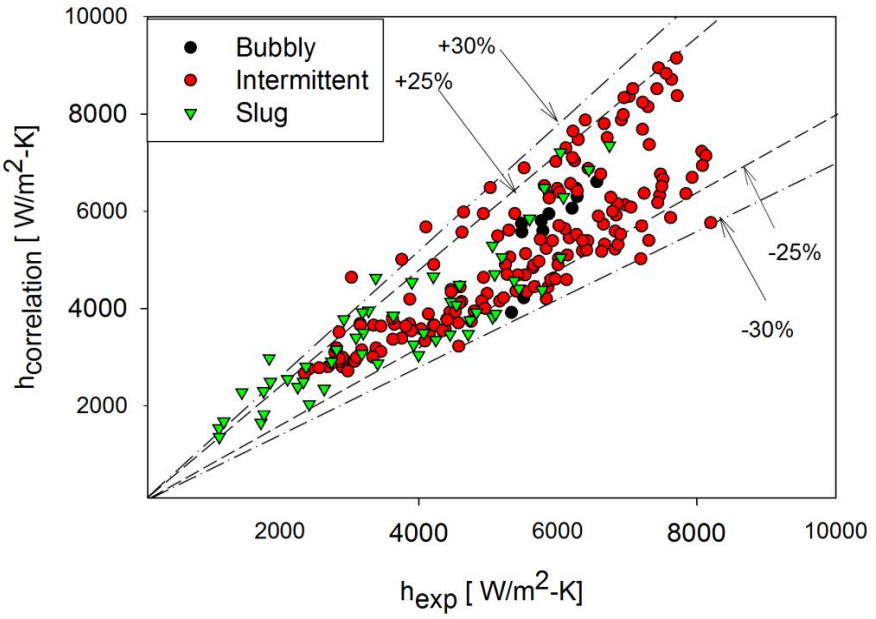

Figure 4.14 Performance of the proposed correlation combining all inclinations

correlations perform particularly well in that flow pattern. Using the new proposed correlation, overall, 96% of the points are predicted between ±30% compared to 84% of the points by Bhagwat *et al.* (2012). The suggested modifications not only improved the accuracy but it also improved the mean absolute error with smaller standard deviation while compared to the other pressure drop based correlations. The predictions have mean absolute error of 14% and standard deviation of 9% which is better than Bhagwat *et al.* (2012) as can be observed from Table 4.8. Specifically, in the slug region, the performance of the correlation improves considerably with 91% of the points within ±30% error compared to 74% of the points by Bhagwat *et al.* (2012). In the intermittent zone among 169 points in all orientation 98% of the points are predicted within ±30%. In Figure 4.14, the performance of the proposed correlation is presented graphically with ±25% and ±30% error band. In Figure 4.14 the points which are still out of the error band after modification occur mostly at Re_{SG} less than 1000. It should be mentioned that in that range heat

transfer coefficient values are small and for a certain difference in the prediction by the correlations is made more severe when percentage error is calculated.

CHAPTER V

SUMMARY, CONCLUSIONS & RECOMMENDATIONS

5.1 Summary of Findings

In the present study, heat transfer in non-boiling two phase air-water flow was studied in horizontal and near horizontal downward flow. The objective of the study was to establish basic understanding of the mechanism of heat transfer in downward inclined flow by analyzing the effect of liquid and gas flow rate, flow pattern and inclination on two-phase heat transfer coefficient and circumferential temperature. In total 400 experimental data points were collected in horizontal, -5^{o},-10^{o} and -20^{o} for the purpose of the research. After plotting and analyzing the data, conclusions were drawn about the heat transfer phenomena in two-phase downward flow which are described below:

(1) Mainly five flow patterns have been observed in horizontal and near horizontal downward flow, bubbly, stratified, slug, intermittent and annular flow. The ongoing experiment focused mainly on bubbly, stratified, slug and intermittent flow regime. In a specific liquid flow rate, two-phase heat transfer coefficient increased with the increase

of gas flow rate as the flow transitions from bubbly to stratified, slug and annular flow regime sequentially. This increase in the heat transfer coefficient was observed due to an increase in the mixture velocity, higher turbulence, and liquid film development at the top surface of the pipe. In the slug region, initially the heat transfer showed steep increase with the increase of Re_{SG} due to increased slug frequency. As the Re_{SG} was increased further due to elongated slugs the slope of h_{TP} became flat which continued to the onset of slug wavy region. As Re_{SG} was increased further due to higher turbulence, increased slug frequency and liquid film development at the top pipe surface steeper slope of h_{TP} was observed. Liquid flow rates had higher impact on heat transfer at low gas flow rates. At low gas flow rates, heat transfer coefficient increased rapidly with the increase of liquid flow rate in all orientations. At higher gas flow rates, the effect of liquid flow rates on heat transfer rate diminished as it remained almost same throughout the range of liquid flow rate.

(2) The effect of inclination on heat transfer shows different trend at different flow regimes. In the stratified flow regime, a maximum of 27% decrease in heat transfer was observed in -20^o orientation from the horizontal. This reduction occurred due to the difference in the flow regime between horizontal and inclined flow; slug flow which is more conducive to heat transfer persisted at horizontal flow compared to stratified flow pattern at inclined orientation. While comparing the downward inclined orientations, in the stratified region, initially, little change in the heat transfer was observed with inclination at low Re_{SG}. When Re_{SG} was increased further, it showed a decrease with the increase of inclination due to decreased frequency of the disturbance waves which locally accelerates the flow causing higher heat transfer. In the slug flow regime, the trend of h_{TP} with inclination was irregular. The reason for such trend was investigated by analyzing the local h_{TP} value at the top and bottom surface of the pipe. Top surface h_{TP} was always

found to be greater than bottom surface h_{TP}. However, it was revealed that the top and bottom surface h_{TP} follows opposing trend with inclination in the slug flow regime. For top surface, h_{TP} decreased with the increase of inclination where as for the bottom surface the trend was opposite. The reason for decreasing h_{TP} at the top surface with increasing inclination is due to the decreasing frequency and higher residence time of the slug (which touches the top surface). On the other hand, the liquid phase, which maintained continuous contact with the bottom surface, was accelerated with the increase of inclination due to gravity force and increased the h_{TP} for the bottom. The opposite trend of increasing and decreasing h_{TP} for top and bottom was found to be the main reason for an irregular trend for average h_{TP}. Moreover, it was also observed that at times slugs were slowed down to the point of complete stop due to buoyancy force in random fashion which might have also contributed to the phenomena. At the onset of intermittent flow regime, the effect of orientation was very prominent as the h_{TP} decreased gradually from horizontal to -20^{o}. This gradual decrease was caused by an increase in the resistance of shear force to the gas phase due to an increase in buoyancy with inclination. This resistance caused the gas phase to slow down decreasing turbulence and also increased the residence time of the slugs in the slug wavy region retarding the heat transfer. In the annular wavy region, the effect of inclination was reduced due to the liquid film development at the top surface of the pipe.

(3) The performance of different heat transfer correlations which are available in the literature and relevant to the current research were investigated using the experimental data collected. Most of the existing correlations didn't perform satisfactorily. Among the general correlations, Shah (1981) and Knott *et al.* (1959) performed satisfactorily and among the Reynolds analogy based correlations Vijay *et al.* (1982) and Bhagwat *et al.* (2013) performed well. Tang and Ghajar (2007) performed well in the slug region. No

correlation was found in the literature that performs well in stratified region. The uncertainty associated with the measurement of inside wall temperature at low gas and liquid flow rates and higher percentage error associated with low heat transfer coefficient value (h_{TP}) could be responsible for such occurrence. Shah (1981) predicted 97% and 93% of all the points within ±30% and ±25% respectively. Due to its exceptional performance and simple structure, no further attempt was made to modify the Shah (1981) correlation or propose a new correlation for the downward inclined flow. For Reynolds analogy correlation, a new correlation was proposed to improve the performance of the Bhagwat *et al.* (2012) correlation which predicted 84% of the points within ±30% without considering the stratified flow points. It specially performed poorly at slug flow regime with only 74% of the points within ±30%. The proposed correlation predicted 96% of the all points within ±30% and 91% of the slug points within ±30%.

5.2 Future Recommendations

(1) A new correlation can be modelled specifically for the stratified flow regime as all the existing correlations in the literature fail to predict the heat transfer coefficient within reasonable accuracy in this flow pattern.

(2) Conduct further experiments at higher downward inclined flow such as -30^{o}, -45^{o}, -60^{o} etc. to observe if any major changes occur in the flow pattern to offset trends of heat transfer which has been established in this research work. Different fluid combination and different pipe diameters can be used to collect more data and establish a more detailed overview of changes in two-phase heat transfer coefficient with inclination covering the entire range from the horizontal to vertical downward inclined flow.

(3) Performance of the new proposed correlations should be tested further for higher downward inclined flow to confirm the validity of the value of the exponents used and its

structure with different gas-fluid combinations. By conducting further investigation the value of the exponents can be refined and potentially be used as a universal correlation for all downward inclined flows.

(4) An experimental setup for microgravity two-phase heat transfer investigation can be constructed for inclined pipe orientation. This is an emerging field which has great future application in space technology and instrumentation and still requires great deal of information regarding the effect of reduced gravity on flow pattern, pressure drop and heat transfer in two-phase flow.

REFERENCES

Aggour, M. A. (1978). Hydrodynamics and Heat Transfer in Two-Phase Two-Component Flow. (Ph.D. Dissertation), University of Manitoba, Canada.

Bhagwat, S. M., Mollamahmutoglu, M., & Ghajar, A. J. (2012). Experimental Investigation and Empirical Analysis of Non-Boiling Gas-Liquid Two Phase Heat Transfer in Vertical Downward Pipe Orientation. *Proceedings of ASME 2012 Summer Heat Transfer Conference (HT2012)*, Puerto Rico, July 8-12.

Chisholm, D. (1973). Void Fraction During Two-Phase Flow. *J. Mechanical Engineering Science, 15*, 235-236.

Chu, Y. C., & Jones, B. G. (1980). Convective Heat Transfer Coefficient Studies in Upward and Downward Vertical Two-Phase Non-Boiling Flows. *AIChE., 7,* 79-90.

Cook, W. L. (2008). An Experimental Apparatus for Measurement of Pressure Drop, Void Fraction, and Non-Boiling Two-Phase Heat Transfer and Flow Visualization in Pipes for All Inclinations. (MS), Oklahoma State University, Stillwater.

Davis, E. J., & David, M. M. (1964). Two-Phase Gas-Liquid Convection Heat Transfer. *I&EC Fundamentals, 3*(2), 111–118.

Deshpande, S. D., Bishop, A. A., & Mkrandikar, B. M. (1991). Heat Transfer to Air-Water Plug-Slug Flow in Horizontal Pipes. *I&EC Research, 30*, 2172–2180.

Dorresteijn, W. R. (1970). Experimental Study of Heat Transfer in Upward and Downward Two Phase Flow of Air and Oil through 700 M Tubes. *Proccedings of the 4th International Heat Transfer Conference*

Drucker, M. I., Dhir, V. K., & Duffey, R. B. (1984). Two Phase Heat Transfer for Flow in Tubes and over Rod Bundles with Blockages. *Trans. of ASME, J. of Heat Transfer*.

Elamvaluthi, G., & Srinivas, N. S. (1984). Two-Phase Heat Transfer in Two Component Vertical Flows. *International Journal of Multiphase Flow, 10*(2), 237-242. doi: http://dx.doi.org/10.1016/0301-9322(84)90021-1

Fedotkin, I. M., & Zarudnev, L. P. (1970). Correlation of Experimental Data on Local Heat Transfer in Heating of Air-Liquid Mixtures in Pipes. *Heat Transfer-Sou. Res., 2*(1), 175-181.

Fogler, H. S. (2008). *Paraffin Research, Porous Media Research Group.* Retrieved June 18, 2014, from <sitemaker.umich.edu/sfogler/paraffin_deposition>

Fried, L. (1954). Pressure Drop and Heat Transfer for Two-Phase, Two-Component Flow. *Chem. Eng. Prog. Symp. Series, 50*(9), 47–51.

Furuholt, E. M. (1988). Multiphase Technology: Is It of Interest for Future Field Developments? *Society of Petroleum Engineers European Petroleum Conference*, London, England.

Gabriel, K. S. (2007). *Microgravity Two-Phase Flow and Heat Transfer*. El Segundo, CA: Microcosm Press and Springer.

Ghajar, A. J. (2005). Non-Boiling Heat Transfer in Gas-Liquid Flow in Pipes: A Tutorial. *Journal of the Brazilian Society of Mechanical Sciences and Engineering, 27*(1), 46-73.

Ghajar, A. J., & Bhagwat, S. M. (2014). Gas-Liquid Two Phase Flow Phenomenon in near Horizontal Upward and Downward Inclined Pipe Orientations. *International Journal of Mechanical, Aerospace, Industrial and Mechatronics Industry, 8*(6), 1039-1053.

Ghajar, A. J., & Kim, J. (2005). A Non-Boiling Two-Phase Flow Heat Transfer Correlation for Different Flow Patterns and Pipe Inclination Angles. *Proc. of 2005 ASME Summer Heat Transfer Conf.*, San Francisco, CA.

Ghajar, A. J., & Kim, L. (2006). *Calculation of Local inside-Wall Convective Heat Transfer Parameters from Measurements of the Local Outside-Wall Temperatures Along an Electrically Heated Circular Tube, Heat Transfer Calculations*. NewYork, NY: Mc-Graw-Hill.

Ghajar, A. J., & Tam, L. M. (1994). Heat Transfer Measurements and Correlations in the Transition Region for a Circular Tube with Three Different Inlet Configurations, Experimental Thermal and Fluid Science. *8*, 79-90.

Gnielinski, V. (1976). New Equations for Heat and Mass Transfer in Turbulent Pipe and Channel Flows. *Int. Chemical Engineering, 16*, 359-368.

Hestroni, G., Mewes, D., Enke, C., Gurevich, M., Mosyak, A., & Rozenblit, R. (2003). Heat Transfer to Two-Phase Flow in Inclined Tubes. *Int. J. of Multiphase Flow, 29*, 173–194.

Hetsroni, G., Hu, B. G., Yi, B. G., Mosyak, A., Yarin, L. P., & Ziskind, G. (1998a). Heat Transfer in Intermittent Air-Water Flow–Part I: Horizontal Tube. *Int. J. Multiphase Flow, 24*(2), 165–188.

Hetsroni, G., Hu, B. G., Yi, B. G., Mosyak, A., Yarin, L. P., & Ziskind, G. (1998b). Heat Transfer in Intermittent Air-Water Flow, Part Ii: Upward Inclined Tube. *Int. J. Multiphase Flow, 24*, 188–212.

Hossainy, T. A., Bhagwat, S. M., & Ghajar, A. J. (2014). Non-Boiling Heat Transfer in Horizontal and near Horizontal Downward Inclined Gas-Liquid Two Phase Flow. *10th International Conference on Heat Transfer, Fluid Mechanics and Thermodynamics*, Orlando, Florida.

Hughmark, G. A. (1965). Holdup and Heat Transfer in Horizontal Slug Gas-Liquid Flow. *Chem. Eng. Sci. , 20*, 1007-1010.

Johnson, H. A., & Abou-Sabe, A. H. (1952). Heat Transfer and Pressure Drop for Turbulent Flow of Air-Water Mixture in a Horizontal Pipe. *Trans. ASME, 50*(9), 47–51.

Kago, T., Saruwari, T., Kashima, M., Morooka, S., & Kato, Y. (1986). Heat Transfer in Horizontal Plug and Slug Flow for Gas-Liquid and Gas-Slurry Systems. *J. Chemical Engineering of Japan, 19*(2), 125–131.

Kalapatapu, S. B. (2014). Non-Boiling Heat Transfer in Horizontal and near Horizontal Upward Inclined Gas-Liquid Two-Phase Flow. MS Thesis. Mechanical and Aerospace Engineering. Oklahoma State University. Stillwater, Oklahoma.

Khoze, A. N., Dunayev, S. V., & Sparin, V. A. (1976). Heat and Mass Transfer in Rising Two-Phase Flows in Rectangular Channels. *Heat Transfer - Soviet Research, 8*(3), 87-90.

Kim, D., & Ghajar, A. J. (2002). Heat Transfer Measurements and Correlations for Air-Water Flow of Different Flow Patterns in a Horizontal Pipe Experimental. *Thermal and Fluid Science, 25*, 659–676.

Kim, D., Ghajar, A. J., & Dougherty, R. L. (2000). Robust Heat Transfer Correlation for Turbulent Gas-Liquid Flow in Vertical Pipes. *Journal of Thermophysics and Heat Transfer, 14*(4), 574-578.

Kim, J., & Ghajar, A. J. (2006). A General Heat Transfer Correlation for Non-Boiling Gas-Liquid Flow with Different Flow Patterns in Horizontal Pipes. *Int. J. Multiphase Flow, 32*, 447–465.

King, C. D. G. (1952). Heat Transfer and Pressure Drop for an Air-Water Mixture Flowing in a 0.737 Inch I.D. Horizontal Tube. (M.S.), University of California, Berkeley, CA.

Kline, S. J., & McClintock, F. A. (1953). Describing Uncertainties in Single Sample Experiments. *Mechanical Engineering, 1*, 3-8.

Knott, R. F., Anderson, R. N., Acrivos, A., & Petersen, E. E. (1959). An Experimental Study of Heat Transfer to Nitrogen-Oil Mixtures. *Industrial and Engineering Chemistry, 51*(11), 1369-1372.

Lockhart, R. W., & Martinelli, R. C. (1949). Proposed Correlation of Data for Isothermal Two-Phase, Two-Component Flow in Pipes. *Chemical Engineering Process, 45*(1), 39–48.

Lunde, K. E. (1961). Heat Transfer and Pressure Drop in Two-Phase Flow. *Chem. Eng. Bog. Symp. Ser., 57*, 104-110.

Martin, B. W., & Sims, G. E. (1971). Forced Convection Heat Transfer to Water with Air Injection in a Rectangular Duct. *I&EC Fundamentals, 14*, 1115–1134.

Mollamahmutoglu, M. (2012). Study of Isothermal Pressure Drop and Non-Boiling Heat Transfer in Vertical Downward Two Phase Flow. (M.S.), Oklahoma State University, Stillwater, Oklahoma.

Nürnberg, F. M. (1970). Two Phase Problem in Nuclear Reactors. *Reactor Physics, 15*(8), 47-52.

Oliver, D. R., & Wright, S. J. (1964). Pressure Drop and Heat Transfer in Gas-Liquid Slug Flow in Horizontal Tubes. *British Chemical Engineering, 9*, 590-596.

Oshinowo, O., Betts, R. C., & Charles, M. E. (1984). Heat Transfer in Co-Current Vertical Two-Phase Flow. *Canadian Journal of Chemical Engineering, 62*, 194-199.

Park, J., Fukuda, K., & Liu, Q. (2012). Chf Phenomena by Photographic Study of Boiling Behavior Due to Transient Heat Inputs. *Science and Technology of Nuclear Installations, 2012*, 12. doi: 10.1155/2012/248923

Pletcher, R. H., & McManus, H. N. (1968). Heat Transfer and Pressure Drop in Horizontal Annular Two-Phase, Two-Component Flow. *J. Heat Mass Transfer, 11*, 1087–1104.

Ravipudi, S. R., & Godbold, T. M. (1978). The Effect of Mass Transfer on Heat Transfer Rates for Two-Phase Flow in Vertical Pipe. *Proc. of the 6th International Heat Transfer Conference*, Toronto, Canada

Rezkallah, K. S., & Sims, G. E. (1987). An Examination of Correlations of Mean Heat Transfer Coefficients in Twophase and Two-Component Flow in Vertical Tubes. *AIChE Symp. Series, 83*, 109-114.

Rzehak, R., & Krepper, E. (2013). Cfd for Subcooled Flow Boiling: Parametric Variations. *Science and Technology of Nuclear Installations, 2013*, 22. doi: 10.1155/2013/687494

Shah, M. M. (1981). Generalized Prediciton of Heat Transfer During Two-Component Gas-Liquid Flow in Tubes and Other Channels. *AIChE Symp. Series, 77*, 140-151.

Shoham, O., Dukler, A. E., & Taitel, Y. (1982). Heat Transfer During Intermittent/Slug Flow in Horizontal Tubes. *Industrial & Engineering Chemistry Fundamentals, 21*(3), 312-319. doi: 10.1021/i100007a020

Sieder, E. N., & Tate, G. E. (1936). Heat Transfer and Pressure Drop of Liquids in Tubes. *Industrial and Engineering Chemistry, 28*, 1429-1435.

Soldo, V., Grozdek, M., Curko, T., & (2006). Two-Phase Heat Transfer During Refrigerant Evaporation in a Solar Collector Tube *61st ATI National Congress – International Session "Solar Heating and Cooling"* Zagreb,Perugia.

Spalding, D. B. (l964). Contribution to the Theory of Heat Transfer across a Turbulent Boundary Layer. *Int. J. Heat Mass Transfer, 7*, 743-761

Spedding, P. L., & Chen, J. J. J. (1984). Holdup in Two Phase Flow. *International Journal of Multiphase Flow, 10*(3), 307–339.

Tang, C. C. (2011). A Study of Heat Transfer in Non-Boiling Two-Phase Gas-Liquid Flow in Pipes for Horizontal, Slightly Inclined, and Vertical Orientations. (Ph.D.), Oklahoma State University, Stillwater, Oklahoma.

Tang, C. C., & Ghajar, A. J. (2007). Validation of a General Heat Transfer Correlation for Non-Boiling Two-Phase Flow with Different Flow Patterns and Pipe Inclination Angles. *Proceedings of the 2005 ASME-JSME Thermal Engineering Heat Transfer Connference*, Vancouver, Canada, July 8-12.

Tang, C. C., & Ghajar, A. J. (2011). A Mechanistic Heat Transfer Correlation for Non-Boiling Two-Phase Flow in Horizontal, Inclined and Vertical Pipes *Proceedings of ASME/JSME 2011(AJTE2011) 8th Thermal Engineering Joint Conference*. Honolulu, Hawaii.

Trevisan, O. V., Franca, F. A., & Lisboa, A. C. (2006). Oil Production in Offshore Fields: An Overview of the Brazilian Technology Development Program. *Proceedings of the 1st World Heavy Oil Conference*, Beijing, China, November 13–15.

Vijay, M. M. (1978). A Study of Heat Transfer in Two-Phase Two-Component Flow in a Vertical Tube. (Ph.D), University of Manitoba, Canada.

Vijay, M. M., Aggour, M. A., & Sims, G. E. (1982). A Correlation of Mean Heat Transfer Coefficients for Two-Phase Two-Component Flow in a Vertical Tube. *Proceedings of the 7th International Heat Transfer Conference*, Munich, Germany

APPENDIX A

UNCERTAINTY ANALYSIS

The heat transfer uncertainty analysis is performed for both single phase and two phase flow for the current research. A method proposed by Kline and McClintock (1953) is utilized for the heat transfer uncertainties calculation for both single phase and two phase heat transfer.

Assume, a measurement *R* is a function of several independent variables.

$$R = f(x_1, x_2, x_3 \ldots\ldots\ldots\ldots\ldots x_n) \tag{A.1}$$

The uncertainty (w_R) of measurement of *R* can be performed by the following formula proposed by Kline and McClintock (1953):

$$w_R = \pm[(\frac{dR}{dx_1}w_1)^2 + (\frac{dR}{dx_2}w_2)^2 + (\frac{dR}{dx_3}w_3)^2 + \quad \ldots\ldots\ldots \quad + (\frac{dR}{dx_n}w_n)^2\ ]^{\frac{1}{2}} \tag{A.2}$$

According to the method, the uncertainty of the independent variables of heat transfer coefficient equation are first separately calculated and then the individual uncertainties are replaced in the

formula to obtain the total uncertainty of the single phase and two phase heat transfer measurements.

The method of heat transfer uncertainty calculation along with all the equations which are used in every step are described in details and after that sample calculations for both single phase and two phase heat transfer uncertainty are presented in Table A.1, A.2, A.3 and A.4.

The heat transfer coefficient equation is:

$$h = \frac{\dot{q}''}{\bar{T}_{wi} - \bar{T}_b} = \frac{\dot{q}''}{\Delta T} \tag{A.3}$$

Applying Kline and McClintock (1953) method we can determine the uncertainty for *h*:

$$w_h = \left[\left(\frac{\partial h}{\partial \dot{q}''} w_{\dot{q}''} \right)^2 + \left(\frac{\partial h}{\partial \Delta T} w_{\Delta T} \right)^2 \right]^{\frac{1}{2}} \tag{A.4}$$

After performing the partial differentiation the equation becomes:

$$w_h = \left[\left(\frac{1}{\Delta T} w_{\dot{q}''} \right)^2 + \left(\frac{-\dot{q}''}{\Delta T} w_{\Delta T} \right)^2 \right]^{\frac{1}{2}} \tag{A.5}$$

From Eq. (A.3) it is evident that to determine the uncertainty for h, uncertainties associated with $\dot{q}'', \bar{T}_{wi}$ and $\bar{T}_b$ have to be determined. The uncertainty regarding ΔT can be determined by summing up the uncertainties of average inside wall surface temperature and average bulk temperature of the two phase flow.

Now, the average wall inside surface temperature can be expressed with the following equation:

$$\bar{T}_{wi} = \dot{q} R_t + \bar{T}_{wo} \tag{A.6}$$

The uncertainty equation:

$$w_{\bar{T}_{wi}} = \left[\left(\frac{\partial \bar{T}_{wi}}{\partial \dot{q}} w_{\dot{q}} \right)^2 + \left(\frac{\partial \bar{T}_{wi}}{\partial R_t} w_{R_t} \right)^2 + \left(\frac{\partial \bar{T}_{wi}}{\partial \bar{T}_{wo}} w_{\bar{T}_{wo}} \right)^2 \right]^{\frac{1}{2}} \tag{A.7}$$

After simplification the equation becomes:

$$w_{\bar{T}_{wi}} = \left[\left(R_t w_{\dot{q}} \right)^2 + \left(\dot{q} w_{R_t} \right)^2 + \left(w_{\bar{T}_{wo}} \right)^2 \right]^{\frac{1}{2}} \tag{A.8}$$

The experimental set up has seven temperature stations with each station having four thermocouples. The average wall outside surface temperature at each station is determined by taking the numerical average of the temperature of the four thermocouples using the following equation:

$$\bar{T}_{wosn} = \frac{\bar{T}_{wo-1} + \bar{T}_{wo-2} + \bar{T}_{wo-3} + \bar{T}_{wo-4}}{4} \tag{A.9}$$

Then the average temperature of the seven stations is determined to calculate the average outside wall surface temperature for the whole setup using the following equation:

$$\bar{T}_{wo} = \frac{\bar{T}_{wo-1} + \bar{T}_{wo-2} + \bar{T}_{wo-3} + \bar{T}_{wo-4} + \bar{T}_{wo-5} + \bar{T}_{wo-6} + \bar{T}_{wo-7}}{7} \tag{A.10}$$

The uncertainty associated with each thermocouple temperature is $\pm 0.5^0$C. The outside wall surface temperature has been determined by taking the average at each station; hence, the associated uncertainty with the average wall outside surface temperature is also taken as $\pm 0.5^0$C.

The equation for thermal resistance for the setup is:

$$R_t = \frac{\ln\left(D_o / D_i \right)}{2\pi k l} \tag{A.11}$$

The uncertainty equation is:

$$w_{R_t} = \left[\left(\frac{\partial R_t}{\partial D_o} w_{D_o} \right)^2 + \left(\frac{\partial R_t}{\partial D_i} w_{D_i} \right)^2 + \left(\frac{\partial R_t}{\partial k} w_k \right)^2 + \left(\frac{\partial R_t}{\partial l} w_l \right)^2 \right]^{\frac{1}{2}} \tag{A.12}$$

After substituting the terms we get:

$$w_{R_t} = \left[\left(\frac{1}{2\pi D_o k l} w_{D_o} \right)^2 + \left(\frac{-1}{2\pi D_i k l} w_{D_i} \right)^2 + \left(\frac{-\ln\left(D_o / D_i \right)}{2\pi k^2 l} w_k \right)^2 + \left(\frac{-\ln\left(D_o / D_i \right)}{2\pi l^2 k} w_l \right)^2 \right]^{\frac{1}{2}} \tag{A.13}$$

The uncertainty value for thermal resistance calculated by using Eq. (A. 13) is $\pm$0.51%. It should be noted that the uncertainty for the thermal conductivity value is considered negligible as the value has been determined from best fit curve of tabulated value.

The heat transfer rate has the following equation:

$$\dot{q} = V_D I \tag{A.14}$$

The uncertainty equation becomes:

$$w_{\dot{q}} = \left[\left(\frac{\partial \dot{q}}{\partial V_D} w_{V_D} \right)^2 + \left(\frac{\partial \dot{q}}{\partial I} w_I \right)^2 \right]^{\frac{1}{2}} \tag{A.15}$$

After performing the manipulation we get:

$$w_{\dot{q}} = \left[\left(I w_{V_D} \right)^2 + \left(V_D w_I \right)^2 \right]^{\frac{1}{2}} \tag{A.16}$$

This uncertainty regarding heat transfer rate is calculated by using the equation for heat input from the welder which takes in account the manufacturer prescribed uncertainties for the voltage (V_D) and current (I). However, there is also heat loss due to the surroundings from the setup and heat storage in the setup. The amount of heat loss can be calculated from the difference between the heat input rate from the welder and heat transfer rate calculated by using the enthalpy equation to the flow which is:

$$\dot{q} = \dot{m}c(T_{b,out} - T_{b,in}) \tag{A.17}$$

This heat balance error is added with the uncertainty obtained by using Eq. (A.16) to obtain the total uncertainty of heat transfer rate.

The heat flux equation is:

$$\dot{q}'' = \frac{V_D I}{\pi D_i L} \tag{A.18}$$

Hence, the uncertainty equation for heat flux is:

$$w_{\dot{q}''} = \left[\left(\frac{\partial \dot{q}''}{\partial V_D} w_{V_D} \right)^2 + \left(\frac{\partial \dot{q}''}{\partial I} w_I \right)^2 + \left(\frac{\partial \dot{q}''}{\partial D_i} w_{D_i} \right)^2 + \left(\frac{\partial \dot{q}''}{\partial l} w_l \right)^2 \right]^{\frac{1}{2}} \tag{A.19}$$

After substituting the appropriate values the heat flux uncertainty equation becomes:

$$w_{\dot{q}''} = \left[\left(\frac{I}{\pi D_i l} w_{V_D} \right)^2 + \left(\frac{V_D}{\pi D_i l} w_I \right)^2 + \left(\frac{-V_D I}{\pi D^2{}_i l} w_{D_i} \right)^2 + \left(\frac{-V_D I}{\pi D_i l^2} w_l \right)^2 \right]^{\frac{1}{2}} \tag{A.20}$$

After calculating all the intermediate uncertainty values, they are replaced in Eq. (A.4) to obtain the total uncertainty of the heat transfer coefficient *h*.

The sample calculations for the best and worst cases of uncertainties are presented in Table A.1 and A.2 for the single phase heat transfer data points and in Table A.3 and A.4 for two-phase heat transfer data points.

Table A.1 Single phase heat transfer uncertainty (Best Case RUN 0001)

Variable	Value	Uncertainty	Uncertainty %
Inner Diameter (D_i) (m)	0.0125	±1.270E-05	±0.1
Outer Diameter (D_o) (m)	0.0171	±1.270E-05	±0.07
Length (l) (m)	1.016	±3.175E-03	0.31
Thermal Conductivity (k) ($W/m\text{-}K$)	13.438	-	-
Ampere (I) (A)	579.2	±5.79	±1.00
Voltage (V_D) (V)	3.96	±0.0396	±1.00
Thermal Resistance (R_t) (K/W)	0.0036	±1.85E-5	±0.51
Average Inner Wall Temperature (T_{wi}) ($°C$)	31.05	±0.5	±1.48
$T_{wi} - T_b$ (ΔT) ($°C$)	17.55	±1.01	±5.6
Heat Transfer Rate ($\dot{q}$) (W)	2290.21	±32.43	±1.36
Heat Flux (W/m^2)	57302.92	±833.50	±1.45
Heat Transfer Coefficient (h) ($W/m^2\text{-}K$)	7783.671	±413.206	±5.31

Table A. 2 Single phase heat transfer uncertainty (Worst case RUN 0018)

Variable	Value	Uncertainty	Uncertainty %
Inner Diameter (D_i) (m)	0.0125	±1.270E-05	±0.1
Outer Diameter (D_o) (m)	0.0171	±1.270E-05	±0.07
Length (l) (m)	1.016	±3.175E-03	0.31
Thermal Conductivity (k) ($W/m\text{-}K$)	13.438	-	-
Ampere (I) (A)	579.2	±5.79	±1.00
Voltage (V_D) (V)	3.96	±0.0396	±1.00
Thermal Resistance (R_t) (K/W)	0.0036	±1.85E-5	±0.51
Average Inner Wall Temperature (T_{wi}) ($°C$)	31.05	±0.5	±1.48
$T_{wi} - T_b$ (ΔT) ($°C$)	13.00	±1.01	±5.6
Heat Transfer Rate ($\dot{q}$) (W)	2310.21	±6.96	±1.36
Heat Flux ($\dot{q}''$) (W/m^2)	492.21	±833.50	±1.45
Heat Transfer Coefficient (h) ($W/m^2\text{-}K$)	596.1	±72.01	±12.08

Table A. 3 Two phase heat transfer uncertainty (Best case RUN 151)

Variable	Value	Uncertainty	Uncertainty %
Inner Diameter (D_i) (m)	0.0125m	±1.27E-5m	±0.10
Outer Diameter (D_o) (m)	0.0171m	±1.27E-5m	±0.07
Length (l) (m)	1.016m	±3.175E-3	±0.31
Thermal Conductivity (k) ($W/m\text{-}K$)	13.438 W/m.K	–	–
Ampere (I) (A)	254.06 A	±2.54 A	±1.00
Voltage (V_D) (V)	1.76 V	±0.017 V	±1.00
Thermal Resistance (R_t) (K/W)	0.0036 K/W	±1.85E-5	±0.51
Average Inner Wall Temperature (T_{wi}) ($°C$)	42.12°C	0.50°C	±1.18
$T_{wi} - T_b$ (ΔT) ($°C$)	16	±1.01	6.31
Heat Transfer Rate ($\dot{q}$) (W)	462.9 W	±6.32 W	±1.36
Heat Flux ($\dot{q}''$) (W/m^2)	11189.31W/m^2	±186.97	±1.67
Heat Transfer Coefficient (h) ($W/m^2\text{-}K$)	729.1 $W/m^2\text{-}K$	±45.65	±6.26

Table A. 4 Two phase heat transfer uncertainty (Worst case RUN 1150)

Variable	Value	Uncertainty	Uncertainty %
Inner Diameter (D_i) (m)	0.0125m	±1.27E-5m	±0.10
Outer Diameter (D_o) (m)	0.0171m	±1.27E-5m	±0.07
Length (l) (m)	1.016m	±3.175E-3	±0.31
Thermal Conductivity (k) ($W/m\text{-}K$)	13.438 W/m.K	–	–
Ampere (I) (A)	245 A	±2.45	±1.00
Voltage (V_D) (V)	1.9 V	±0.019	±1.00
Thermal Resistance (R_t) (K/W)	0.0036 W	±1.85E-5	±0.51
Average Inner Wall Temperature (T_{wi}) ($°C$)	13.87°C	±0.55°C	±3.96
$T_{wi} - T_b$ (ΔT) ($°C$)	3	±1.01	33.66
Heat Transfer Rate ($\dot{q}$) (W)	466.53 W	±6.61 W	±1.56
Heat Flux ($\dot{q}''$) (W/m^2)	11672.22 W/m^2	±195.37	±1.67
Heat Transfer Coefficient (h) ($W/m^2\text{-}K$)	3065.83 $W/m^2\text{-}K$	±966.85	±31.54

VITA

Tabassum Aziz Hossainy

Candidate for the Degree of

Master of Science

Thesis: NON-BOILING HEAT TRANSFER IN HORIZONTAL AND NEAR HORIZONTAL DOWNWARD TWO PHASE GAS-LIQUID FLOW

Major Field: Mechanical Engineering

Biographical:

Born in Chittagong, Bangladesh in March 28, 1988. Finished primary school from Chittagong Collegiate School in 2003 and high school from Chittagong Ispahani College in 2005. Completed BS Degree in Mechanical Engineering from Islamic University of Technology (IUT), Gazipur, Bangladesh in 2009. Worked as a lecturer at IUT for 3 years before applying for higher studies at Oklahoma State University, USA.

Education:

Completed the requirements for the Master of Science in Mechanical Engineering at Oklahoma State University, Stillwater, Oklahoma in July, 2014.

Completed the requirements for the Bachelor of Science Mechanical Engineering at Islamic University of Technology, Gazipur, Bangladesh in 2009.

Experience:
3 year as a lecturer at Islamic University of Technology
2 year Research/Teaching Assistant at Oklahoma State University